AN ANALYSIS OF SELF-COOLING WITH INFILTRATED POROUS COMPOSITES INCLUDING THE EFFECT OF THE MELT LAYER

by

Maurice Robert Berry, Jr.

Thesis Submitted to the Graduate Faculty of the
Virginia Polytechnic Institute
in Partial Fulfillment for the Degree of
MASTER OF SCIENCE
in
Mechanical Engineering

APPROVED: _____

Chairman, Dr. Martin Crawford

_____ _____

Dr. H. L. Wood Dr. F. R. DeJarnette

April, 1968

Blacksburg, Virginia

TABLE OF CONTENTS

LIST OF FIGURES

LIST OF TABLES

NOMENCLATURE

A	Intercept of Vapor Pressure-Temperature Curve (lb/ft^2)
a_c	Thermal Diffusivity of Infiltrant (ft^2/hr)
a_m	Thermal Diffusivity of Matrix (ft^2/hr)
B	Slope of Vapor Pressure-Temperature Curve (lb^oR/ft^2)
c_c	Specific Heat of Coolant (BTU/lb^oR)
c_m	Specific Heat of Matrix (BTU/lb^oR)
g_c	Conversion Factor ($4.169 \times 10^8 lb_m ft/lb_f hr^2$)
h_o	Convective Heat-Transfer Coefficient to the Heated Surface With No Vaporization or Transpiration Effects of the Coolant ($BTU/hr\ ft^2\ ^oR$)
k_c	Thermal Conductivity of Infiltrant ($BTU/hr\ ft^oR$)
k_m	Thermal Conductivity of Matrix ($BTU/hr\ ft^oR$)
L	Distance From the Insulated Surface to the Original Surface of the Matrix (ft)
ℓ_a	Distance to Nearest Point of Known Temperature Above Point in Question (ft)
ℓ_b	Distance to Nearest Point of Known Temperature Below Point in Question (ft)
M	Molecular Weight of the Coolant (lb/lb mole)
$\dot{m}_\ell$	Mass Rate of Flow of Liquid Coolant Per Unit Surface Area ($lb/hr\ ft^2$)
$\bar{m}_\ell$	Rate of Formation of Liquid ($lb/hr\ ft^2$)
$\dot{m}_v$	Mass Rate of Flow of Coolant in Vapor Form Per Unit Surface Area ($lb/hr\ ft^2$)
$\bar{m}_v$	Rate of Formation of Vapor ($lb/hr\ ft^2$)
n	Nodal point at the Original Surface
P	Porosity of the Matrix; Fraction of Infiltrant Volume as Compared to the Total Volume

P_o	Ambient Pressure of the Hot-Gas Stream (lb/ft^2)
P_v	Vapor Pressure of the Coolant (lb/ft^2)
q_o	Heat Convected by the Hot-Gas Stream ($BTU/hr\ ft^2$)
q_1	Heat Conducted Into a Finite-Difference Element ($BTU/hr\ ft^2$)
q_2	Heat Conducted Out of a Finite-Difference Element ($BTU/hr\ ft^2$)
R_u	Universal Gas Constant (1545.4 ft lb/lb mole ^oR)
T	Temperature (^oR)
T_a	Temperature of Nearest Nodal Point Above Point in Question (^oR)
T_b	Temperature of Nearest Nodal Point Below Point in Question (^oR)
T_c	Critical Temperature of the Coolant (^oR)
T_m	Melting Temperature of the Coolant (^oR)
T_{mm}	Melting Temperature of the Matrix (^oR)
T_{nb}	Normal Boiling Temperature of the Coolant (^oR)
T_o	Ambient Temperature of the Hot-Gas Stream (^oR)
T_v	Vaporization Temperature of Coolant (^oR)
T_{xi}	Initial Temperature Distribution Throughout the Composite (^oR)
x	Distance Normal to Surface Measured From Insulated Back Face (ft)
Δx	Distance Increment (ft)
α	Viscous Flow Coefficient (ft^{-2})
β	Inertial Flow Coefficient (ft^{-1})
δ_1	Distance From Insulated Back Face to Liquid-Solid Interface (ft)
δ_2	Distance From Insulated Back Face to Vapor-Liquid Interface (ft)

θ	Time (hr)
$\Delta\theta$	Time Increment (hr)
θ_1	Time at Which Temperature at the Original Surface Equals the Melting Temperature of the Coolant (hr)
θ_2	Time at Which the Surface Temperature of the Liquid Layer Equals the Vaporization Temperature of the Coolant at Ambient Pressure (hr)
θ_3	Time at Which Liquid Layer Starts to Recede Below the Original Surface (hr)
θ_4	Time at Which All Coolant has Vaporized (hr)
θ_{crit}	Time at Which Heated Surface Temperature Equals the Melting Temperature of the Matrix (hr)
λ_m	Latent Heat of Fusion of the Coolant (BTU/lb)
λ_{nb}	Latent Heat of Vaporization of the Coolant at Normal Boiling Point (BTU/lb)
λ_v	Latent Heat of Vaporization of the Coolant (BTU/lb)
ρ_c	Density of the Coolant (lb/ft^3)
ρ_m	Density of the Matrix (lb/ft^3)
μ	Viscosity of the Coolant Vapor (lb/ft hr)

Subscripts

$c\ell$	Coolant in Liquid Phase
cs	Coolant in Solid Phase
cv	Coolant in Vapor Phase
i	Any Internal Nodal Point
m	Nodal Point at the Liquid-Solid Interface ($x = \delta_1$) or Matrix in Solid Phase
mc	Weighted Property of Matrix and Coolant Composite
$m\ell$	Weighted Property of Matrix and Liquid Coolant Composite
ms	Weighted Property of Matrix and Solid Coolant Composite

mv	Weighted Property of Matrix and Vapor Coolant Composite
ml	Nodal Point Immediately Above Liquid-Solid Interface
m2	Nodal Point Immediately Below Liquid-Solid Interface
v	Nodal Point at Vapor-Liquid Interface ($x = \delta_2$)
vl	Nodal Point Immediately Above Vapor-Liquid Interface
v2	Nodal Point Immediately Below Vapor-Liquid Interface
$\Big\vert_{I,II}$	Regions Existing During Various Time Periods
1,2...	Quantity at a Particular Nodal Point

Superscripts

$(\quad)'$	Quantity at Time $\theta + \Delta\theta$

I. INTRODUCTION

The development of high-energy aluminized propellants with flame temperatures in excess of 6000°F has created the need for a new non-eroding nozzle-throat insert material for solid rocket motors. The nozzle wall temperatures attained with these propellants during a reasonable firing duration exceed even the maximum practical operating temperatures of uncooled tungsten. However, by infiltrating a porous tungsten matrix with a coolant material that is subject to melting and vaporizing, it is possible to retard the rapid temperature rise at the surface and permit increased exposure to the hot-gas stream. This concept has been termed "self-cooling" by Schwarzkopf and Weisert (1).

In a previous study (2), the transient behavior of an infiltrated tungsten composite was investigated from the standpoint of one- dimensional, finite-thickness, flat-plate model. In that study, the plate is initially at a uniform temperature. The hot-gas flow is initiated, and the surface temperature of the plate increases until the coolant begins to vaporize. As vaporization proceeds, a porous tungsten region develops through which the gaseous coolant flows to the hot surface, whose temperature continues to increase with time. The gaseous-solid coolant interface recedes from the surface with time. The effect of the phase change of the coolant from solid to liquid was not considered. Ungar and Touryan (3) have recently shown that,

due to the expansion involved in the change of phase from a solid to a liquid, there exists a period of time when the infiltrant forms a stable liquid layer on the surface exposed to the hot-gas flow. Also, it was observed that this melt layer has a significant influence on the transient temperature response of the matrix surface in that, during this time period, the surface is insulated from the hot-gas flow and remains essentially at the temperature of the liquid layer. Therefore, during this time period, there exists a relatively flat portion on the temperature-time curve of the matrix surface temperature.

The object of this investigation is to develop an analysis of the self-cooling concept which will include the effects of the melting process and of the liquid layer on the temperature response at the original matrix surface.

II. REVIEW OF LITERATURE

A. Previous Investigations

Initial development of the infiltrated porous tungsten self-cooling concept was carried out by Maloff (4) and Davies and Smith (5) with copper and lithium hydride respectively. Subsequently, Gessner, Ingram, and Seader (2) initiated an analytical investigation of the mechanics of the self-cooling concept. The application of the analysis was to aid in the selection of coolant materials, to indicate the effects of the porous structure of the matrix and to provide guidance in the interpretation of the experimental data obtained from small solid-propellant motor firings. The self-cooling process was described physically in the following manner: After hot-gas flow is initiated, the temperature of the composite surface rises rapidly until the vaporization temperature of the coolant is reached. All effects of the phase change of the coolant at the melting point were assumed negligible. At the instant the vaporization temperature is obtained at the surface, the coolant begins to vaporize and a porous tungsten layer develops through which the gaseous coolant flows to the exposed surface. This results in a vapor-liquid coolant interface which recedes with time. The rate of recession of the interface and, consequently, the gaseous coolant mass flow rate are functions of the temperature distribution within the composite and of the pressure drop through the porous structure caused by viscous and inertial

effects on the coolant mass flow. Thus, the interface recession rate and the corresponding mass flow rate of the coolant, as well as the interface temperature, are time-dependent variables. The vaporization process continues until the coolant is exhausted. The cooling mechanisms employed in the analysis include: heat absorbed at the interface due to the vaporizing coolant, convective cooling as the gaseous coolant flows through the porous structure, the reduction of the convective heat transfer coefficient by mass addition into the boundary layer. The heat absorbed by the melting coolant and all chemical reactions were neglected due to the complexity of the problem. It was noted (2) that exothermic chemical reactions between the gaseous coolant and hot-gas would have an unfavorable effect on heat transfer.

Gessner et al. (2) indicated that in an extensive search of previous investigations, a more complex model than those existing for transpiration and ablation cooling was needed to adequately describe the self-cooling process. The transpiration models examined consider one-dimensional, steady-state heat transfer, and thus do not consider the coolant flow rate as function of time. The ablation models discussed more closely approximate the physical situation of the self-cooling process than do the transpiration models. However, the ablation models reviewed are based upon semiempirical relationships and quasisteady analyses that are not applicable to the self-cooling process with infiltrated tungsten composites. A comprehensive tabulation of thirteen transpiration and ablation models is contained in reference (2).

The general model employed by Gessner considers the thickness of the nozzle liner as small compared to the diameter of the nozzle throat and thus approximates an infinite flat plate of finite thickness. The liner consists of a constant-porosity composite utilizing a tungsten matrix impregnated with a single coolant that vaporizes below the melting point of tungsten. The plate, initially at a constant temperature, is suddenly subjected to intense convective heating on one surface. The other surface or back face is considered as thermally insulated. One-dimensional, unsteady-state heat transfer continues in the plate until the vaporization temperature of the coolant at the heated surface is attained. At that instant, the flow of coolant vapor begins and the vapor-solid interface recedes through the porous structure. This interface recession continues until a reasonable firing time is attained or until all coolant is exhausted. Throughout the analysis, equal matrix and coolant temperatures at a given depth in the porous structure are assumed. Other assumptions made include those of negligible heat conduction through the gaseous coolant, negligible radiation at the heated surface, and no diffusion or chemical reactions. Also, since the liquid phase was not considered, the effect of melting of the coolant on the temperature distribution was neglected.

A closed-form solution for the complete set of differential equations applicable to Gessner's (2) analysis did not appear feasible at the time and, therefore, a finite-difference numerical approach for solving the set of equations was developed and

programmed for a digital computer. The transpiration effect of the coolant vapor on the hot-gas stream was included in the analysis. However, in a later report (6), Gessner indicates that the reduction in convective heat transfer due to transpiration effects for cases studied is less than three percent.

Several case studies were made with eight different coolants infiltrated in tungsten matrices of various porosities. From the data, conclusions were drawn as to the desirable properties of an ideal infiltrant. The ideal coolant should have large values of vapor specific heat, solid density, and latent heat of vaporization, and also a low boiling point. Gessner, Ingram, and Seader (2) also indicated that compatibility problems were evident and that these problems are discussed in detail in volume I of their report, which is classified.

In an earlier report, Grosh (7) developed an analytical solution to the differential equations applicable to the self-cooling process, but with restricted boundary conditions. His objective was to examine the simultaneous effects of transpiration and change of phase. The model formulated was a semi-infinite porous plate initially at uniform temperature and suddenly subjected to a step increase in temperature at the surface. Solutions for the temperature distributions were given in terms of tabulated functions. However, the phase-front positions were determined by solving a set of non-linear, algebraic equations whose solutions are presented in the form of a nomogram for the case where only one phase change occurs in the solid. For more than one phase

change the solution proved quite difficult without the aid of a computer.

While conducting tests in an arc jet on a copper-infiltrated tungsten matrix, Ungar and Touryan (3) observed a copper film on the surface of the test specimen. Accompanying the existence of the copper film, the temperature of the matrix surface remained somewhat less than the vaporization temperature of the copper. The tests were repeated with several variations, but in all cases, the formation and retention of a relatively stable liquid layer strongly influenced the time to failure of this specimen and its temperature history. These observations indicate that the self-cooling process must include the effect of the liquid layer and that the process can be separated into five time domains:

> "1) The initial heat-up period prior to any phase changes,
> 2) The period during which coolant melts and flows onto the surface to form a liquid layer but with no vaporization,
> 3) The period during which the liquid metal coolant vaporizes and is renewed at the surface as the melting process continues,
> 4) The period after the liquid layer has been depleted during which the liquid coolant vaporizes within the refractory matrix, and
> 5) The final period during which the base tungsten fails." (Ref. 3, pg. 1949)

Ungar and Touryan (3) also note that this important phenomenon seemed to have been overlooked in previous studies (2).

A similar temperature plateau was observed by Resnick, et. al (8). Molten pools appeared on the surfaces of test specimens during the early stages of the heating period, accompanied by a noticeable decline in the rate of temperature rise of the surface. Resnick also

observed that the molten pools were more pronounced for larger porosities.

B. Manufacturing Process

The manufacturing process described briefly by Resnick (8) was as follows: Tungsten particles of different sizes were used. Various porosities were achieved by varying the compacting pressure which was in the order of 50,000 to 100,000 PSI. The matrix was then sintered. Infiltration was accomplished by placing excess infiltrant in contact with the sintered matrix and heating to a temperature above the melting point of the infiltrant in a hydrogen atmosphere. A similar manufacturing process was indicated by Schwarzkopf and Weisert (9). Both Resnick (8) and Schwarzkopf and Weisert (9) observed that matrices fabricated from tungsten particles of small diameters restricted the flow of coolant and infiltrant remained in the matrix after the tungsten at the surface failed. Gessner (2) indicated a minimum particle size of 10 microns for unrestricted flow.

C. Experimental Tests

An extensive testing program has been carried out using small-scale rocket nozzles to develop the concept of self-cooled composites (9). Several conclusions were drawn from the experimental data obtained. It was found that the maximum thermal protection can be achieved with graded matrices in which a layer having low porosity forms the exposed surface and is backed by a high-porosity layer. In addition, these data indicate a

requirement for graded porosity in the axial direction. The test data also show the thermal expansion and expulsion of liquid coolant onto the surface. In most cases, the data obtained do not appear to be comparable to the analytical results presented by Gessner (2) due to severe erosion which occurs at the nozzle throat. However, these tests substantiate the belief that the self-cooling mechanism provides an inherent form of thermal protection.

III. THE ANALYSIS

A. Introduction and Theoretical Model

A detailed theoretical model and analysis are developed to describe the self-cooling process in infiltrated composites. The general model considered is similar to that assumed by Gessner (2) in that a porous matrix infiltrated with a coolant of a somewhat lower melting temperature, initially at a uniform temperature, is suddenly subjected to a strong convective heat input at the exposed surface. The composite is considered as an infinite flat plate of finite thickness. The remaining surface, or back face, is considered as thermally insulated. To show the effect of the liquid infiltrant on the overall self-cooling process, particular emphasis is given to the phase change from solid to liquid, and the resulting liquid layer which expands onto the exposed surface. Also, an extensive search was conducted to determine the dependence of the thermophysical properties upon temperature.

The process is divided into five time periods for purposes of analysis, similar to those suggested by Ungar and Touryan (3). Briefly, these time periods are as follows:

Time Period I: Once convective heating at the exposed surface has begun, the composite will undergo an initial heat-up period prior to any phase change. The temperature of the exposed surface approaches the melting temperature of the coolant.

Time Period II: When the melting temperature of the coolant is attained at the exposed surface, the coolant begins to melt. The expansion of the coolant due to phase change forces liquid coolant onto the surface. The interface between the solid and liquid coolant continues to recede through the matrix, sustaining the flow of liquid onto the surface. The evaporation of coolant from the surface will be neglected until the vaporization temperature of the coolant is attained at the surface. Therefore, the melt layer continues to grow until vaporization occurs.

Time Period III. A flow of vapor begins from the surface of the melt layer once the vaporization temperature is attained. Initially this effect will tend to reduce the rate of build-up of the liquid layer. The mass rate of flow of vapor will continue to increase until it becomes greater than the flow of liquid onto the surface and the thickness of the layer will diminish. Figure 1 shows the model during time periods II and III.

Time Period IV: As the flow of vapor continues, the vapor-liquid interface will recede throughout the matrix, having a transpiration effect on the convective heating at the exposed surface (Figure 2). The vapor-liquid interface recedes to the back face of the matrix at which time all coolant is exhausted.

Time Period V: In the final period of interest, heating continues in the base tungsten matrix, until the melting temperature

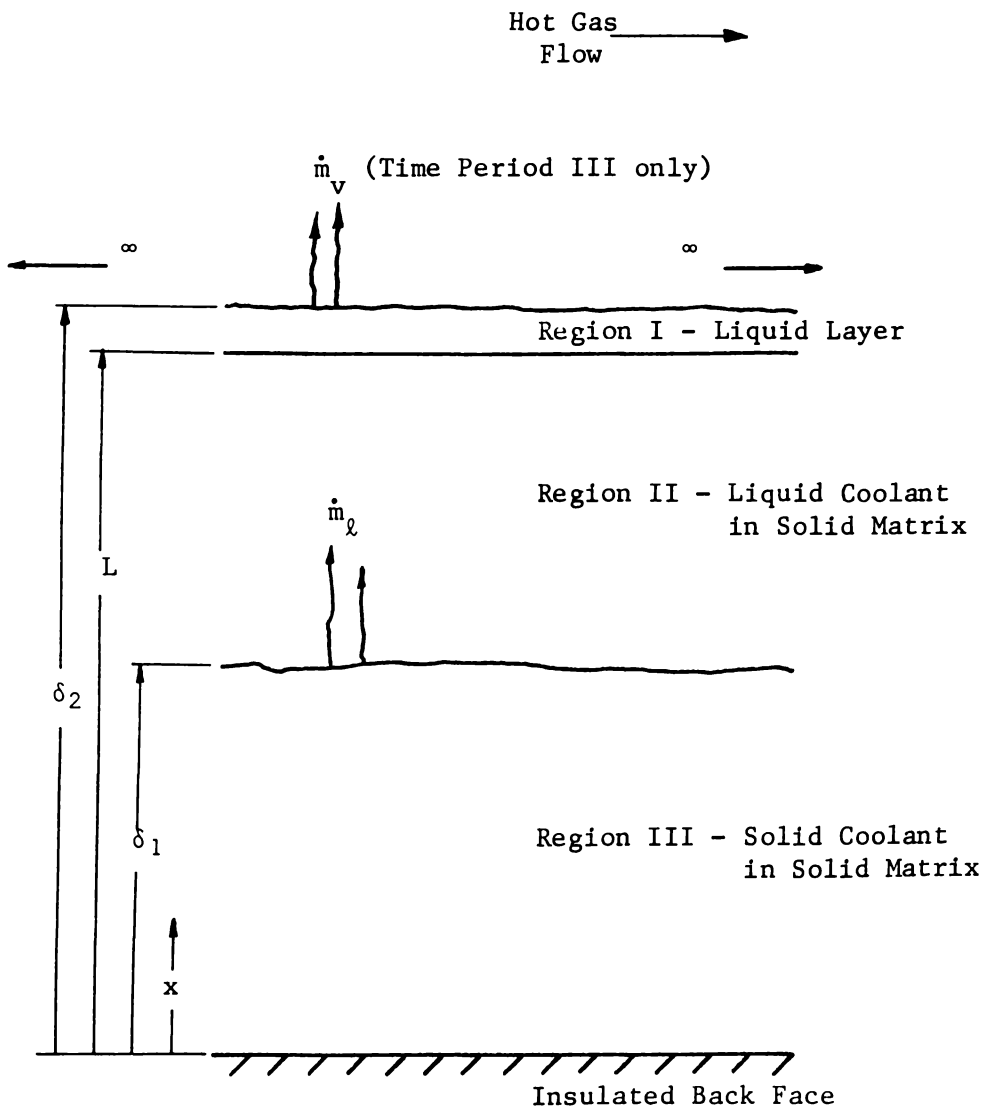

Figure 1: Theoretical Model, Time Periods II and III

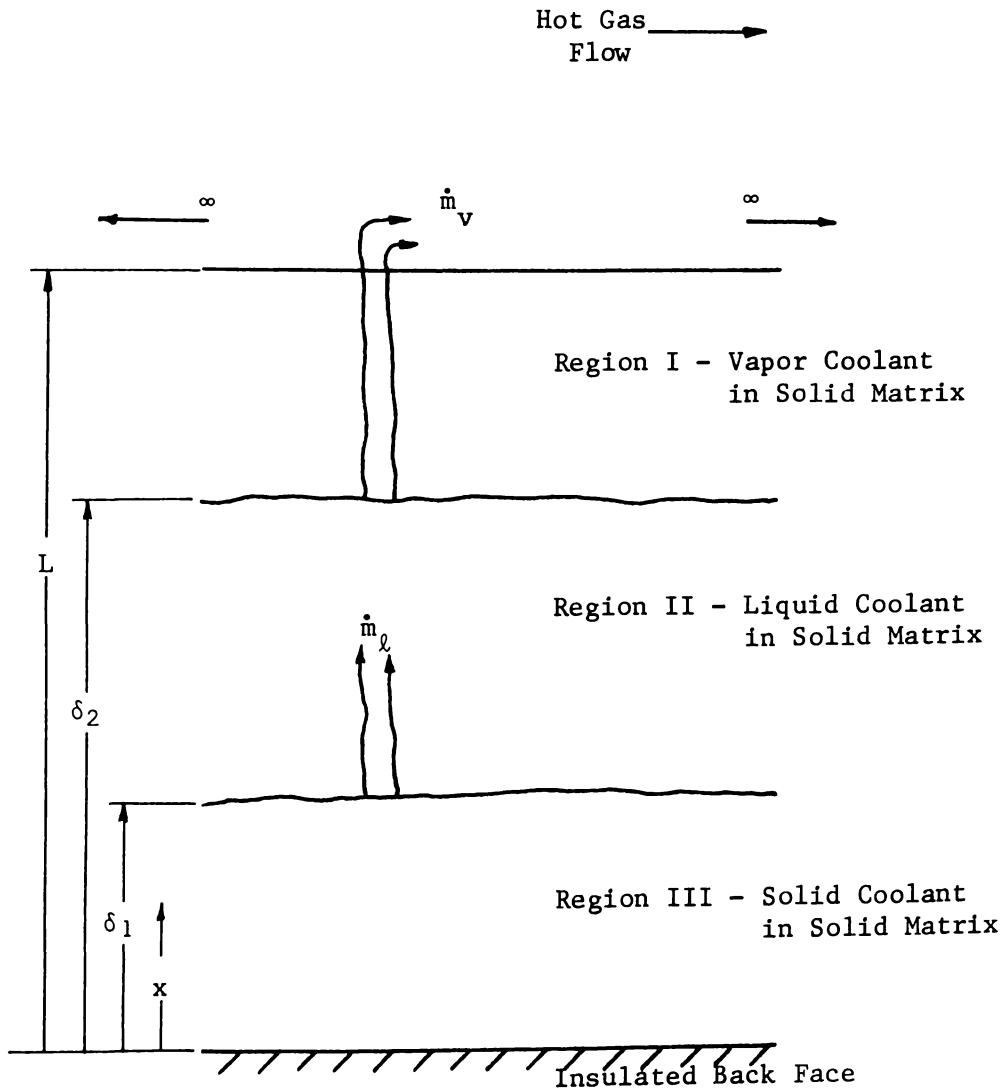

Figure 2: Theoretical Model, Time Period IV

of the tungsten at the exposed surface is exceeded. It is possible that the melting temperature of the tungsten will be exceeded before time period V even begins. This time will be considered as the critical time and the analysis is complete.

The major cooling mechanisms employed in the analysis are the heats absorbed on the phase change at the liquid-solid and vapor-liquid interfaces. Other mechanisms include: convective cooling as the gaseous and/or liquid coolant flows through the porous structure, reduction of the convective heating at the exposed surface by mass addition, and the insulating effect of the melt layer above the exposed surface.

Several simplifying assumptions are made. Equal matrix and coolant temperatures at any given depth in the porous matrix are assumed. This has been substantiated by Weinbaum and Wheeler (10) in their analysis of heat transfer in sweat-cooled metals. In addition, heat conducted through the coolant in the vapor phase is assumed negligible as compared to that conducted through the matrix. Due to the complexity of the problem, erosion at the exposed surface and diffusion or chemical reaction between coolant vapor and hot-gas are neglected. Also, radiation from the hot gas to the heated surface is assumed negligible compared to the convective heating.

B. Detailed Theoretical Analysis

A detailed theoretical analysis is developed for the various time periods described in Section A of this chapter.

1. Time Period I $(0 \leq \theta \leq \theta_1)$

Since the temperature difference between the matrix and the coolant is assumed negligible, it is convenient to define an apparent thermal conductivity for the matrix and solid coolant composite,

$$k_{ms} = k_m (1-P) + k_{cs} P \tag{3.1}$$

and heat capacity per unit volume as,

$$(\rho c)_{ms} = \rho_m c_m (1-P) + \rho_{cs} c_{cs} P \tag{3.2}$$

which will be assigned locally to the composite. After heating has begun but before the surface temperature has reached the melting temperature of the infiltrant, an energy balance on any internal element can be written as:

$$\frac{\partial}{\partial x}\left[k_{ms}\frac{\partial T}{\partial x}\right] = (\rho c)_{ms}\frac{\partial T}{\partial \theta} \tag{3.3}$$

The corresponding initial condition and boundary conditions are as follows:

$$\text{When } \theta = 0,\ T = T_{xi} \tag{3.3a}$$

$$\text{at } x = L,\ k_{ms}\frac{\partial T}{\partial x} = h_o(T_o - T) \tag{3.3b}$$

$$\text{at } x = 0,\ \frac{\partial T}{\partial x} = 0 \tag{3.3c}$$

Solutions to the above equation, with constant properties, are presented in the form of charts in most heat transfer texts (for example, 11). Since these charts assume constant thermal properties, they are not applicable to this analysis and can

be used only as an approximate check to the solution obtained.

2. Time Period II ($\theta_1 < \theta \leq \theta_2$)

After melting of the infiltrant at the surface begins, there exists a time period during which a liquid layer grows onto the surface due to expansion of the coolant upon melting. The various regions that may exist are shown in Figure 1. Whenever the liquid layer exists on the surface, there are three regions in which a heat balance must be written. The first region is the liquid layer itself. The heat balance can be written as follows:

Region I - ($L \leq x \leq \delta_2$)

$$\frac{\partial}{\partial x}\left[k_{c\ell}\frac{\partial T}{\partial x}\right] - \dot{m}_{\ell}\frac{\partial}{\partial x}c_{c\ell}T = \rho_{c\ell}c_{c\ell}\frac{\partial T}{\partial \theta} \tag{3.4}$$

Where initially the temperature distribution is that determined from time period I at $\theta = \theta_1$, and the boundary conditions are:

$$\text{at } x = \delta_2,\ k_{c\ell}\frac{\partial T}{\partial x} = h_o(T_o - T) \tag{3.4a}$$

$$\text{where } T < T_v(P_o)$$

$$\text{at } x = L,\ k_{c\ell}\frac{\partial T}{\partial x}\bigg|_I = k_{m\ell}\frac{\partial T}{\partial x}\bigg|_{II} \tag{3.4b}$$

Where again an apparent conductivity of the matrix and liquid coolant is written as,

$$k_{m\ell} = k_m(1-P) + k_{c\ell}P \tag{3.4c}$$

It is seen that the solution for this region is dependent on the temperature gradients in region II and the mass flow rate of the liquid coolant. An energy balance at the melting interface yields the following expression for mass flow rate of liquid infiltrant per unit area:

$$\dot{m}_{\ell} = \frac{\rho_{cs} - \rho_{c\ell}}{\rho_{cs}\lambda_m}\left[k_{m\ell}\frac{\partial T}{\partial x}\bigg|_{II} - k_{ms}\frac{\partial T}{\partial x}\bigg|_{III}\right] \tag{3.5}$$

Thus region I is also dependent on the temperature gradient in region III and therefore all regions must be solved simultaneously. The mass flow rate of liquid may also be written as:

$$\dot{m}_{\ell} = (\rho_{c\ell} - \rho_{cs})P\frac{d\delta_1}{d\theta} \tag{3.6}$$

so that the recession rate of the melting interface may be determined from:

$$\frac{d\delta_1}{d\theta} = \frac{\dot{m}_{\ell}}{(\rho_{c\ell} - \rho_{cs})P} \tag{3.7}$$

subject to the conditions

$$\text{at } x = \delta_1,\ T = T_m \tag{3.7a}$$

when $\theta = \theta_1$, $\delta_1 = L$ (3.7b)

The growth rate of the liquid layer on the surface may also be determined from the mass flow rate of the liquid onto the surface. This can be written as:

$$\dot{m}_\ell = \rho_{c\ell} \frac{d\delta_2}{d\theta} \tag{3.8}$$

or,

$$\frac{d\delta_2}{d\theta} = \frac{\dot{m}_\ell}{\rho_{c\ell}} \tag{3.9}$$

In making this analysis, it is assumed that thermal expansion is negligible except during a phase change. A detailed development of the mass flow rate expressions are contained in Section C of the finite-difference analysis.

Region II - $(\delta_1 \leq x < L)$

For the region where there exists liquid coolant in a solid matrix a heat balance may be written as follows:

$$\frac{\partial}{\partial x}\left[k_{m\ell}\frac{\partial T}{\partial x}\right] - \dot{m}_\ell \frac{\partial}{\partial x} c_{c\ell} T = (\rho c)_{m\ell}\frac{\partial T}{\partial \theta} \tag{3.10}$$

where initially the temperature distribution is that determined from time period I at $\theta = \theta_1$, and the boundary condition is:

$$\text{at } x = \delta_1,\ k_{m\ell}\frac{\partial T}{\partial x}\bigg|_{II} - k_{ms}\frac{\partial T}{\partial x}\bigg|_{III} = \frac{\dot{m}_\ell \rho_{cs} \lambda_m}{(\rho_{cs}-\rho_{c\ell})} \qquad (3.10a)$$

Region III - $(0 \leq x < \delta_1)$

In region III, there exists solid coolant within the matrix so that the differential equation will be the same as that presented in time period I. The initial condition is again the temperature distribution from time period I at $\theta = \theta_1$ and the boundary condition at $x = 0$ remains:

$$\text{when } x = 0,\ \frac{\partial T}{\partial x} = 0 \qquad (3.11)$$

It should be noted that the existence of region III is dependent on the location of the liquid-solid interface (δ_1). If $\delta_1 \leq 0$, region III does not exist and the boundary condition (3.10a) for region II becomes:

$$\text{when } x = \delta_1 = 0,\ \frac{\partial T}{\partial x} = 0 \qquad (3.12)$$

Also, it is understood that once the melting interface recedes to the back face of the matrix the formation of liquid coolant no longer takes place.

3. Time Period III $(\theta_2 < \theta \leq \theta_3)$

The temperature of the liquid at the surface of the liquid layer exposed to hot-gas flow will continue to rise until its vaporization temperature corresponding to the free-stream pressure is attained. The vaporization temperature can be expressed in terms of vapor pressure by the general equation:

$$T_v = \frac{B}{A - \log P_v} \tag{3.13}$$

Once vaporization begins, the heat associated with this change of phase is absorbed at the surface of the layer. The effect of vaporization temperature on the latent heat of vaporization will be computed from Watson's equation as presented in reference (12).

$$\lambda_v = \lambda_{nb} \left[\frac{T_c - T_v}{T_c - T_{nb}} \right]^{0.38} \tag{3.14}$$

To use this equation, it is required that λ_{nb}, the latent heat at the normal boiling point, T_{nb}, be known. The latent heat at all other reduced temperatures can then be computed from equation (3.14), if the critical temperature of the coolant, T_c, is available.

The rate of formation of vapor per unit area may be calculated from an energy balance at the surface of the liquid layer as:

$$\bar{m}_v = \frac{1}{\lambda_v} \left[h_o(T_o - T_v) - k_{c\ell} \frac{\partial T}{\partial x} \bigg|_I \right] \tag{3.15}$$

Assuming all vapor formed leaves the surface,

$$\dot{m}_v = \bar{m}_v \tag{3.15a}$$

The regions that may exist for this time period correspond to those defined in time period II. The mass flow rate of vapor leaving the liquid layer will tend to reduce the growth rate of the liquid layer

until eventually the mass flow rate of vapor exceeds the mass flow rate of liquid onto the surface. At that time the thickness of the liquid layer will begin to recede toward the original surface. Equation (3.9) can now be rewritten to give the recession rate of the liquid-vapor interface as:

$$\frac{d\delta_2}{d\theta} = \frac{\dot{m}_\ell - \dot{m}_v}{\rho_{c\ell}} \tag{3.16}$$

The differential equation describing the liquid layer remains:

$$\frac{\partial}{\partial x}\left[k_{c\ell}\frac{\partial T}{\partial x}\right] - \dot{m}_\ell \frac{\partial}{\partial x} c_{c\ell} T = \rho_{c\ell} c_{c\ell} \frac{\partial T}{\partial \theta} \tag{3.17}$$

with boundary conditions:

$$\text{at } x = \delta_2,\ h_o(T_o - T_v) - k_{c\ell}\frac{\partial T}{\partial x}\bigg|_I = \bar{m}_v \lambda_v \tag{3.17a}$$

$$\text{at } x = L,\ k_{c\ell}\frac{\partial T}{\partial x}\bigg|_I = k_{m\ell}\frac{\partial T}{\partial x}\bigg|_{II} \tag{3.17b}$$

and with the initial condition that the temperature profile at $\theta = \theta_2$ is known from time period II.

The regions below the original surface for time period III will remain the same as in time period II. It is essential to note that during the periods in which there exists a liquid layer above the surface, the underlying structure remains at a temperature

less than the coolant vaporization temperature at free-stream pressure.

4. Time Period IV ($\theta_3 < \theta \leq \theta_4$)

After the liquid layer recedes to the original surface ($\theta = \theta_3$) the coolant will begin to vaporize from within the matrix. The various regions that may exist are shown in Figure 2.

Region I - ($\delta_2 \leq x \leq L$)

When the vapor-liquid interface has receded below the original surface the heat balance for region I is as follows, assuming that the thermal conductivity and heat capacity of the vapor are negligible in comparison to those of the matrix,

$$\frac{\partial}{\partial x}\left[k_m(1-P)\frac{\partial T}{\partial x}\right] - \dot{m}_v \frac{\partial}{\partial x} c_{cv} T = \rho_m c_m (1-P)\frac{\partial T}{\partial \theta} \qquad (3.18)$$

where initially the temperature distribution is that determined from time period III at $\theta = \theta_3$, and the boundary conditions are:

$$\text{at } x = L, \quad k_m(1-P)\frac{\partial T}{\partial x} = h_o(T_o - T) \qquad (3.18a)$$

$$\text{at } x = \delta_2, \quad k_m(1-P)\frac{\partial T}{\partial x}\bigg|_I - k_{m\ell}\frac{\partial T}{\partial x}\bigg|_{II} = \bar{m}_v \lambda_v \qquad (3.18b)$$

In the above equations, h_o is the convective heat-transfer coefficient at the original surface. The effect of mass addition to the boundary layer is neglected on the basis of data presented by Gessner et al. (2) as previously discussed.

The mass flow rate of the coolant in vapor form through the porous matrix will be reduced due to a pressure drop between the interface and original surface. As suggested by Greenberg and Weger (13) and Green and Duwez (14), most experimental results for one-dimensional flow through porous materials may be correlated by an equation of the type:

$$-\frac{dp}{dx} = \alpha\mu V + \beta\rho V^n \tag{3.19}$$

where α and β are constants, n is an exponent between 1.0 and 2.0 and V is the velocity of the fluid. The constants α and β, defined respectively as the viscous and inertial coefficients, characterize the porous structure and are independent of the physical properties of the fluid. The viscous coefficient is the inverse of the permeability coefficient defined by Darcy's Law. The first term on the right-hand side of equation (3.19) represents the portion of the pressure gradient due to friction, while the second term represents the inertial effects. The inertial coefficient is thought to account for the irregularity of the flow passages and the contraction and expansion of the fluid rapidly changing direction in the flow path. Letting

$$\dot{m}_v = \rho_{cv} V \tag{3.20}$$

and using the perfect-gas law, equation (3.19) can be written as:

$$\frac{P_2^2 - P_1^2}{\Delta x} = \frac{2\alpha\mu R_u T \dot{m}_v}{g_c M} + \frac{2\beta R_u T \dot{m}_v^2}{g_c M} \qquad (3.21)$$

Gessner, et al. (2) suggest that to account for the non-isothermal flow of the coolant vapor to the surface equation (3.21) can be used to calculate the interface pressure by writing:

$$P_v = \left[P_o^2 + \frac{2\dot{m}_v R_u}{g_c M} (\alpha\mu + \beta\dot{m}_v) \int_{\delta_2}^{L} T dx\right]^{1/2} \qquad (3.22)$$

The dependence of α and β on temperature and pressure have also been studied (2). It is concluded that β is independent of temperature and pressure over the ranges anticipated in this analysis. Although α is independent of pressure, its dependency on temperature is significant, but at present its dependency has not been substantiated and will not be included in this analysis. It is also noted that the viscous and inertial coefficients are also independent of matrix porosity (2).

The coolant-vapor viscosity variation with temperature is calculated from the relation presented by Gambill (15, equation 15) with units modified:

$$\mu = \frac{(MT_{nb})^{1/2}}{V_{nb}^{2/3}} \left[\frac{0.0742\ (T/T_{nb})^{0.645} - 0.0249}{(1.18T/T_{nb})^{0.9 \log (1.18T/T_{nb})}}\right] \qquad (3.23)$$

where V_{nb} is the molar gas volume at the normal boiling point. Applying the perfect-gas law, the molar gas volume at the normal boiling point becomes:

$$V_{nb} = \frac{R_u T_{nb}}{P_{nb}} \tag{3.24}$$

or,

$$V_{nb} = 0.73\ T_{nb} \tag{3.25}$$

Substituting equation (3.25) into (3.23) the viscosity expression becomes:

$$\mu = \frac{M^{1/2}}{T_{nb}^{1/6}} \left[\frac{0.0915\ (T/T_{nb})^{0.645} - 0.0307}{(1.18\ T/T_{nb})^{0.9 \log (1.18\ T/T_{nb})}} \right] \tag{3.26}$$

The temperature at the vaporization interface may now be determined from the vapor pressure-temperature relationship (3.13). Also the latent heat of vaporization will be available from Watson's equation (3.14). The mass flow rate of coolant vapor per unit surface area is then determined from an energy balance at the vapor-liquid interface,

$$\dot{m}_v = \frac{\rho_{c\ell} - \rho_{cv}}{\rho_{c\ell} \lambda_v} \left[k_m (1-P) \frac{\partial T}{\partial x} \bigg|_I - k_{m\ell} \frac{\partial T}{\partial x} \bigg|_{II} \right] \tag{3.27}$$

and the location of the vapor-liquid interface from a mass balance,

$$\frac{d\delta_2}{d\theta} = \frac{\dot{m}_v - \dot{m}_\ell}{P(\rho_{cv}-\rho_{c\ell})} \tag{3.28}$$

It is again evident that the solutions to the above equations are not only dependent on each other but also on those of the other regions that exist during this time period.

The analysis of regions below the vapor-liquid interface is the same as presented previously in time period II. The existance of region III will cease during this time period, as must that of region II, since this time period is defined to include the vaporization of all coolant. When the vapor-liquid interface recedes to the insulated surface, the coolant will be depleted. This will conclude time period IV.

5. Time Period V ($\theta_4 < \theta \leq \theta_{crit}$)

After all coolant is exhausted only one region will exist--that of a porous matrix. The differential equation can be written as:

$$\frac{\partial}{\partial x}\left[k_m(1-P)\frac{\partial T}{\partial x}\right] = \rho_m c_m (1-P)\frac{\partial T}{\partial \theta} \tag{3.29}$$

with as initial condition the resulting temperature distribution from the preceeding time period, and the boundary conditions; at the exposed surface,

$$k_m(1-P)\frac{\partial T}{\partial x} = h_o(T_o - T) \qquad (3.29a)$$

and at the insulated back face,

$$\frac{\partial T}{\partial x} = 0 \qquad (3.29b)$$

This equation will be employed until the temperature at the matrix surface (x = L) is equal to the melting temperature of the matrix. This time will be considered the critical time and the analysis complete.

C. Methods of Solution

As previously mentioned, the solution of the differential equation applicable to time period I is presented in most elementary heat-transfer texts for the case of constant thermal properties. Unfortunately, a closed-form solution to equation (3.3) is not as readily obtainable, due to difficulties arising in the separation of variables technique of solution.

At the instant melting occurs at the original surface, a difficulty arises in specifying the boundary conditions in addition to the complication of the dependency of the thermal properties on temperature. The coolant mass flow rate, the growth rate of liquid layer above the surface, and the recession rate of the liquid-solid interface are not prescribed functions but are interdependent. Therefore, the boundary conditions at the original

surface and the interface are not uniquely specified. Furthermore, the various regions that exist at any instant of time are coupled at the interface and cannot be solved independently. Similar difficulties exist at the vapor-liquid interface, with the added complication of the dependence of the vaporization temperature on pressure.

Due to the above complications, a closed-form solution does not seem feasible at this time. When closed-form solutions are not possible, the approach often used for transient conduction problems is a finite-difference solution similar to that discussed by Dusinberre (16). A finite-difference analysis will be used to evaluate the temperature distributions within the composite, and the surface temperature variation, interface locations, and mass flow rates of the coolant with time.

IV. THE FINITE-DIFFERENCE ANALYSIS

A. The Finite-Difference Model and General Equations

The finite-difference approximations to the theoretical models presented in Chapter III are shown in Figures 3 and 4. The composite is divided into n-1 equal elements of height Δx and unit area, yielding n nodal points. The nodal points are counted as: 1, located at the thermally insulated back face, through n, on the original surface.

It is convenient to first derive an explicit finite-difference equation for a general internal nodal point, i, which will be used for several regions throughout the entire heating period by selectively substituting the proper conditions at the time of application. This equation will be used to evaluate the temperatures of the internal elements, excluding boundary elements and those elements adjacent to interfaces, for all regions throughout the entire heating period. The differential equation for an internal element, in its most general form, can be written as:

$$\frac{\partial}{\partial x}\left[k_{mc}\frac{\partial T_i}{\partial x}\right] - \dot{m}_c\frac{\partial}{\partial x}(c_c T_i) = (\rho c)_{mc}\frac{\partial T_i}{\partial \theta} \qquad (4.1)$$

In order to derive an explicit finite-difference equation as an approximation to equation (4.1), consider a heat balance on a finite-difference element as shown in Figure 5. The term explicit is used to denote that the temperature of the element after one

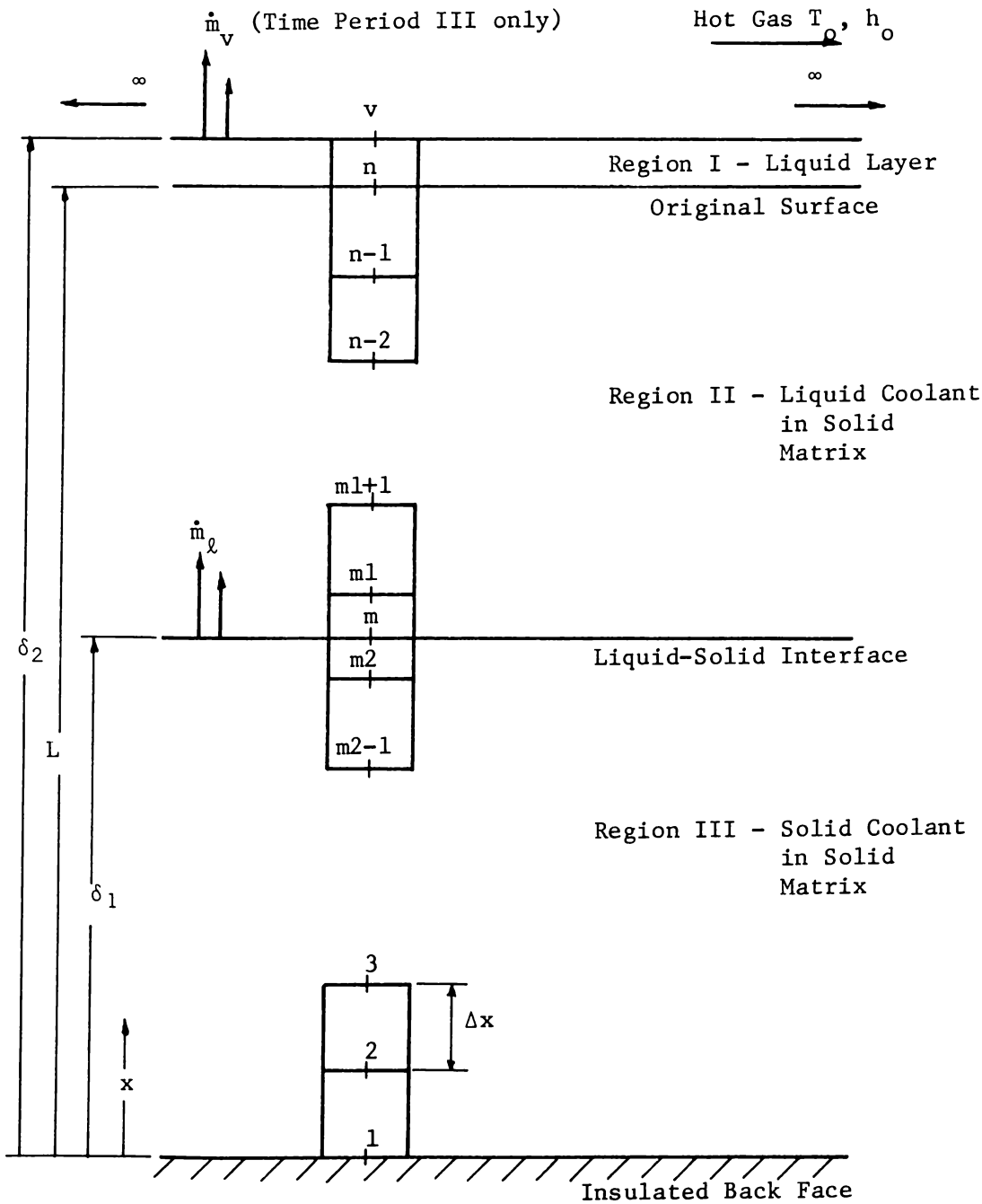

Figure 3: Finite-Difference Model, Time Periods II and III

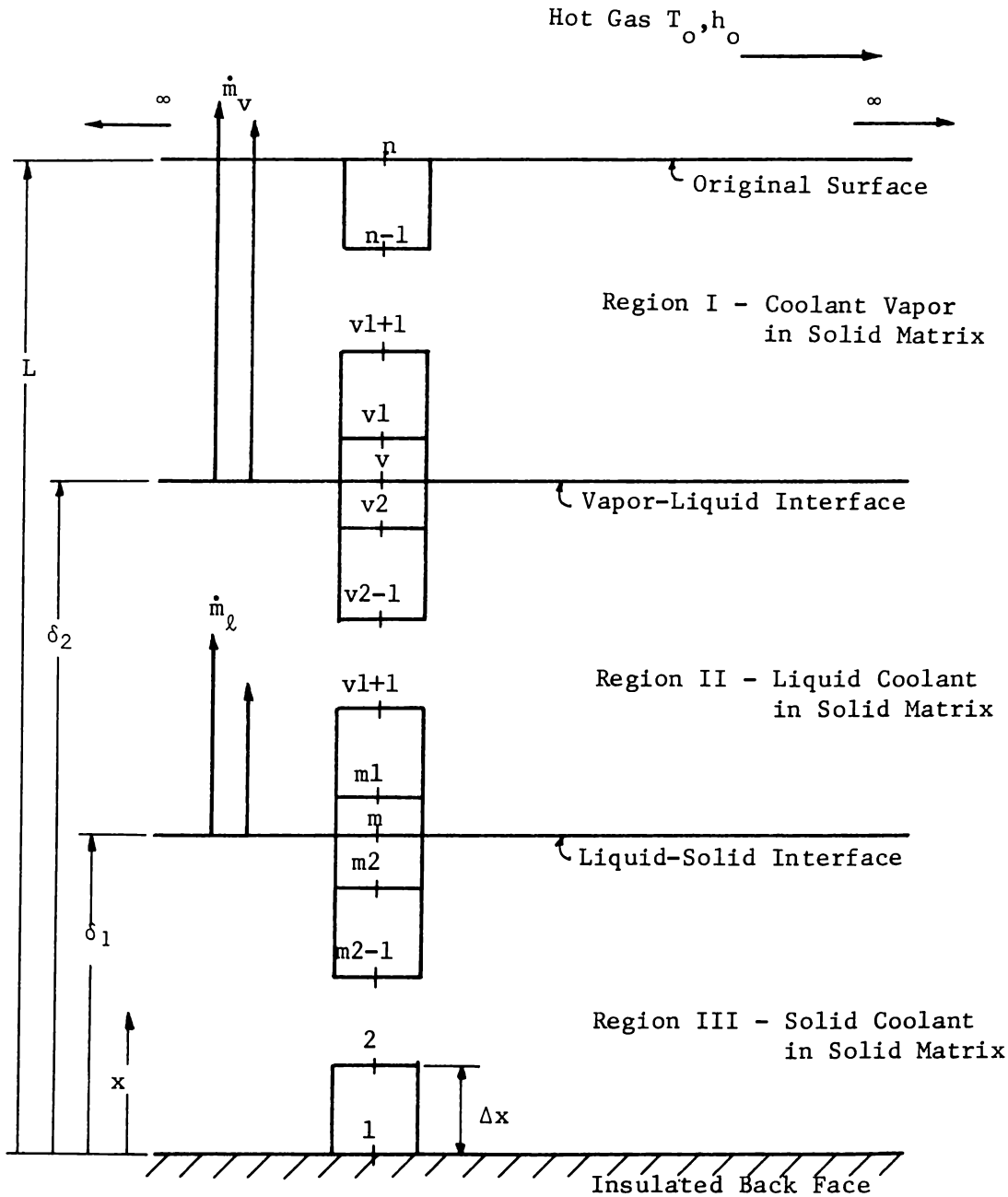

Figure 4: Finite-Difference Model, Time Period IV

time increment (T_i' at $\theta + \Delta\theta$) is evaluated from the temperatures of adjacent nodal points (T_{i+1} and T_{i-1}) at time θ. Later on the term implicit is used to denote that the temperature of the element after one time increment (T_i' at $\theta + \Delta\theta$) is evaluated from the temperature of the adjacent nodal points (T_{i+1}' and T_{i-1}') at time $\theta + \Delta\theta$.

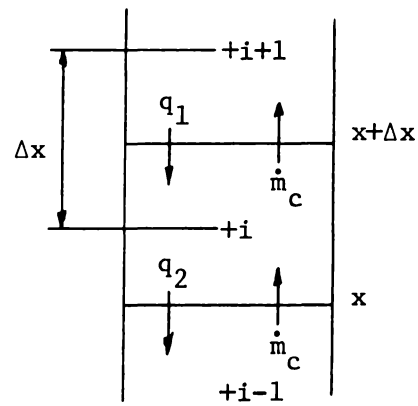

Figure 5

A General Internal Finite-Difference Element

An energy balance on the element shown in Figure 5 yields,

$$q_1 - q_2 + \dot{m}_c c_{cx} T_x - \dot{m}_c c_{cx+\Delta x} T_{x+\Delta x} = (\rho c)_{mc} \frac{\partial T}{\partial \theta} \Delta x \qquad (4.2)$$

or, using finite-difference approximations:

$$k_{mc} \left(\frac{T_i + T_{i+1}}{2} \right) \frac{T_{i+1} - T_i}{\Delta x} - k_{mc} \left(\frac{T_i + T_{i-1}}{2} \right) \frac{T_i - T_{i-1}}{\Delta x}$$

$$+ \dot{m}_c \left[c_c \left(\frac{T_i + T_{i-1}}{2} \right) \frac{T_i + T_{i-1}}{2} - c_c \left(\frac{T_i + T_{i+1}}{2} \right) \frac{T_i + T_{i+1}}{2} \right]$$

$$= (\rho c)_{mc} (T_i) \frac{T_i' - T_i}{\Delta\theta} \Delta x \qquad (4.3)$$

Throughout the finite-difference analysis, the temperature enclosed in parentheses following a thermal property will indicate the temperature at which that property is to be evaluated. Solving equation (4.3) for T_i' yields:

$$T_i' = T_i + \frac{\Delta\theta}{(\rho c)_{mc}(T_i)}\left[k_{mc}\left(\frac{T_i+T_{i-1}}{2}\right)\frac{T_{i-1}-T_i}{\Delta x^2}\right.$$

$$+ k_{mc}\left(\frac{T_i+T_{i+1}}{2}\right)\left.\frac{T_{i+1}-T_i}{\Delta x^2}\right] + \frac{\dot{m}_c\Delta\theta}{(\rho c)_{mc}(T_i)\Delta x}\left[c_c\left(\frac{T_i+T_{i-1}}{2}\right)\frac{T_i+T_{i-1}}{2}\right.$$

$$\left. - c_c\left(\frac{T_i+T_{i+1}}{2}\right)\frac{T_i+T_{i+1}}{2}\right] \qquad (4.4)$$

The above equation is then the general equation for a region consisting of solid, liquid, or gaseous coolant in a solid matrix. The thermal properties and the mass flow rate of the coolant must be suitably selected. For explicit equations such as equation (4.4), there is a certain criterion which must be satisfied to assure stability of the calculated temperature values. This is accomplished by reducing the time increment sufficiently for a given nodal spacing so that the coefficient of the unprimed temperature is positive. For equation (4.4) the coefficient is:

$$1 - \frac{\Delta\theta}{\Delta x^2(\rho c)_{mc}(T_i)}\left[k_{mc}\left(\frac{T_i+T_{i-1}}{2}\right) + k_{mc}\left(\frac{T_i+T_{i+1}}{2}\right)\right]$$

$$+ \frac{\dot{m}_c\Delta\theta}{2(\rho c)_{mc}(T_i)\Delta x}\left[c_c\left(\frac{T_i+T_{i-1}}{2}\right) - c_c\left(\frac{T_i+T_{i+1}}{2}\right)\right] \qquad (4.4a)$$

and the required stability becomes:

$$\Delta\theta \leq 1 \Bigg/ \left\{ \frac{1}{\Delta x^2 (\rho c)_{mc}(T_i)} \left[k_{mc}\left(\frac{T_i+T_{i-1}}{2}\right) + k_{mc}\left(\frac{T_i+T_{i+1}}{2}\right)\right] \right. \tag{4.4b}$$

$$\left. - \frac{\dot{m}_c}{2\Delta x(\rho c)_{mc}(T_i)} \left[c_c\left(\frac{T_i+T_{i-1}}{2}\right) - c_c\left(\frac{T_i+T_{i+1}}{2}\right)\right]\right\}$$

Equation (4.4) may also be modified to apply at the insulated back face. If $i = 1$, $T_{i-1} = T_{i+1}$, and $\dot{m}_c = 0$ for the back face element of height $\Delta x/2$ equation (4.4) is written as:

$$T_1' = T_1 + \frac{2\Delta\theta}{(\rho c)_{mc}(T_1)} \; k_{mc}\left(\frac{T_1+T_2}{2}\right) \; \frac{T_2-T_1}{\Delta x^2} \tag{4.5}$$

It is also possible to derive a general implicit equation for the nodal point at the original surface under normal conditions; that is, when a liquid layer does not exist above the surface and all interfaces, if they exist, have receded below nodal point n-1. The differential equation is:

$$\frac{\partial}{\partial x}\left[k_{mc}(T_n')\frac{\partial T_n'}{\partial x}\right] - \dot{m}_c \frac{\partial}{\partial x}\left[c_c(T_n')T_n'\right] = (\rho c)_{mc}(T_n')\frac{\partial T_n'}{\partial \theta} \tag{4.6}$$

or, expanding:

$$k_{mc}(T_n')\frac{\partial^2 T_n'}{\partial x^2} + \left[\frac{\partial k_{mc}(T_n')}{\partial x} - \dot{m}_c c_c(T_n')\right]\frac{\partial T_n'}{\partial x}$$

$$- \dot{m}_c T_n' \frac{\partial c_c(T_n')}{\partial x} = (\rho c)_{mc}(T_n')\frac{\partial T_n'}{\partial \theta} \tag{4.7}$$

At the exposed surface, we may also write that the convective heat input to the surface is equal to the heat conducted into the composite:

$$h_o(T_o - T_n') = k_{mc}(T_n') \frac{\partial T_n'}{\partial x} \tag{4.8}$$

or,

$$\frac{\partial T_n'}{\partial x} = \frac{h_o(T_o - T_n')}{k_{mc}(T_n')} \tag{4.9}$$

Writing the Taylor-series expansions, neglecting third-order and higher derivatives for the temperature at the surface yields:

$$T_{n-1}' = T_n' - \Delta x \frac{\partial T_n'}{\partial x} + \frac{\Delta x^2}{2} \frac{\partial^2 T_n'}{\partial x^2} \tag{4.10}$$

or,

$$\frac{\partial^2 T_n'}{\partial x^2} = \frac{2(T_{n-1}' - T_n')}{\Delta x^2} + \frac{2}{\Delta x} \frac{\partial T_n'}{\partial x} \tag{4.11}$$

and,

$$T_n = T_n' - \Delta\theta \frac{\partial T_n'}{\partial \theta} \tag{4.12}$$

or,

$$\frac{\partial T_n'}{\partial \theta} = \frac{T_n' - T_n}{\Delta\theta} \tag{4.13}$$

Also for the thermal properties:

$$k_{mc}(T_n'-1) = k_{mc}(T_n') - \Delta x \frac{\partial k_{mc}(T_n')}{\partial x} \tag{4.14}$$

or,

$$\frac{\partial k_{mc}(T_n')}{\partial x} = \frac{k_{mc}(T_n') - k_{mc}(T_n'-1)}{\Delta x} \tag{4.15}$$

and similarly:

$$\frac{\partial c_c(T_n')}{\partial x} = \frac{c_c(T_n') - c_c(T_n'-1)}{\Delta x} \tag{4.16}$$

Substituting equations (4.9), (4.11), (4.13), (4.15), and (4.16) into equation (4.7) and solving for the temperature of the surface gives:

$$T_n' = \left\{ \frac{(\rho c)_{mc}(T_n')}{\Delta\theta} T_n + 2 \frac{k_{mc}(T_n')}{\Delta x^2} T_n'-1 + \frac{h_o T_o}{k_{mc}(T_n')} \left[\frac{3k_{mc}(T_n') - k_{mc}(T_n'-1)}{\Delta x} - \dot{m}_c c_c(T_n') \right] \right\} \Bigg/ \left\{ \frac{(\rho c)_{mc}(T_n')}{\Delta\theta} + 2\frac{k_{mc}(T_n')}{\Delta x^2} + \frac{h_o}{k_{mc}(T_n')} \left[\frac{3k_{mc}(T_n') - k_{mc}(T_n'-1)}{\Delta x} - \dot{m}_c c_c(T_n') \right] \right\} \tag{4.17}$$

The above equation is then the general implicit equation applicable at the original surface for the conditions previously discussed. Implicit finite-difference equations require no stability criterion.

B. Time Period I ($0 \leq \theta \leq \theta_1$)

During the initial heating period, the composite consists of solid coolant in the solid matrix. The temperatures of the internal nodal points are given by the general explicit equation (4.4) as follows:

Nodal points 2 through n-1

$$k_{mc} = k_{ms}$$

$$(\rho c)_{mc} = (\rho c)_{ms} \qquad (4.18)$$

$$\dot{m}_c = 0.0$$

The temperature at the insulated back face is determined from explicit equation (4.5):

Nodal point 1

$$k_{mc} = k_{ms}$$

$$(\rho c)_{mc} = (\rho c)_{ms} \qquad (4.19)$$

The general implicit equation for the original surface is applicable at the exposed surface:

Nodal point n

$$k_{mc} = k_{ms}$$

$$(\rho c)_{mc} = (\rho c)_{ms} \qquad (4.20)$$

$$\dot{m}_c = 0.0$$

The time at which the temperature at the exposed surface is the same as the normal melting point of the coolant will be denoted as θ_1 and will terminate time period I.

C. Time Period II ($\theta_1 < \theta \leq \theta_2$)

There may exist three separate and distinct regions during this heating period as indicated in Figure 3. The general explicit equation (4.4) will be used to calculate the temperatures of the interior nodal points for these regions as follows:

Nodal points 2 through m2-1

$$k_{mc} = k_{ms}$$

$$(\rho c)_{mc} = (\rho c)_{ms} \qquad (4.21)$$

$$\dot{m}_c = 0.0$$

Nodal points m1 + 1 through n-1

$$k_{mc} = k_{m\ell}$$

$$(\rho c)_{mc} = (\rho c)_{m\ell} \qquad (4.22)$$

$$\dot{m}_c = \dot{m}_\ell$$

$$c_c = c_{c\ell}$$

The temperature of the back face will again be determined from equation (4.5) with:

Nodal point 1

$$k_{mc} = k_{ms} \qquad (4.23)$$

$$(\rho c)_{mc} = (\rho c)_{ms}$$

At this point, it must be noted that the existence of the region consisting of the solid coolant within a solid matrix depends on the location of the liquid-solid interface and, therefore, the point within the composite where the temperature is equal to the melting temperature of the coolant. Since the temperature gradient

near the insulated back face of the composite is small compared to that nearer the heated surface, it is convenient to let the temperature of the back face be equal to the melting temperature of the coolant when the liquid-solid interface recedes below nodal point 2. At subsequent times, the liquid-solid interface will not exist and the temperature of the back face will be determined from equation(4.5) with:

Nodal point 1

$$k_{mc} = k_{m\ell} \qquad (4.24)$$

$$(\rho c)_{mc} = (\rho c)_{m\ell}$$

Also, at the time when the interface recedes below nodal point 2, the formation of liquid will cease and for subsequent calculations, $\dot{m}_{\ell} = 0$.

The remaining nodal points require a separate analysis due to the heat absorption accompanying melting at the liquid-solid interface and due to the liquid layer above the original surface. It is convenient to develop two equations that apply at different times depending on the location of the liquid-solid interface. First, however, an expression will be developed relating the mass rate of flow of the liquid, the rate of formation of the liquid, and the recession date of the liquid-solid interface.

Consider the element defined by the liquid-solid interface at times θ and $\theta + \Delta\theta$ as shown in Figure 6.

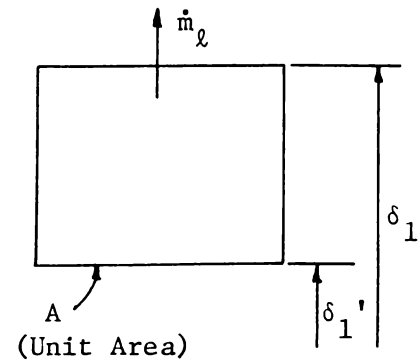

Figure 6

Element Defined by Liquid-Solid Interface

at Times θ and $\theta + \Delta\theta$

The rate of formation of liquid is:

$$\bar{m}_\ell \Delta\theta A = \rho_{cs} PA(\delta_1 - \delta_1') \tag{4.25}$$

or,

$$\bar{m}_\ell = \rho_{cs} P \frac{(\delta_1 - \delta_1')}{\Delta\theta} \tag{4.26}$$

The mass of the coolant at time θ, M_θ, may be written as:

$$M_\theta = \rho_{cs} PA(\delta_1 - \delta_1') \tag{4.27}$$

and at time $\theta + \Delta\theta$:

$$M_{\theta+\Delta\theta} = \rho_{c\ell} PA(\delta_1 - \delta_1') \tag{4.28}$$

Substracting equations (4.28) from (4.27):

$$M_\theta - M_{\theta+\Delta\theta} = \dot{m}_\ell A\Delta\theta = PA(\rho_{cs} - \rho_{c\ell})(\delta_1 - \delta_1') \tag{4.29}$$

so that:

$$\dot{m}_\ell = P(\rho_{cs} - \rho_{c\ell}) \frac{(\delta_1 - \delta_1')}{\Delta\theta} \tag{4.30}$$

Combining equations (4.26) and (4.30), we also obtain the relation between the mass flow rate and the rate of formation of the liquid coolant as:

$$\bar{m}_{\ell} = \frac{\rho_{cs}}{(\rho_{cs}-\rho_{c\ell})} \dot{m}_{\ell} \tag{4.31}$$

1. Liquid-Solid Interface Above Nodal Point n-1

In the development of the equations for the liquid-solid interface recession, first consider the case where the interface lies between the original surface and nodal point n-1. The temperature of nodal points 1 through n-2 are determined explicitly as previously discussed. To develop an implicit finite-difference equation for the location of the liquid-solid interface, consider the following system as shown schematically in Figure 7.

It is assumed that while the liquid-solid interface lies above nodal point n-1, the quantity of liquid that has accumulated above the original surface is negligible and therefore the thickness of the liquid layer above the surface (δ_2 - L) is sufficiently small so that we may let $T_v = T_n$. This allows us to write:

$$q_1 = h_o(T_o - T_n) = k_{m\ell}\left(\frac{T_n - T_m}{L - \delta_1}\right) \tag{4.32}$$

An implicit equation for the heat conducted out of the element (q_2) will be developed for a general case later.

The shaded area of Figure 7 represents the change of internal energy of the element, ΔU, and may be written as:

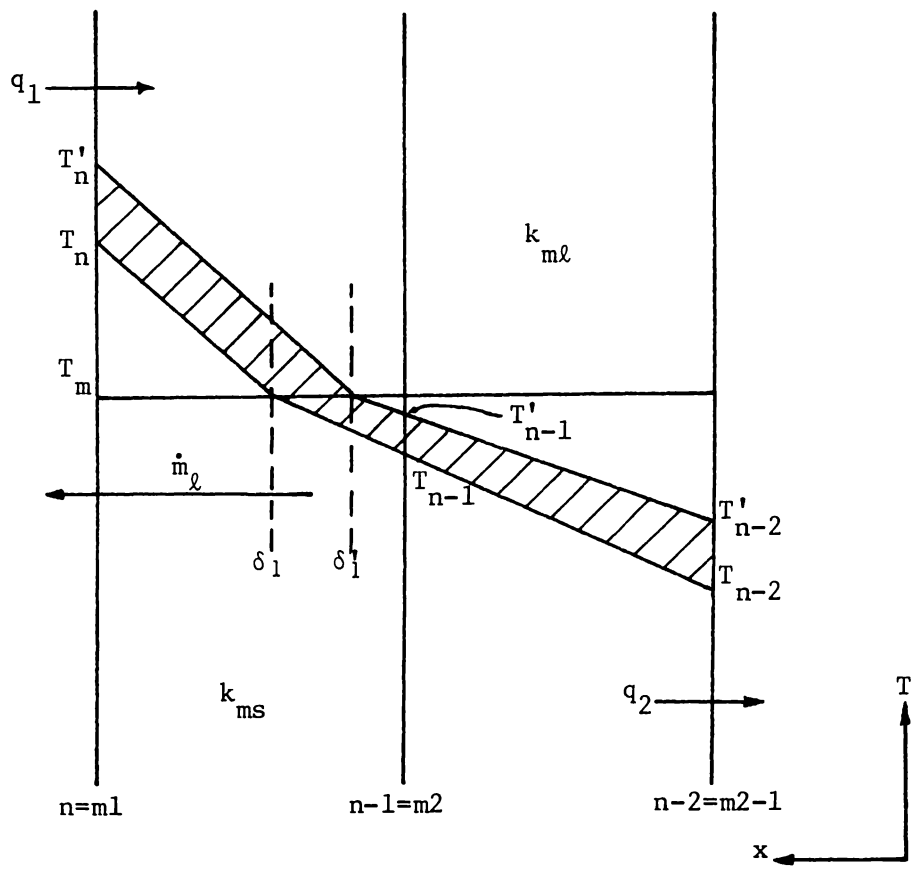

Figure 7: Schematic of Liquid-Solid Interface Above Nodal Point n-1.

$$\Delta U = 1/2(\rho c)_{m\ell}(T_n'-T_n)(L - \delta_1) + 1/2(\rho c)_{m\ell}(\delta_1-\delta_1')(T_n'-T_m)$$
$$+ 1/2(\rho c)_{ms}(T_n'_{-2}-T_{n-2})[\delta_1-(n-3)\Delta x]$$
$$+ 1/2(\rho c)_{ms}(\delta_1-\delta_1')(T_m-T_n'_{-2}) \qquad (4.33)$$

With some algebra equation (4.33) may be rewritten as:

$$2\Delta U = (L - \delta_1')[(\rho c)_{m\ell}(T_n'-T_m) + (\rho c)_{ms}(T_m-T_n'_{-2})]$$
$$- (L - \delta_1)[(\rho c)_{m\ell}(T_n-T_m) + (\rho c)_{ms}(T_m-T_n'_{-2})] \qquad (4.34)$$
$$+ (\rho c)_{ms}(T_n'_{-2}-T_{n-2})[\delta_1-(n-3)\Delta x]$$

An energy balance on the element yields:

$$(q_1 - q_2)\Delta\theta - \Delta U = \bar{m}_{\ell}\lambda_m\Delta\theta \qquad (4.35)$$

and substitution of equations (4.31) and (4.30) into the energy balance:

$$2(q_1-q_2)\Delta\theta - 2\Delta U = 2\rho_{cs}\lambda_m P(L-\delta_1') - 2\rho_{cs}\lambda_m P(L-\delta_1) \qquad (4.36)$$

Substitution of equation (4.34) into (4.36) yields:

$$A_3 - A_2 - (L-\delta_1')\,[(\rho c)_{m\ell}(T_n'-T_m) + A_4] = 0 \qquad (4.37)$$

by defining the following constants:

$$A_2 \equiv (\rho c)_{ms}(T_n'_{-2}-T_{n-2})[\delta_1-(n-3)\Delta x]$$
$$A_3 \equiv 2(q_1-q_2)\Delta\theta + 2\rho_{cs}\lambda_m P(L-\delta_1)$$
$$+ (L-\delta_1)[(\rho c)_{m\ell}(T_n-T_m) + (\rho c)_{ms}(T_m-T_n'_{-2})] \qquad (4.38)$$
$$A_4 \equiv (\rho c)_{ms}(T_m-T_n'_{-2}) + 2\rho_{cs}\lambda_m P$$

Using the same assumption that led to equation (4.32), we may write:

$$h_o(T_o-T_n') = k_{m\ell}\left[\frac{T_n'-T_m}{L-\delta_1'}\right] \qquad (4.39)$$

or solving for T_n',

$$T_n' = \frac{k_{m\ell} T_m + h_o(L-\delta_1')T_o}{k_{m\ell} + h_o(L-\delta_1')} \tag{4.40}$$

Substitution of equation (4.40) reduces (4.37) to a quadratic equation in the unknown $(L - \delta_1')$,

$$h_o[A_4+(\rho c)_{m\ell}(T_o-T_m)](L-\delta_1')^2 - [(A_3-A_2)h_o-A_4k_{m\ell}](L-\delta_1') - (A_3-A_2)k_{m\ell} = 0 \tag{4.41}$$

from which the solution is:

$$(L-\delta_1') = \left\{\left[(A_3-A_2)h_o-A_4k_{m\ell}\right] \pm \sqrt{\left[(A_3-A_2)h_o-A_4k_{m\ell}\right]^2 + 4h_o\left[A_4 + (\rho c)_{m\ell}(T_o-T_m)\right](A_3-A_2)k_{m\ell}}\right\} \Big/ 2h_o\left[A_4+(\rho c)_{m\ell}(T_o-T_m)\right] \tag{4.42}$$

Close inspection reveals that the positive sign must be used to insure $\delta_1' < \delta_1$.

Equation (4.42) enables one to calculate the location of the liquid-solid interface and thus the mass flow rate of the liquid from equation (4.30).

To determine the temperature at the original surface, we will develop an implicit equation to be used whenever equation (4.42) is employed. Consider again Figure 7 and the discussion that led to equation (4.32). The heat transfer may be written:

$$q_1 = h_o(T_o-T_n') = k_{m\ell}\frac{\partial T_n'}{\partial x} \tag{4.43}$$

The differential equation at the surface is:

$$\frac{\partial^2 T_n'}{\partial x^2} - \frac{\dot{m}_\ell' c_{c\ell}}{k_{m\ell}} \frac{\partial T_n'}{\partial x} = \frac{1}{a_{m\ell}} \frac{\partial T_n'}{\partial \theta} \tag{4.44}$$

Write the Taylor-series expansions:

$$T_n = T_n' - \Delta\theta \frac{\partial T_n'}{\partial \theta} \tag{4.45}$$

or,

$$\frac{\partial T_n'}{\partial \theta} = \frac{T_n' - T_n}{\Delta\theta} \tag{4.46}$$

and,

$$T_m = T_n' - (L-\delta_1') \frac{\partial T_n'}{\partial x} + \frac{(L-\delta_1')^2}{2} \frac{\partial^2 T_n'}{\partial x^2} \tag{4.47}$$

or,

$$\frac{\partial^2 T_n'}{\partial x^2} = \frac{2}{(L-\delta_1')^2} (T_m - T_n') + \frac{2}{(L-\delta_1')} \frac{\partial T_n'}{\partial x} \tag{4.48}$$

Substituting equations (4.46) and (4.48) into the differential equation and solving for the temperature gradient at the original surface yields:

$$\frac{\partial T_n'}{\partial x} = \frac{\frac{1}{a_{m\ell}} \frac{(T_n' - T_n)}{\Delta\theta} - \frac{2}{(L-\delta_1')^2} (T_m - T_n')}{\frac{2}{(L-\delta_1')} - \frac{\dot{m}_\ell' c_{c\ell}}{k_{m\ell}}} \tag{4.49}$$

Substitution of equation (4.49) into (4.43) and solving for T_n' gives:

$$T_n' = \frac{h_o T_o \left[\frac{2}{(L-\delta_1')} - \frac{\dot{m}_\ell' c_{c\ell}}{k_{m\ell}}\right] + T_n \frac{k_{m\ell}}{a_{m\ell}\Delta\theta} + \frac{2k_{m\ell} T_m}{(L-\delta_1')^2}}{\frac{k_{m\ell}}{a_{m\ell}\Delta\theta} + \frac{2k_{m\ell}}{(L-\delta_1')^2} + h_o\left[\frac{2}{(L-\delta_1')} - \frac{\dot{m}_\ell' c_{c\ell}}{k_{m\ell}}\right]} \tag{4.50}$$

A generalized interpolation equation, based on the differential equation, for determining the unknown temperature T_{n-1}' or T_{m2} will be developed later as will the expressions for calculating the other variables T_v' and δ_2'.

2. Liquid-Solid Interface Below Nodal Point n-1

The second set of equations which will be developed for predicting the recession of the liquid-solid interface implicitly assumes the interface has receded below nodal point n-1. The procedure is similar to the previous analysis. Consider Figure 8. Again, assume the temperatures of nodes 1 through m2-1 and m1+1 through n-1 have been calculated from the general explicit equation as previously discussed. The generalized equations to calculate the heat conducted into and out of the element as well as the interpolation equation for nodes m1 and m2 will be developed later as previously mentioned.

The shaded area shown in Figure 8 again represents the change in internal energy and is written as:

$$\Delta U = 1/2(\rho c)_{m\ell}(T_{m1+1}'-T_{m1+1})[(m1)\Delta x - \delta_1]$$

$$+ 1/2(\rho c)_{m\ell}(\delta_1-\delta_1')(T_{m1+1}'-T_m) + 1/2(\rho c)_{ms}(T_{m2-1}'-T_{m2-1})$$

$$[\delta_1-(m2-2)\Delta x] + 1/2(\rho c)_{ms}(\delta_1-\delta_1')(T_m-T_{m2-1}') \qquad (4.51)$$

The energy balance on the element is again given by equation (4.36). Substituting equation (4.51) into the energy balance and solving for the new location of the liquid-solid interface yields:

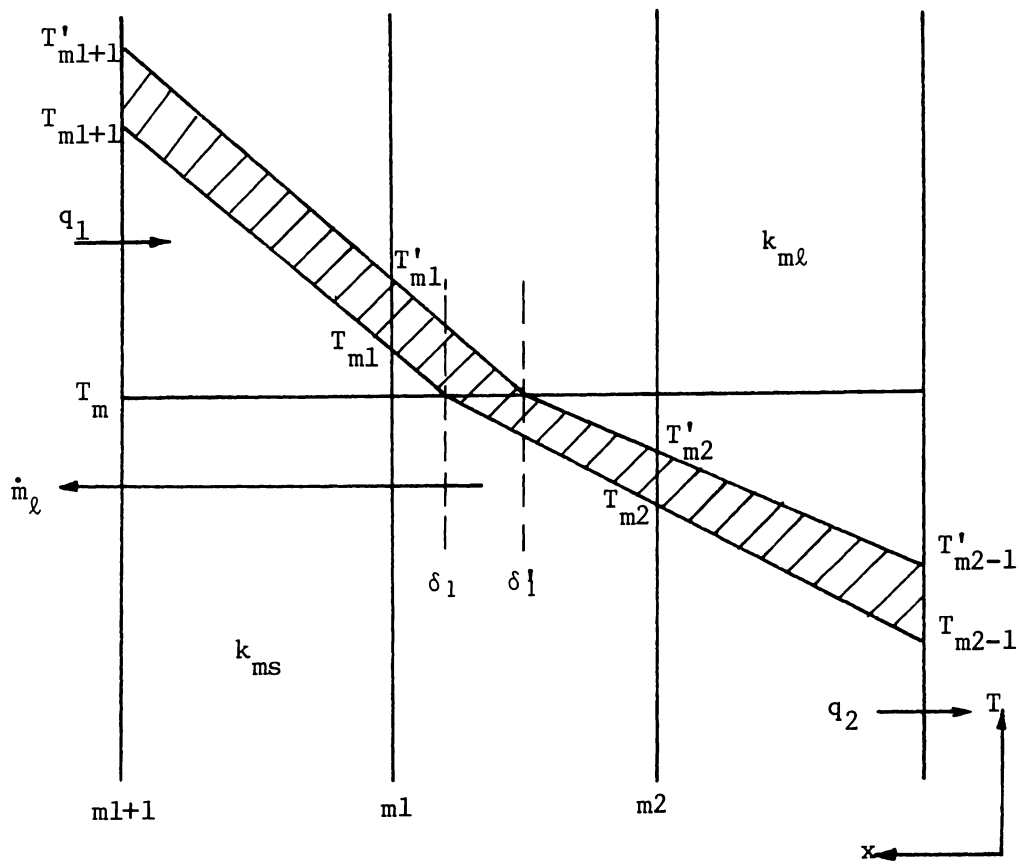

Figure 8: Schematic of Liquid-Solid Interface Below Nodal Point n-1.

$$\delta_1' = \delta_1 + \Big\{(\rho c)_{m\ell}(T'_{m1+1}-T_{m1+1})[(m1)\Delta x-\delta_1] \qquad (4.52)$$

$$+ (\rho c)_{ms}(T'_{m2-1}-T_{m2-1})[\delta_1-(m2-2)\Delta x] + 2\Delta\theta(q_2-q_1)\Big\}$$

$$\Big/ [(\rho c)_{m\ell}(T'_{m1+1}-T_m) + (\rho c)_{ms}(T_m-T'_{m2-1}) + 2\rho_{cs}\lambda_m P]$$

Once the location of the liquid-solid interface is obtained from equation (4.52) the mass flow rate of liquid may be calculated from equation (4.30), as in the case where the interface is located above nodal point n-1 and for which equation (4.42) is employed.

There remains to be developed an explicit expression to determine the temperature at the original surface when the interface has receded below node n-1. We may neglect the heat storage in the liquid layer since its maximum thickness for anticipated coolants is at most 5.0 percent of the total composite thickness, assuming extremely high porosity. A more realistic maximum thickness would not exceed 2.0 percent of the total composite thickness since it is not expected that the liquid-solid interface will recede to the back face before the vaporization temperature is reached at the exposed surface of the liquid layer. Making this assumption, we may write:

$$q_o = h_o(T_o-T_v) = k_{c\ell}\frac{T_v-T_n}{\delta_2-L} = k_{m\ell}\frac{\partial T_n}{\partial x} \qquad (4.53)$$

Solving for the temperature gradient at the original surface from these relations:

$$\frac{\partial T_n}{\partial x} = \frac{h_o}{k_{m\ell}}\left[T_o - \frac{h_o T_o(\delta_2-L) + k_{c\ell}T_n}{h_o(\delta_2-L) + k_{c\ell}}\right] \qquad (4.54)$$

The differential equation is:

$$k_{m\ell}(T_n)\frac{\partial^2 T_n}{\partial x^2}+\left[\frac{\partial k_{m\ell}(T_n)}{\partial x}-\dot{m}_\ell c_{c\ell}\right]\frac{\partial T_n}{\partial x}=(\rho c)_{m\ell}\frac{\partial T_n}{\partial \theta} \tag{4.55}$$

Again using Taylor-series expansions, we may write:

$$\frac{\partial T_n}{\partial \theta}=\frac{T_n'-T_n}{\Delta\theta} \tag{4.56}$$

$$\frac{\partial^2 T_n}{\partial x^2}=\frac{2(T_{n-1}-T_n)}{\Delta x^2}+\frac{2}{\Delta x}\frac{\partial T_n}{\partial x} \tag{4.57}$$

$$\frac{\partial k_{m\ell}(T_n)}{\partial x}=\frac{k_{m\ell}(T_n)-k_{m\ell}(T_{n-1})}{\Delta x} \tag{4.58}$$

Substituting equations (4.54) and (4.56) through (4.58) into (4.55) and solving for T_n' yields:

$$T_n'=T_n+a_{m\ell}(T_n)\Delta\theta\left\{\frac{2}{\Delta x^2}(T_{n-1}-T_n)+\frac{1}{k_{m\ell}{}^2(T_n)}\,\frac{\left[\frac{3k_{m\ell}(T_n)-k_{m\ell}(T_{n-1})}{\Delta x}-\dot{m}_\ell c_{c\ell}\right](T_o-T_n)}{\frac{(\delta_2-L)}{k_{c\ell}}+\frac{1}{h_o}}\right\} \tag{4.59}$$

Since this is an explicit equation, the following stability criterion must be satisfied whenever equation (4.59) is employed.

$$\Delta\theta\le 1\Bigg/\left\{\frac{2a_{m\ell}(T_n)}{\Delta x^2}+\frac{h_o k_{c\ell} a_{m\ell}(T_n)}{k_{m\ell}{}^2(T_n)(\delta_2-L)}\left[\frac{\frac{3k_{m\ell}(T_n)-k_{m\ell}(T_{n-1})}{\Delta x}-\dot{m}_\ell c_{c\ell}}{h_o+\frac{k_{c\ell}}{(\delta_2-L)}}\right]\right\} \tag{4.60}$$

3. Generalized Equations for Heat Conducted Into and Away From a Finite-Difference Element

A Generalized equation will be derived to predict the temperature gradient at a given nodal point, i, which leads to an expression of the following form for the heat conducted into an element:

$$q_1 = k_{mc} \frac{\partial T_i}{\partial x} \tag{4.61}$$

It is assumed that both the old and new temperatures, T_i and T_i' as well as the temperature, T_b, at a small distance, ℓ_b, below nodal point i are known. The differential equation can be written as:

$$k_{mc}(T_i) \frac{\partial^2 T_i}{\partial x^2} + \left[\frac{\partial k_{mc}(T_i)}{\partial x} - \dot{m}_c c_c(T_i) \right] \frac{\partial T_i}{\partial x} = (\rho c)_{mc}(T_i) \frac{\partial T_i}{\partial \theta} \tag{4.62}$$

By writing the Taylor-series expansions, we obtain:

$$\frac{\partial T_i}{\partial \theta} = \frac{T_i' - T_i}{\Delta \theta} \tag{4.63}$$

$$\frac{\partial^2 T_i}{\partial x^2} = \frac{2}{\ell_b^2} (T_b - T_i) + \frac{2}{\ell_b} \frac{\partial T_i}{\partial x} \tag{4.64}$$

$$\frac{\partial k_{mc}(T_i)}{\partial x} = \frac{k_{mc}(T_i) - k_{mc}(T_b)}{\ell_b} \tag{4.65}$$

Substituting equations (4.63), (4.64), and (4.65) into the differential equation, we may solve for the temperature gradient at nodal point i, so that with equation (4.61) the heat conducted into the element becomes:

$$q_1 = k_{mc}^2(T_i)\frac{\dfrac{T_i'-T_i}{a_{mc}(T_i)\Delta\theta} - \dfrac{2(T_b-T_i)}{\ell_b^2}}{\dfrac{3k_{mc}(T_i) - k_{mc}(T_b)}{\ell_b} - \dot{m}_c c_c(T_i)} \tag{4.66}$$

When this equation is used in connection with equation (4.52), the variables are:

$$\begin{aligned} T_i &= T_{m1+1} & k_{mc} &= k_{m\ell} \\ T_i' &= T_{m1+1}' & a_{mc} &= a_{m\ell} \\ T_b &= T_{m1} & \dot{m}_c &= \dot{m}_\ell \\ \ell_b &= \Delta x & c_c &= c_{c\ell} \end{aligned} \tag{4.67}$$

In a similar manner, we may develop an expression for the heat conducted away from an element:

$$q_2 = k_{mc}^2(T_i)\frac{\dfrac{T_i'-T_i}{a_{mc}(T_i)\Delta\theta} - \dfrac{2(T_a-T_i)}{\ell_a^2}}{\dfrac{k_{mc}(T_a) - 3k_{mc}(T_i)}{\ell_a} - \dot{m}_c c_c(T_i)} \tag{4.68}$$

where T_i and T_i' are the old and new temperatures at a given nodal point and T_a is the known temperature at a small distance, ℓ_a, above the nodal point. This expression is used in connection with both equation (4.52) where:

$$\begin{aligned} T_i &= T_{m2-1} & k_{mc} &= k_{ms} \\ T_i' &= T_{m2-1}' & a_{mc} &= a_{ms} \\ T_a &= T_{m2} & \dot{m}_c &= 0.0 \\ \ell_a &= \Delta x \end{aligned} \tag{4.69}$$

and equation (4.38) where,

$$
\begin{aligned}
T_i &= T_{n-2} & k_{mc} &= k_{ms} \\
T_i' &= T_{n-2}' & a_{mc} &= a_{ms} \\
T_a &= T_{n-1} & \dot{m}_c &= 0.0 \\
\ell_a &= \Delta x
\end{aligned}
\tag{4.70}
$$

Equation (4.68) will also be used in the development of an expression to calculate the mass flow rate of vapor leaving the surface in time period III.

4. Generalized Interpolation Equation

We must derive a general interpolation equation based on the differential equation in order to determine the temperatures of the remaining nodal points in the vicinity of the liquid-solid interface. Consider the system shown in Figure 9.

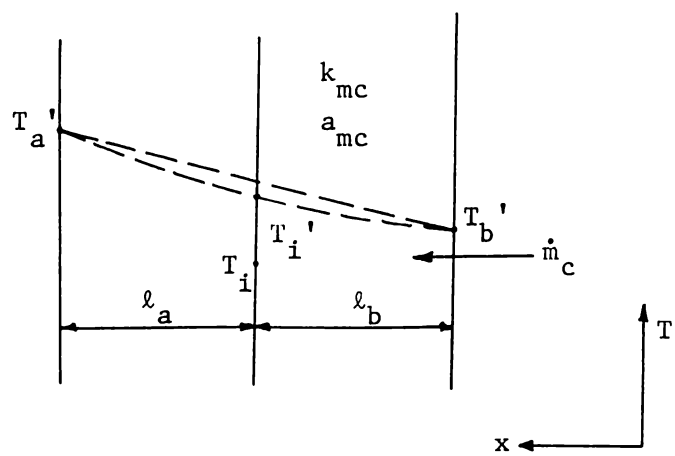

Figure 9

Interpolation Model

The differential equation is: (4.71)

$$k_{mc}(T_i') \frac{\partial^2 T_i'}{\partial x^2} + \left[\frac{\partial k_{mc}(T_i')}{\partial x} - \dot{m}_c c_c(T_i') \right] \frac{\partial T_i'}{\partial x} = \frac{k_{mc}(T_i')}{a_{mc}(T_i')} \frac{\partial T_i'}{\partial \theta}$$

We may write the following Taylor-series expansions:

$$T_i = T_i' - \Delta\theta \frac{\partial T_i'}{\partial \theta} \tag{4.72}$$

$$T_a' = T_i' + \ell_a \frac{\partial T_i'}{\partial x} + \frac{\ell_a^2}{2} \frac{\partial^2 T_i'}{\partial x^2} \tag{4.73}$$

$$T_b' = T_i' - \ell_b \frac{\partial T_i'}{\partial x} + \frac{\ell_b^2}{2} \frac{\partial^2 T_i'}{\partial x^2} \tag{4.74}$$

$$k_{mc}(T_a') = k_{mc}(T_i') + \ell_a \frac{\partial k_{mc}(T_i')}{\partial x} \tag{4.75}$$

$$k_{mc}(T_b') = k_{mc}(T_i') - \ell_b \frac{\partial k_{mc}(T_i')}{\partial x} \tag{4.76}$$

$$k_{mc}(T_i') = k_{mc}(T_i) + \Delta\theta \frac{\partial k_{mc}(T_i)}{\partial \theta} \tag{4.77}$$

From equation (4.72), we may write:

$$\frac{\partial T_i'}{\partial \theta} = \frac{T_i' - T_i}{\Delta\theta} \tag{4.78}$$

Substracting equations (4.73) and (4.74) yields:

$$\frac{\partial T_i'}{\partial x} = \frac{\ell_b^2 T_a' - \ell_a^2 T_b'}{\ell_a \ell_b (\ell_a + \ell_b)} + \frac{(\ell_a - \ell_b) T_i'}{\ell_a \ell_b} \tag{4.79}$$

Adding the same equations yields:

$$\frac{\partial^2 T_i'}{\partial x^2} = 2\,\frac{\ell_b T_a' - \ell_a T_b'}{\ell_a \ell_b (\ell_a + \ell_b)} - 2\,\frac{T_i'}{\ell_a \ell_b} \tag{4.80}$$

Also substracting equations (4.76) from (4.75) yields:

$$\frac{\partial k_{mc}(T_i')}{\partial x} = \frac{k_{mc}(T_a') - k_{mc}(T_b')}{\ell_a + \ell_b} \tag{4.81}$$

and adding these equations:

$$k_{mc}(T_i') = \frac{\ell_b k_{mc}(T_a') + \ell_a k_{mc}(T_b')}{\ell_a + \ell_b} \tag{4.82}$$

Similarly, we may obtain:

$$a_{mc}(T_i') = \frac{\ell_b a_{mc}(T_a') + \ell_a a_{mc}(T_b')}{\ell_a + \ell_b} \tag{4.83}$$

Substitution of equations (4.78) through (4.83) into the differential equation (4.71) and solving for the unknown temperature leads to the following interpolation equation:

$$T_i' = \left\{ \frac{T_i}{\Delta\theta}\,\frac{\ell_b k_{mc}(T_a')+\ell_a k_{mc}(T_b')}{\ell_b a_{mc}(T_a')+\ell_a a_{mc}(T_b')} - \dot{m}_c c_c(T_i)\,\frac{\ell_b^2 T_a' - \ell_a^2 T_b'}{\ell_a \ell_b (\ell_a+\ell_b)} \right.$$

$$\left. + \frac{k_{mc}(T_a')[3\ell_b^2 T_a' + \ell_a(2\ell_b - \ell_a)T_b'] + k_{mc}(T_b')[3\ell_a^2 T_b' + \ell_b(2\ell_a - \ell_b)T_a']}{\ell_a \ell_b (\ell_a+\ell_b)^2} \right\}$$

$$\Bigg/ \left\{ \frac{(3\ell_b - \ell_a)k_{mc}(T_a') + (3\ell_a - \ell_b)k_{mc}(T_b') + (\ell_a^2 - \ell_b^2)\dot{m}_c c_c(T_i)}{\ell_a \ell_b (\ell_a+\ell_b)} \right.$$

$$\left. + \frac{1}{\Delta\theta}\,\frac{\ell_b k_{mc}(T_a')+\ell_a k_{mc}(T_b')}{\ell_b a_{mc}(T_a')+\ell_a a_{mc}(T_b')} \right\} \tag{4.84}$$

Selectively substituting for the arbitrary variables in the above equation allows one to obtain the temperature of any internal nodal point by knowing the temperatures at the arbitrary distances ℓ_a and ℓ_b above and below the nodal point. When used for determining the temperatures of the nodal points above and below the interface, it is convenient to use the temperature of the interface as one of the known temperatures.

5. The Growth of the Liquid Layer

The only remaining unknowns in time period II are the thickness of the liquid above the original suface and the temperature at the exposed surface of the liquid layer.

Consider a mass balance on the coolant above the liquid-solid interface at any time. Neglecting any thermal expansion other than that due to phase change, we may write, on a unit area basis:

$$\rho_{c\ell}(T_m)(\delta_2'-L) = [\rho_{cs}(T_m) - \rho_{c\ell}(T_m)]\, P(L-\delta_1') \qquad (4.85)$$

so that solving for the thickness of the liquid layer yields:

$$\delta_2' = L + P(L-\delta_1')\left[\frac{\rho_{cs}(T_m)}{\rho_{c\ell}(T_m)} - 1\right] \qquad (4.86)$$

The discussion which led to equation (4.53) allows one to write:

$$k_{c\ell}\left[\frac{T_v'-T_n'}{\delta_2'-L}\right] = h_o(T_o-T_v') \qquad (4.87)$$

and solving for the temperature at the exposed surface of the liquid layer gives:

$$T_v' = \frac{h_o T_o(\delta_2'-L) + k_{c\ell} T_n}{h_o(\delta_2'-L) + k_{c\ell}} \qquad (4.88)$$

When the temperature at the exposed surface of the liquid layer becomes equal to the vaporization temperature of the coolant at ambient pressure, the time will be designated θ_2 and time period II will be complete.

D. Time Period III $(\theta_2 < \theta \leq \theta_3)$

1. Below the Original Surface

The determination of all temperatures, the location of the liquid-solid interface, and the mass flow rate of the liquid coolant below the original surface are obtained from the same equations discussed in time period II. It is assumed that the location of the liquid-solid interface, if it exists, is below nodal point n-1.

2. The Depletion of the Liquid Layer

When the temperature at the exposed surface of the liquid layer exceeds the vaporization temperature of the coolant at ambient pressure the liquid begins to vaporize at the surface. New equations which account for this effect are required for the temperature of the original surface and for the mass flow rate of vapor leaving the surface of the liquid layer.

In the development of an implicit equation for the temperature of the original surface the differential equation is:

$$k_{m\ell}(T_n')\frac{\partial^2 T_n'}{\partial x^2} + \left[\frac{\partial k_{m\ell}(T_n')}{\partial x} - \dot{m}_\ell c_{c\ell}(T_n')\right]\frac{\partial T_n'}{\partial x} = \frac{k_{m\ell}(T_n')}{a_{m\ell}(T_n')}\frac{\partial T_n'}{\partial \theta} \tag{4.89}$$

and Taylor-series expansions may be written as in equations (4.56) through (4.58) so that substitution into the differential equation yields:

$$T_n'\left[\frac{k_{m\ell}(T_n')}{a_{m\ell}(T_n')\Delta\theta} + \frac{2k_{m\ell}(T_n')}{\Delta x^2}\right] = \frac{k_{m\ell}(T_n')}{a_{m\ell}(T_n')\Delta\theta}T_n + \frac{2k_{m\ell}(T_n')}{\Delta x^2}T_{n-1}' + \left[\frac{3k_{m\ell}(T_n') - k_{m\ell}(T_{n-1}')}{\Delta x} - \dot{m}_\ell c_{c\ell}(T_n')\right]\frac{\partial T_n'}{\partial x} \tag{4.90}$$

Again, neglecting the heat storage in the liquid layer and realizing that the exposed surface of the liquid layer remains at a constant temperature, we write:

$$k_{c\ell}\frac{T_v - T_n'}{\delta_2' - L} = k_{m\ell}(T_n')\frac{\partial T_n'}{\partial x} \tag{4.91}$$

or

$$\frac{\partial T_n'}{\partial x} = \frac{k_{c\ell}}{k_{m\ell}(T_n')}\frac{T_v - T_n'}{\delta_2' - L} \tag{4.92}$$

where the conductivity of the liquid coolant may be evaluated at the average temperature of the liquid layer. Substitution of equation (4.92) into equation (4.90) and solving for the temperature at the original surface yields:

$$T_n' = \left\{ \frac{(\delta_2'-L)T_n}{a_{m\ell}(T_n')\Delta\theta} + \frac{2(\delta_2'-L)T_{n-1}'}{\Delta x^2} \right.$$

$$\left. + \frac{k_{c\ell}T_v}{k_{m\ell}^2(T_n')} \left[\frac{3k_{m\ell}(T_n') - k_{m\ell}(T_{n-1}')}{\Delta x} - \dot{m}_\ell' c_{c\ell}(T_n') \right] \right\}$$

$$\Bigg/ \left\{ \frac{(\delta_2'-L)}{a_{m\ell}(T_n')\Delta\theta} + \frac{2(\delta_2'-L)}{\Delta x^2} \right. \tag{4.93}$$

$$\left. + \frac{k_{c\ell}}{k_{m\ell}^2(T_n')} \left[\frac{3k_{m\ell}(T_n') - k_{m\ell}(T_{n-1}')}{\Delta x} - \dot{m}_\ell' c_{c\ell}(T_n') \right] \right\}$$

A mass balance on the liquid layer over an increment of time is:

$$\rho_{c\ell}(\delta_2'-\delta_2) = \left[\frac{\dot{m}_\ell'+\dot{m}_\ell}{2} - \frac{\dot{m}_v'+\dot{m}_v}{2} \right] \Delta\theta \tag{4.94}$$

from which we may solve for δ_2' as:

$$\delta_2' = \delta_2 + \frac{(\dot{m}_\ell'+\dot{m}_\ell-\dot{m}_v'-\dot{m}_v)\Delta\theta}{2\rho_{c\ell}} \tag{4.95}$$

Since the new mass rate of flow of the vapor, $\dot{m}_v'$, remains to be determined, rewrite equation (4.95) as:

$$\delta_2' = \delta_2 + \frac{(\dot{m}_\ell'+\dot{m}_\ell-2\dot{m}_v)\Delta\theta}{2\rho_{c\ell}} \tag{4.96}$$

in which form it is to be used in connection with equation (4.93). In the evaluation of the thermal properties it is also necessary to replace T_n' with T_n.

With the aid of the generalized equation for heat conducted away from an element, equation (4.68), the heat conducted into the composite at the original surface is:

$$q_2' = [k_{m\ell}(T_n')]^2 \frac{\frac{T_n'-T_n}{a_{m\ell}(T_n')\Delta\theta} - 2\frac{T_{n-1}'-T_n}{\Delta x^2}}{\frac{3k_{m\ell}(T_n')-k_{m\ell}(T_{n-1}')}{\Delta x} - \dot{m}_\ell' c_{c\ell}(T_n')} \tag{4.97}$$

An energy balance on the liquid layer, neglecting heat storage, is:

$$\dot{m}_v' \lambda_v(T_v) = h_o(T_o-T_v) - q_2' \tag{4.98}$$

Substitution of equation (4.97) into the energy balance, equation (4.98), and solving for the mass flow rate of the vapor yields:

$$\dot{m}_v' = \frac{1}{\lambda_v(T_v)} \left\{ h_o(T_o-T_v) - [k_{m\ell}(T_n')]^2 \frac{\frac{T_n'-T_n}{a_{m\ell}(T_n')\Delta\theta} - 2\frac{T_{n-1}'-T_n'}{\Delta x^2}}{\frac{3k_{m\ell}(T_n')-k_{m\ell}(T_{n-1}')}{\Delta x} - \dot{m}_\ell' c_{c\ell}(T_n')} \right\} \tag{4.99}$$

After the mass flow rate of the vapor has been determined, the thickness of the liquid layer is determined from equation (4.95). When the location of the vapor-liquid interface coincides with the original surface of the composite, time period III is complete, and the time when this occurs is denoted as θ_3.

E. Time Period IV ($\theta_3 < \theta \leq \theta_4$)

The various regions that may exist in time period IV are shown in Figure 4. As previously discussed, the methods of determining the temperatures, location of the liquid-solid interface, if present, and the mass flow rate of the liquid coolant for nodal points 1 through v2-1 are the same as in time periods II and III. Additional quantities to be calculated in time period IV are the location of the vapor-liquid interface and the mass flow rate of the coolant vapor leaving the interface.

1. The Temperature at the Vapor-Liquid Interface

The temperature at the vapor-liquid interface will not remain constant as was the case at the liquid-solid interface due to the increased pressure which results from the flow of vapor through the porous matrix. We may rewrite equation(3.22) developed in the theoretical analysis for this pressure in finite-difference form as follows:

$$P_{v1} = \sum_{i=v1}^{n-1} \left\{ P_{i+1}^2 + \frac{2\dot{m}_v R_u}{g_c M} \left[\alpha \mu_i + \beta \dot{m}_v \right] \frac{(T_{i+1}+T_i)}{2} \Delta x \right\}^{1/2} \tag{4.100}$$

where,

$$\mu_i = \mu \left(\frac{T_{i+1}+T_i}{2} \right) \tag{4.101}$$

is obtained from equation (3.26) as:

$$\mu_i = \frac{M^{1/2}}{T_{nb}^{1/6}} \frac{\left[0.0915\left(\frac{T_{i+1}+T_i}{2T_{nb}}\right)^{0.645} - 0.0307\right]}{\left[1.18\left(\frac{T_{i+1}+T_i}{2T_{nb}}\right)\right]^{0.91\log\left[1.18\left(\frac{T_{i+1}+T_i}{2T_{nb}}\right)\right]}} \tag{4.102}$$

Adding the contribution of the partial distance increment immediately above the interface yields:

$$P_v = \left\{P_{v1}^2 + \frac{2\dot{m}_v R_u}{g_c M}\left[\alpha\mu_v + \beta\dot{m}_v\right]\frac{(T_{v1}+T_v)}{2}\left[(v1-1)\Delta x - \delta_2\right]\right\}^{1/2} \tag{4.103}$$

where again,

$$\mu_v = \mu\left(\frac{T_{v1}+T_v}{2}\right) \tag{4.104}$$

and is obtained as in equation (4.102).

The vapor-liquid interface temperature may now be obtained from the relation:

$$T_v = \frac{B}{A - \log P_v} \tag{4.105}$$

as well as the latent heat of vaporization from the relation:

$$\lambda_v = \lambda_{nb}\left[\frac{T_c - T_v}{T_c - T_{nb}}\right]^{.38} \tag{4.106}$$

as were discussed in the theoretical analysis.

2. Vapor-Liquid Interface Above Nodal Point n-1

As was the procedure for the liquid-solid interface, it is again convenient to derive two equations to predict the location of the vapor-liquid interface. First, however, we must derive relations between the mass flow rate of the vapor, the rate of formation of the vapor, and the interface recession. Consider a mass balance on the element defined by the vapor-liquid interface at time θ and $\theta + \Delta\theta$ as shown in Figure 10.

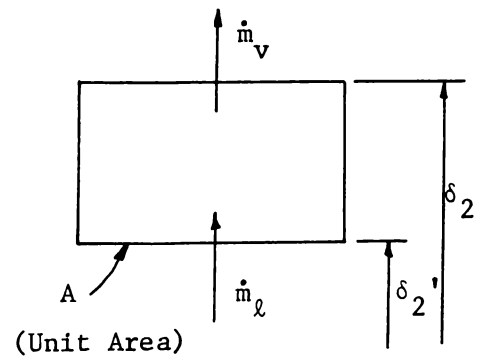

Figure 10

Element Defined By Vapor-Liquid Interface At Times θ and $\theta + \Delta\theta$

The rate of formation of the vapor is:

$$\bar{m}_v \Delta\theta A = \rho_{c\ell}\, PA(\delta_2 - \delta_2') + \dot{m}_\ell A \Delta\theta \tag{4.107}$$

or,

$$\bar{m}_v = \dot{m}_\ell + \rho_{c\ell}\, P \frac{(\delta_2 - \delta_2')}{\Delta\theta} \tag{4.108}$$

The mass of the coolant at time θ, M_θ, may be written as:

$$M_\theta = \rho_{c\ell} PA(\delta_2 - \delta_2') \tag{4.109}$$

and at time $\theta + \Delta\theta$:

$$M_{\theta+\Delta\theta} = \rho_{cv} PA(\delta_2 - \delta_2') \tag{4.110}$$

subtracting:

$$M_{\theta} - M_{\theta+\Delta\theta} = (\dot{m}_v - \dot{m}_\ell)A\Delta\theta = PA(\rho_{c\ell} - \rho_{cv})(\delta_2 - \delta_2') \tag{4.111}$$

so that,

$$\dot{m}_v = \dot{m}_\ell + P(\rho_{c\ell} - \rho_{cv})\frac{(\delta_2 - \delta_2')}{\Delta\theta} \tag{4.112}$$

Combining equations (4.112) and (4.108), the relation between the rate of flow and rate of formation of the vapor may also be obtained as:

$$\bar{m}_v = \frac{\rho_{c\ell}\dot{m}_v - \rho_{cv}\dot{m}_\ell}{\rho_{c\ell} - \rho_{cv}} \tag{4.113}$$

An implicit equation for the location of the vapor-liquid interface, assuming it lies between nodal points n and n-1 will now be developed. Consider Figure 11. The development follows closely to that of the liquid-solid interface. The shaded area is again the change in internal energy of the element and may be written as in equation (4.33) with subscripts modified to agree with Figure 11. The heat input to the element is:

$$q_1 = q_o = h_o(T_o - T_n) \tag{4.114}$$

and the heat leaving the element by conduction, q_2, may be obtained from the generalized equation (4.68) where:

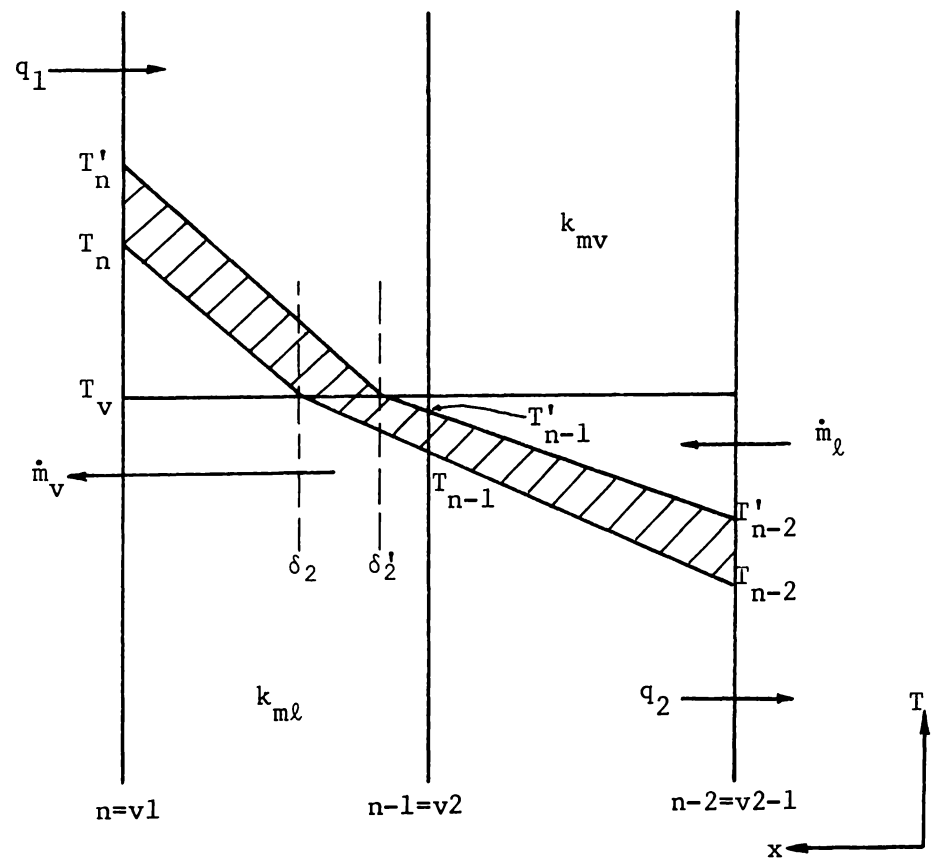

Figure 11: Schematic of Vapor-Liquid Interface Above Nodal Point n-1.

$$T_i = T_{n-2} \qquad k_{mc} = k_{m\ell}$$
$$T_a = T_{n-1} \qquad a_{mc} = a_{m\ell}$$
$$\ell_a = \Delta x \qquad c_c = c_{c\ell} \tag{4.115}$$

As an approximation let:

$$k_{mv}\left[\frac{T_n'-T_v}{L-\delta_2'}\right] = h_o(T_o-T_n') \tag{4.116}$$

so that:

$$T_n' = \frac{h_o T_o(L-\delta_2') + k_{mv}T_v}{h_o(L-\delta_2') + k_{mv}} \tag{4.117}$$

The heat-balance equation differs from that of the liquid-solid interface due to the flow of liquid into the element in addition to the flow of vapor due to interface recession. It becomes:

$$(q_1 - q_2)\Delta\theta + \dot{m}_\ell c_{c\ell}(T_{n-2}-T_v)\Delta\theta - \dot{m}_v c_{cv}(T_n-T_v)\Delta\theta - \Delta U = \bar{m}_v\lambda_v\Delta\theta \tag{4.118}$$

Following the same methods of solution that led to equation (4.42), solve for the location of the vapor-liquid interface as:

$$L-\delta_2' = \left\{[(A_3-A_2)h_o - k_{mv}A_4] + \sqrt{[h_o(A_2-A_3)+k_{mv}A_4]^2+4h_o[A_4+(\rho c)_{mv}(T_o-T_v)](A_3-A_2)k_{mv}}\right\} \Big/ 2h_o[(\rho c)_{mv}(T_o-T_v)+A_4h_o] \tag{4.119}$$

where the constants are defined as:

$$A_2 \equiv (\dot{m}_\ell+\dot{m}_\ell')\lambda_v\Delta\theta + 2\dot{m}_\ell c_{c\ell}(T_v-T_{n-2})\Delta\theta$$
$$+ 2\dot{m}_v c_{cv}(T_n-T_v)\Delta\theta + (\rho c)_{m\ell}(T_{n-2}'-T_{n-2})[\delta_2-(n-3)\Delta x]$$

$$A_3 \equiv (L-\delta_2)[(\rho c)_{m\ell}(T_v-T_{n-2}') + (\rho c)_{mv}(T_n-T_v) + 2P\rho_{c\ell}\lambda_v]$$
$$+ 2(q_1-q_2)\Delta\theta$$

$$A_4 \equiv (\rho c)_{m\ell}(T_v-T_{n-2}') + 2P\rho_{c\ell}\lambda_v \qquad (4.120)$$

With the aid of equation (4.120), it is possible to calculate the mass flow rate of vapor leaving the element from equation (4.112). A more accurate approximation for the temperature of the original surface similar to equation (4.50) may be derived as:

$$T_n' = \frac{h_o T_o\left[\frac{2}{(L-\delta_2')} - \frac{\dot{m}_v' c_{cv}}{k_{mv}}\right] + \frac{k_{mv}T_n}{a_{mv}\Delta\theta} + \frac{2k_{mv}T_v}{(L-\delta_2')^2}}{\frac{k_{mv}}{a_{mv}\Delta\theta} + \frac{2k_{mv}}{(L-\delta_2')^2} + h_o\left[\frac{2}{(L-\delta_2')} - \frac{\dot{m}_v' c_{cv}}{k_{mv}}\right]} \qquad (4.121)$$

The generalized interpolation equation (4.84) previously developed will be employed to determine the remaining unknown, T_{n-1}'.

3. Vapor-Liquid Interface Below Nodal Point n-1

When the vapor-liquid interface has receded below nodal point n-1, the general equation (4.4) for an internal element may be used to determine the temperatures of nodal points vl+1 through n-1 with:

$$k_{mc} = k_m(1-P) \qquad \dot{m}_c = \dot{m}_v$$
$$(\rho c)_{mc} = \rho_m c_m(1-P) \qquad c_c = c_{cv} \qquad (4.122)$$

Also, the general implicit equation (4.17) may be employed at the original surface, subject to the same conditions, (4.122).

Assume that the vapor-liquid interface lies below nodal point n-1 and may be shown schematically as in Figure 12. The shaded area represents the change in internal energy and may be written from equation (4.51) for the liquid-solid interface by changing the subscripts. The heat into and out of the element by conduction may again be obtained from the generalized relations. An energy balance on the element is given by equation (4.118) so that following the same methods of solution that lead to equation (4.52) leads to an expression for the location of the vapor-liquid interface as:

$$\delta_2' = \delta_2 - \Big\{(q_1-q_2)\Delta\theta - \dot{m}_\ell c_{c\ell}(T_v-T_{v2-1})\Delta\theta$$

$$- \dot{m}_v c_{cv}(T_{v1+1}-T_v)\Delta\theta - \frac{\dot{m}_\ell+\dot{m}_\ell'}{2}\lambda_v\Delta\theta$$

$$- 1/2(\rho c)_{mv}(T_{v1+1}'-T_{v1+1})[(v1)\Delta x-\delta_2]$$

$$- 1/2(\rho c)_{m\ell}(T_{v2-1}'-T_{v2-1})[\delta_2-(v2-2)\Delta x]\Big\}$$

$$\Big/\ \rho_{c\ell}P\lambda_v + 1/2[(\rho c)_{mv}(T_{v1+1}'-T_v) + (\rho c)_{m\ell}(T_v-T_{v2-1}')] \qquad (4.123)$$

The mass flow rate of the vapor leaving the interface will be obtained from equation (4.112) and the remaining unknown temperatures, T_{v1} and T_{v2}, from the generalized interpolation equation (4.84).

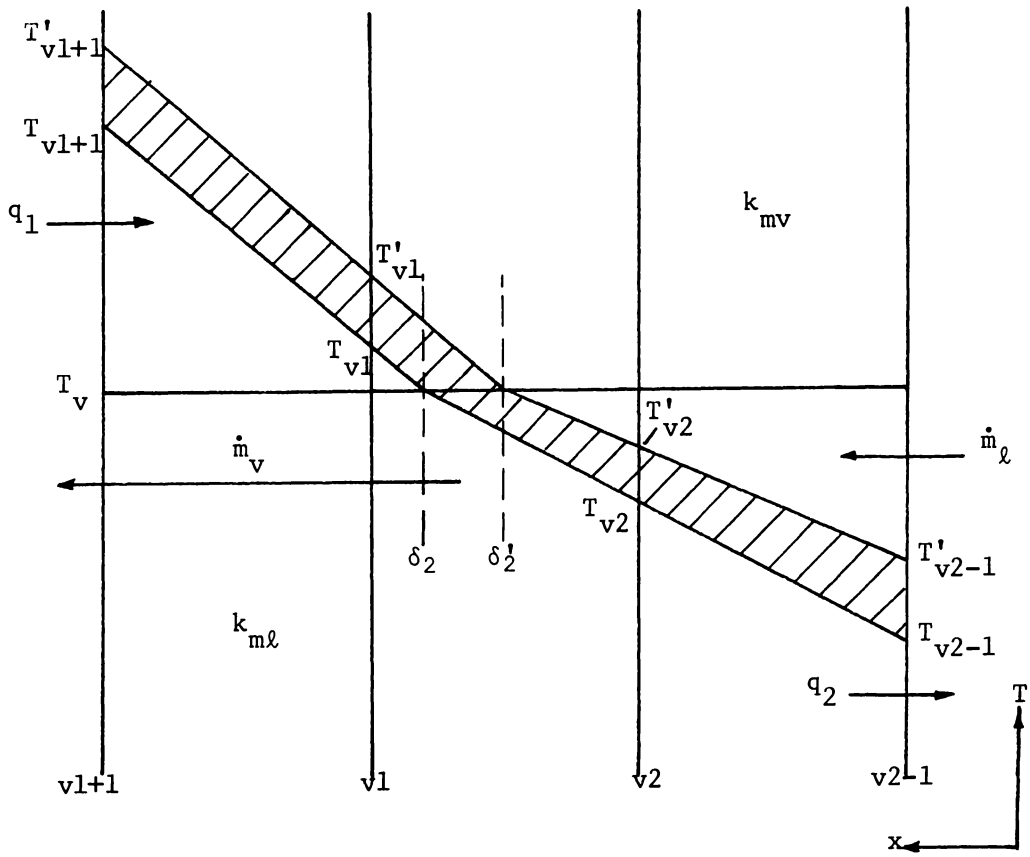

Figure 12: Schematic of Vapor-Liquid Interface Below Nodal Point n-1.

The above analysis applies until that time at which the vapor-liquid interface recedes below nodal point 2. At that time, the following will be assumed:

$$T_1 = T_v \qquad \dot{m}_v = 0.0$$
$$\delta_2' = 0.0 \qquad \theta = \theta_4 \tag{4.124}$$

which will complete the analysis for time period IV.

F. Time Period V $(\theta_4 < \theta \leq \theta_{crit})$

Once the coolant has vaporized completely, the composite consists of a porous matrix only. The temperatures of the internal nodal points are given by the general explicit equation (4.4) as follows:

Nodal points 2 through n-1

$$k_{mc} = k_m(1-P)$$
$$(\rho c)_{mc} = \rho_m c_m(1-P)$$
$$\dot{m}_c = 0.0 \tag{4.125}$$

The temperature at the insulated back face is determined from explicit equation (4.5) and the general implicit equation for the original surface, equation (4.17), is applicable at the exposed surface, both subject to the above conditions. The time at which the exposed surface reaches the melting temperature of the matrix will end time period V and the analysis is complete.

V. MATERIAL PHYSICAL PROPERTIES

An extensive search was conducted to determine the thermophysical properties of seven different metallic coolants: silver, magnesium, copper, tin, lithium, zinc, and lead. In general, the values obtained for the conductivities and specific heats of the coolants, as well as the tungsten matrix, are seen to be strong functions of temperature over the temperature range anticipated. The data collected were plotted so that properties could be evaluated from the following relations:

$$c = a_1 + a_2 T + a_3 T^2 \tag{5.1}$$

$$k = b_1 + b_2 T + b_3 T^2 \tag{5.2}$$

The constants are given in Tables I and II for the coolants and for the tungsten matrix in the various phases expected to exist in the analysis. Conveniently, straight lines approximate much of the data to within the variations reported in the references, and the last terms in the above equations are not needed. For those properties where the second-order term is necessary, a least squares fit of the data was performed. The conductivities of the coolants in vapor form are considered negligible for this analysis.

The densities of the coolants and matrix in the solid phase were obtained from volumetric expansion coefficients. These properties are most conveniently related in the following forms:

$$\rho_m = \frac{1}{d_{m1} + d_{m2} T} \tag{5.3}$$

$$\rho_{cs} = \frac{1}{d_{cs1} + d_{cs2}T} \tag{5.4}$$

The densities of the coolants in liquid phase which were obtained from the references are given by the following relation:

$$\rho_{c\ell} = d_{c\ell 1} + d_{c\ell 2}T \tag{5.5}$$

These constants for the matrix and for the coolants in solid and liquid phase are given in Table III.

Densities of the coolants in vapor phase are obtained from the perfect-gas relation:

$$\rho_{cv} = \frac{P_v M}{R_u T} \tag{5.6}$$

In some instances, the properties of the coolants in liquid phase were not obtained, in which case the property was assumed constant and equal to the value obtained for the liquid coolant at its normal melting point.

Other pertinent properties and constants for the coolants and tungsten matrix are given in Table IV. The constants A, the intercept of the vapor pressure-temperature curve, and B, the slope of the vapor pressure-temperature curve, are in general taken from reference (2). In cases where these constants were not reported plots of the vapor pressure-temperature data from other references were made so that these constants could be evaluated.

The values of the viscous-flow coefficient and the inertial-flow coefficient used for the determination of the pressure drop of the vapor through the matrix are those reported by Gessner (2). These values are characteristic of a tungsten matrix fabricated

from tungsten powder of about fifty microns in diameter. They are:

$$\alpha = 3.71 \times 10^{11} \text{ ft}^{-2} \tag{5.7}$$

$$\beta = 1.525 \times 10^{7} \text{ ft}^{-1} \tag{5.8}$$

These values will be considered independent of temperature, pressure, and matrix porosity as previously discussed.

TABLE I

SPECIFIC HEATS

Element	Phase	$a_1 \times 10^1$	$a_2 \times 10^5$	$a_3 \times 10^9$	Reference
	cs	0.850	1.510	0.000	20
Cu	cℓ	1.200	0.000	0.000	-
	cv	0.480	1.000	0.000	25
	cs	2.040	7.290	0.000	20
Mg	cℓ	2.680	2.950	0.000	19
	cv	1.990	0.175	0.000	25
	cs	0.520	0.706	0.000	20
Ag	cℓ	0.692	0.000	0.000	19
	cv	0.461	0.000	0.000	25
	cs	0.450	1.730	0.000	24
Sn	cℓ	0.480	1.120	0.000	29
	cv	0.521	0.000	0.000	2
	cs	10.000	0.000	0.000	2
Li	cℓ	10.000	0.000	0.000	19
	cv	8.043	-5.330	8.060	25
	cs	0.705	4.070	0.000	24
Zn	cℓ	1.420	-1.820	0.000	19
	cv	0.760	0.000	0.000	25
	cs	0.430	-1.390	0.000	29
Pb	cℓ	0.284	-0.194	0.000	29
	cv	0.240	0.000	0.000	2
W	m	0.300	0.137	0.000	28

TABLE II

CONDUCTIVITIES

Element	Phase	$b_1 \times 10^{-2}$	$b_2 \times 10^{2}$	$b_3 \times 10^{6}$	Reference
	cs	2.370	-2.250	0.000	20
Cu	cℓ	1.820	0.000	0.000	-
Mg	cs	0.770	0.000	0.000	20
	cℓ	0.770	0.000	0.000	-
Ag	cs	2.757	-5.180	0.000	20
	cℓ	1.607	0.000	0.000	-
Sn	cs	0.452	-1.330	0.000	29
	cℓ	0.204	-0.103	0.000	19
Li	cs	0.280	0.000	0.000	2
	cℓ	0.218	0.000	0.000	19
Zn	cs	0.723	-1.350	0.000	29
	cℓ	0.354	-0.141	0.000	19
Pb	cs	0.235	-0.615	0.000	14
	cℓ	0.090	0.000	0.000	-
W	m	0.939	-1.403	1.155	20

Note: Conductivity of Coolant in Vapor Phase Assumed Negligible

TABLE III

DENSITIES

Element	Phase	d_1	d_2	Reference
Cu	cs	$1.756 \times 10_2^{-3}$	5.197×10^{-8}	26
	cℓ	5.183×10^{2}	0.000	21
Mg	cs	$9.092 \times 10_1^{-3}$	4.106×10^{-7}	26
	cℓ	9.810×10^{1}	0.000	19
Ag	cs	$1.520 \times 10_2^{-3}$	5.364×10^{-8}	26
	cℓ	6.500×10^{2}	-3.110×10^{-2}	19
Sn	cs	$2.164 \times 10_2^{-3}$	8.750×10^{-8}	26
	cℓ	4.560×10^{2}	-2.362×10^{-2}	19
Li	cs	$2.875 \times 10_1^{-2}$	2.826×10^{-6}	26
	cℓ	3.400×10^{1}	-2.850×10^{-3}	19
Zn	cs	$2.040 \times 10_2^{-3}$	9.740×10^{-8}	26
	cℓ	4.588×10^{2}	-2.153×10^{-2}	19
Pb	cs	$1.380 \times 10_2^{-3}$	7.120×10^{-8}	26
	cℓ	7.040×10^{2}	-3.980×10^{-2}	19
W	m	8.513×10^{-4}	6.154×10^{-9}	26

Note: Densities of Coolant in Vapor Phase are Obtained From Perfect Gas Relation.

TABLE IV

CONSTANT PROPERTIES

Element	M	A	$Bx10^{-4}$	T_m	T_{nb}	T_c	λ_m	λ_{nb}
Cu	63.54	8.92 (22)	2.93 (22)	2440 (20)	5239 (22)	9900 (27)	91.1 (20)	2110 (20)
Mg	24.32	8.35 (2)	1.25 (2)	1664 (19)	2477 (19)	4954 (2)	148.0 (19)	2407 (19)
Ag	107.87	8.79 (2)	2.44 (2)	2221 (19)	4473 (19)	8940 (2)	43.4 (19)	1001 (19)
Sn	118.70	9.34 (19)	2.75 (19)	909 (18)	4578 (19)	7190 (2)	26.1 (19)	1031 (19)
Li	6.94	8.29 (2)	1.44 (2)	817 (18)	2875 (18)	4595 (2)	284.0 (19)	8424 (19)
Zn	65.38	8.39 (2)	1.08 (2)	1247 (19)	2123 (19)	4246 (2)	43.9 (19)	755 (19)
Pb	207.21	7.93 (19)	1.67 (19)	1081 (19)	3619 (19)	6900* (27)	10.6 (19)	368 (19)
W	183.92	--	--	6560 (2)	--	--	--	--

( ) - Indicates Reference

*$T_c = 1.47(T_{nb})^{1.03}$

VI. RESULTS AND DISCUSSION

A computer program of the finite-difference analysis was written for use with the IBM 7040/1401 digital computing system to compare the relative effectiveness of the seven different coolants previously discussed. The program and a discussion is contained in Appendix A. The results and computer program presented carry the analysis through time period III, the time at which the liquid layer recedes to the original surface and vaporization begins from within the matrix. A program for the completion of the analysis was written, but at this time, the reliability of the results has not been established. The reader is referred to reference (2) for the effect of vaporization from within the matrix on the self-cooling process.

A. General Conditions

There are certain variables in the analysis that must be specified. The ambient temperature and pressure are typical of the flame temperature and throat pressure of a high-energy solid-propellant rocket motor. The convective heat-transfer coefficient is also typical of that at the throat of such a motor having a throat diameter of about 2 inches. The general conditions specified to be used for all cases are as follows:

$T_o = 6660^o$ R

$P_o = 226$ psia

$h_o = 1303$ BTU/hr ft^{2o}R

$L = 2.0$ inches

$T_{xi} = 530^{o}R$

These conditions are also those presented by Gessner, et al. (2). It was anticipated that the results could be compared so that the effects of varying thermal properties and of the melting process could be shown. However, the specific heat of the tungsten matrix reported in (2) was approximately 18 percent higher than the average value obtained for this analysis and, therefore, any comparsion merely indicates this difference. It is interesting to note, although, that with other properties about the same, the difference in specific heats accounted for as much as a 5 percent variation in the temperature of the original surface at any time. The effect of considering properties that vary with temperature is shown in Section B of this chapter.

B. Case Studies

Data were obtained for seven different metallic coolants using the general conditions stated and the properties as previously presented. The variations of original surface temperatures, recession rates of the liquid-solid interface, and the growth and depletion of the liquid layers are given in Figures 13 through 18 for a constant porosity of 20 percent. As mentioned earlier in this chapter, results were obtained up to the point where the coolant begins to vaporize from within the matirx ($\theta = \theta_3$). This is the point where

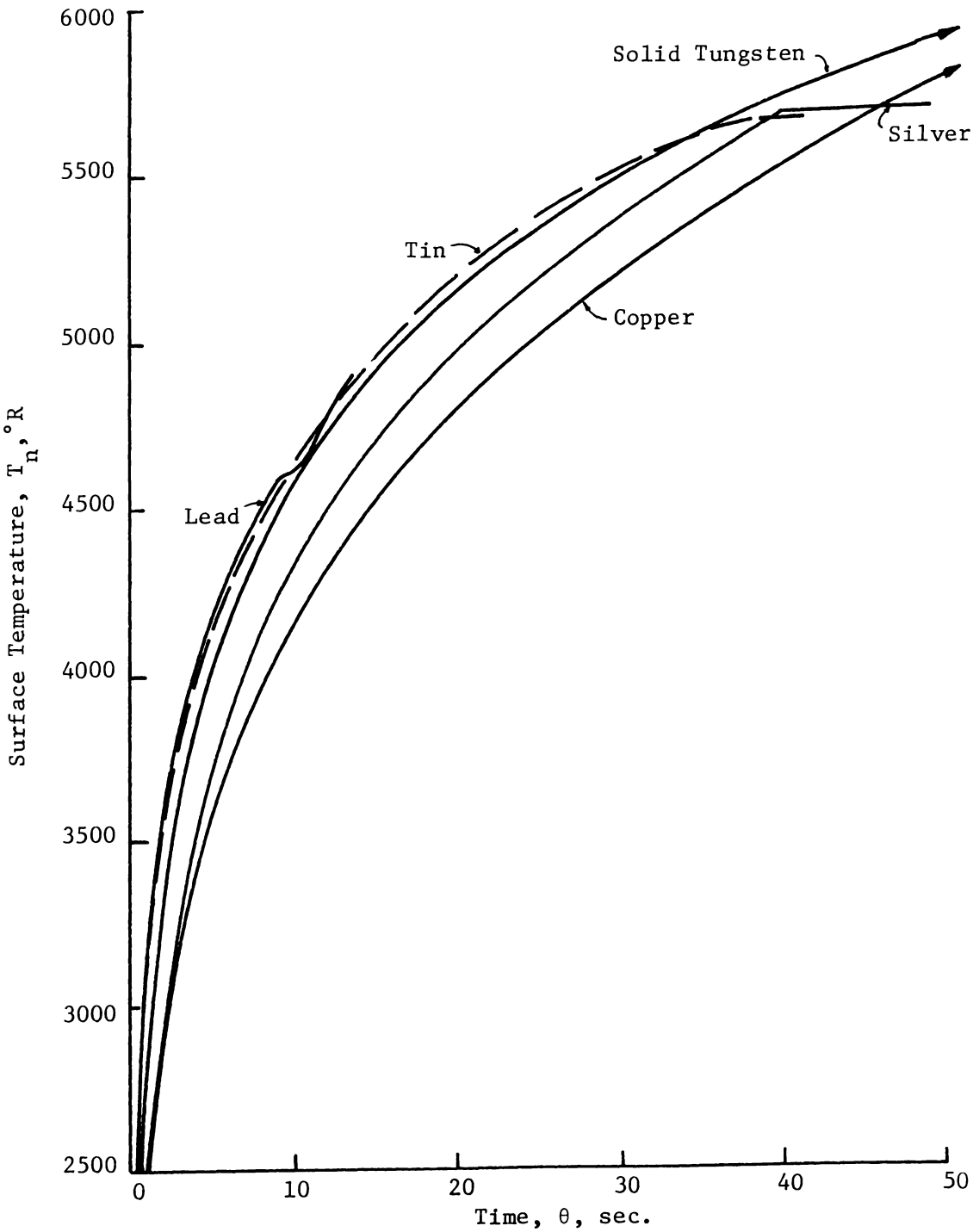

Figure 13: Surface-Temperature Response, Various Coolants, P=0.2

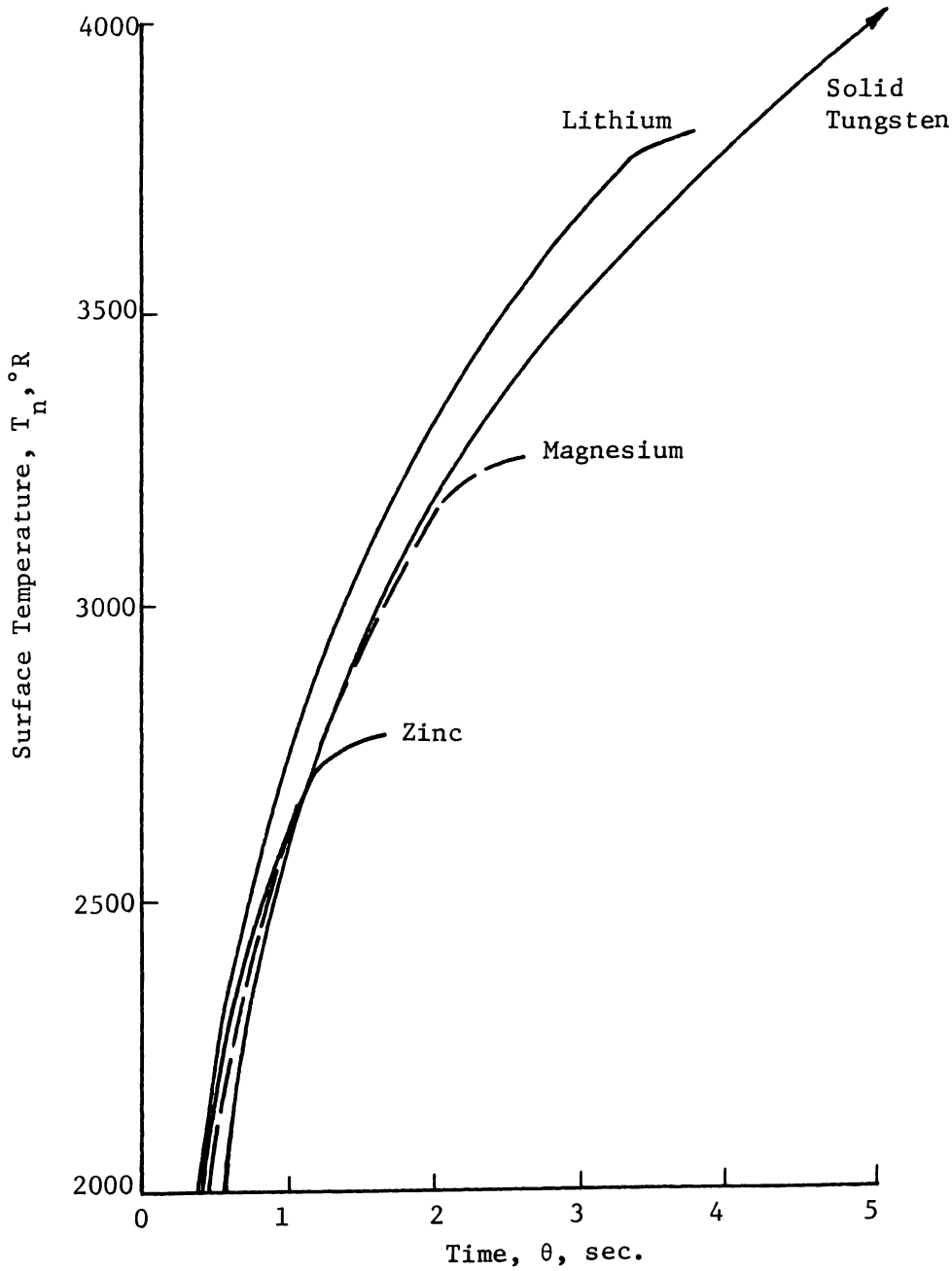

Figure 14: Surface-Temperature Response, Various Coolants, P=0.2

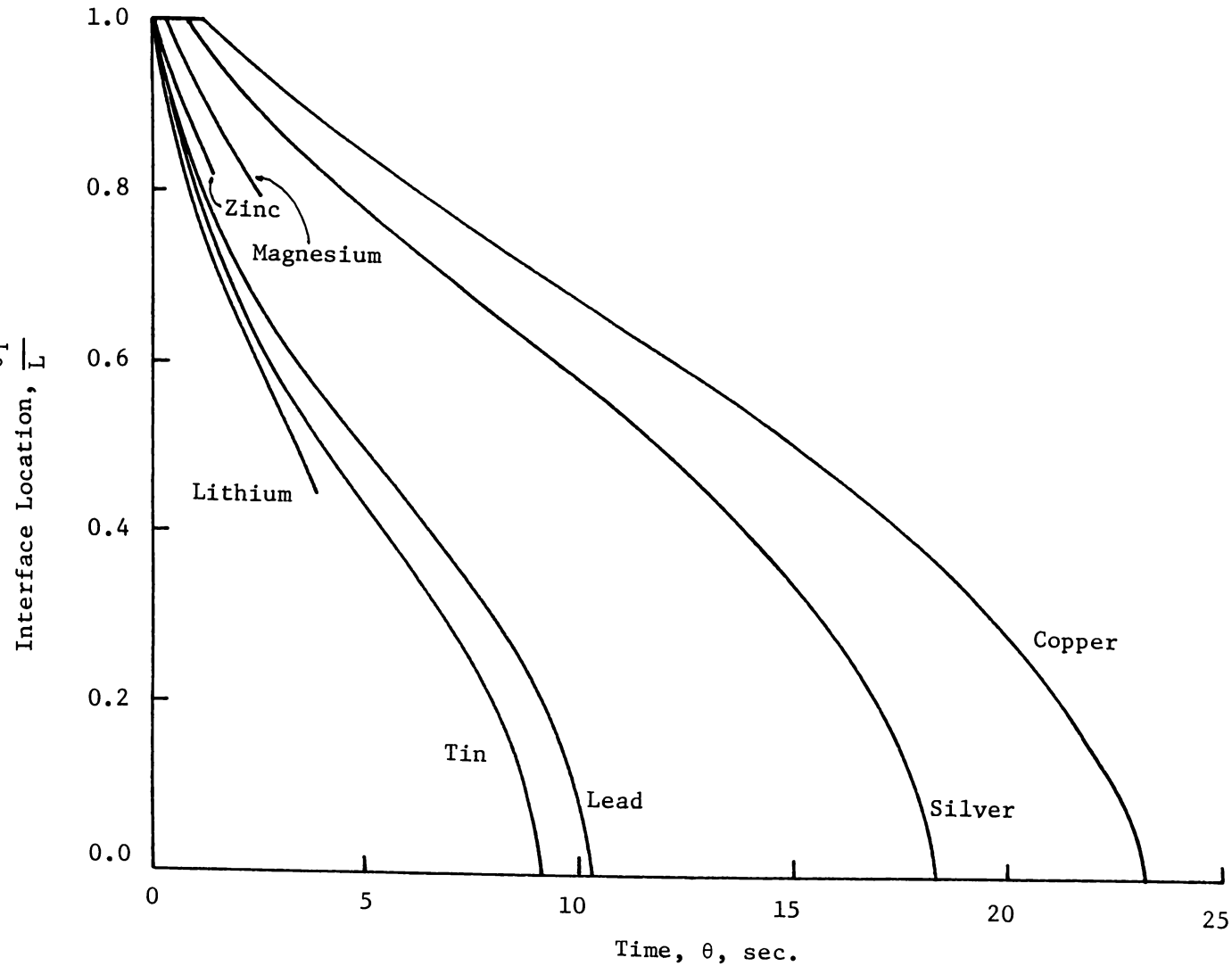

Figure 15: Liquid-Solid Interface Recession, Various Coolants, P=0.2

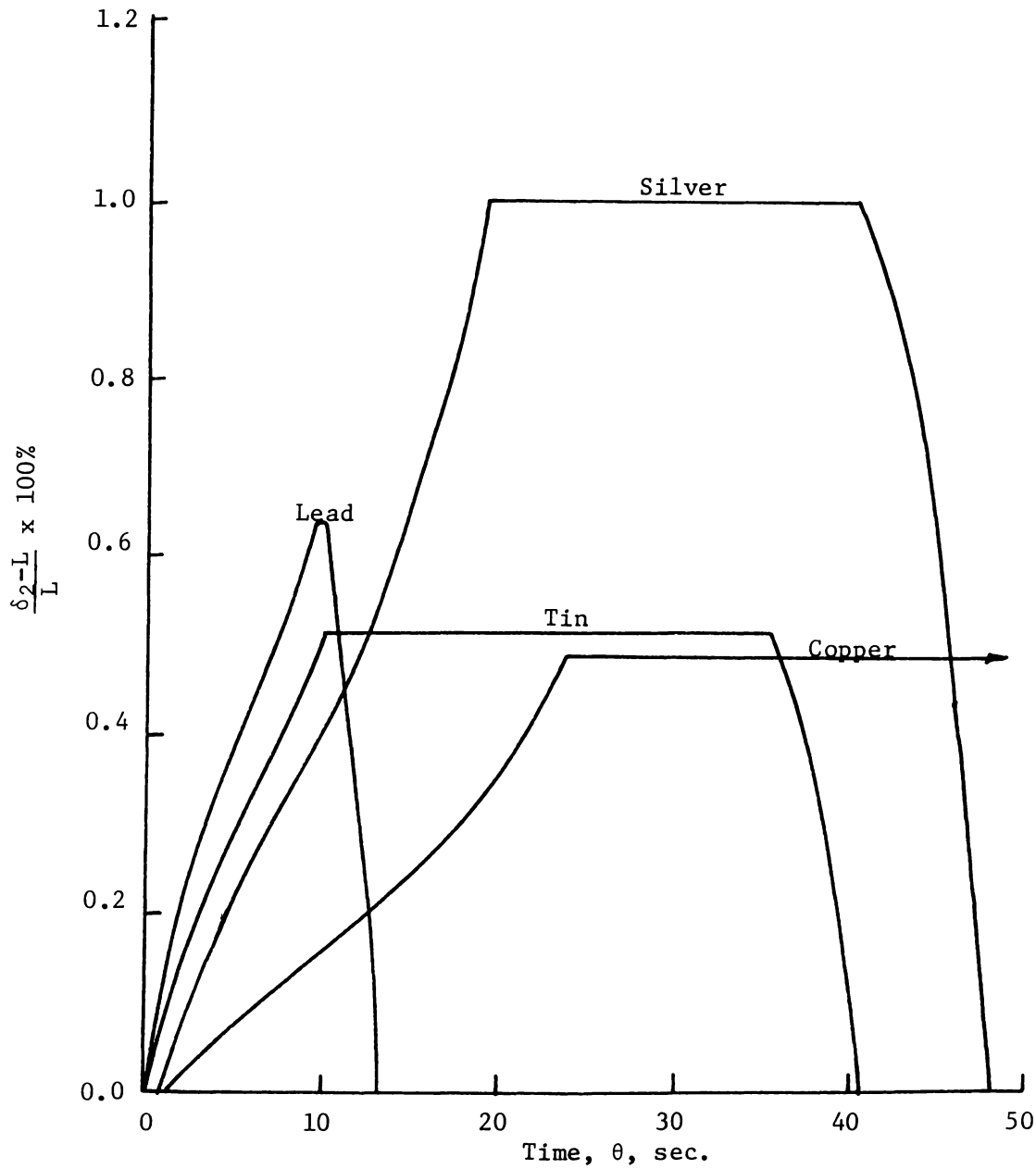

Figure 16: Growth and Depletion of Liquid Layer, Various Coolants, P=0.2

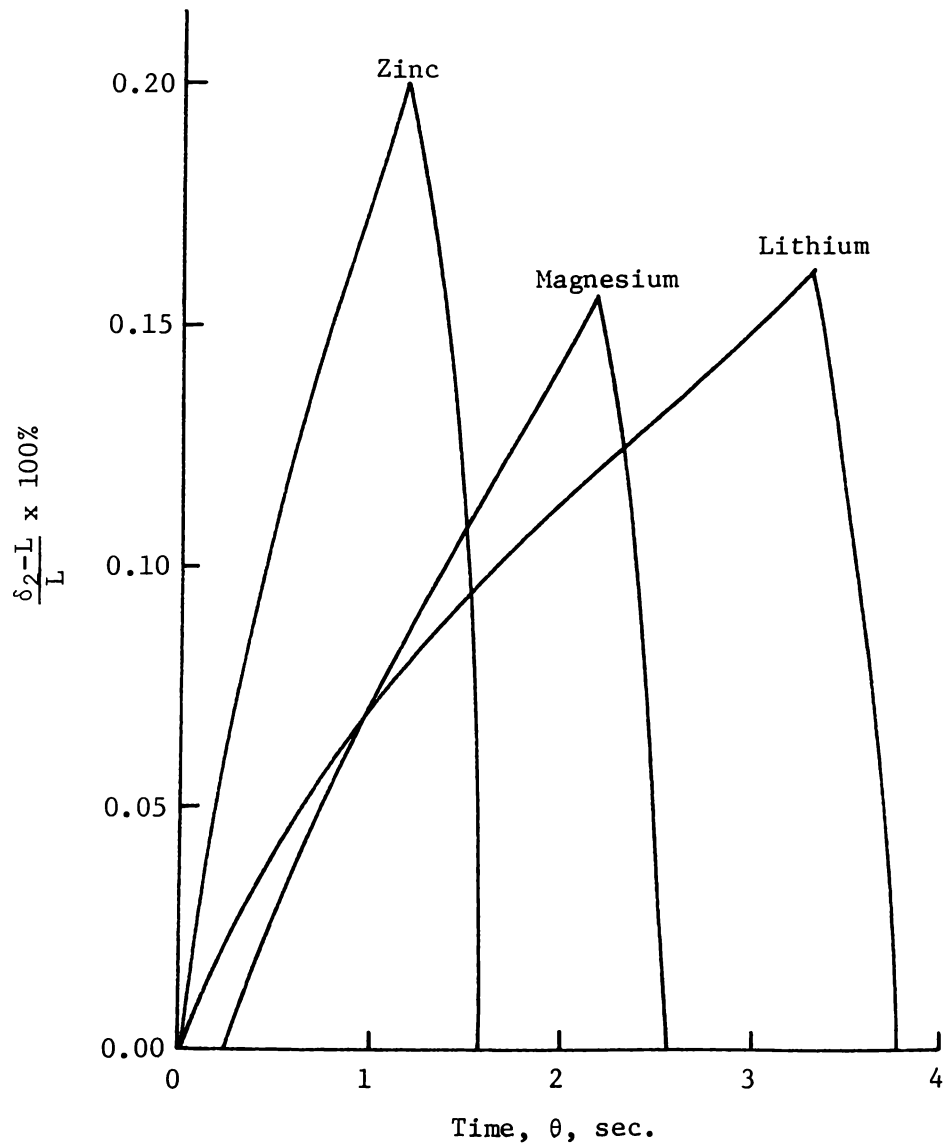

Figure 17: Growth and Depletion of Liquid Layer, Various Coolants, P=0.2

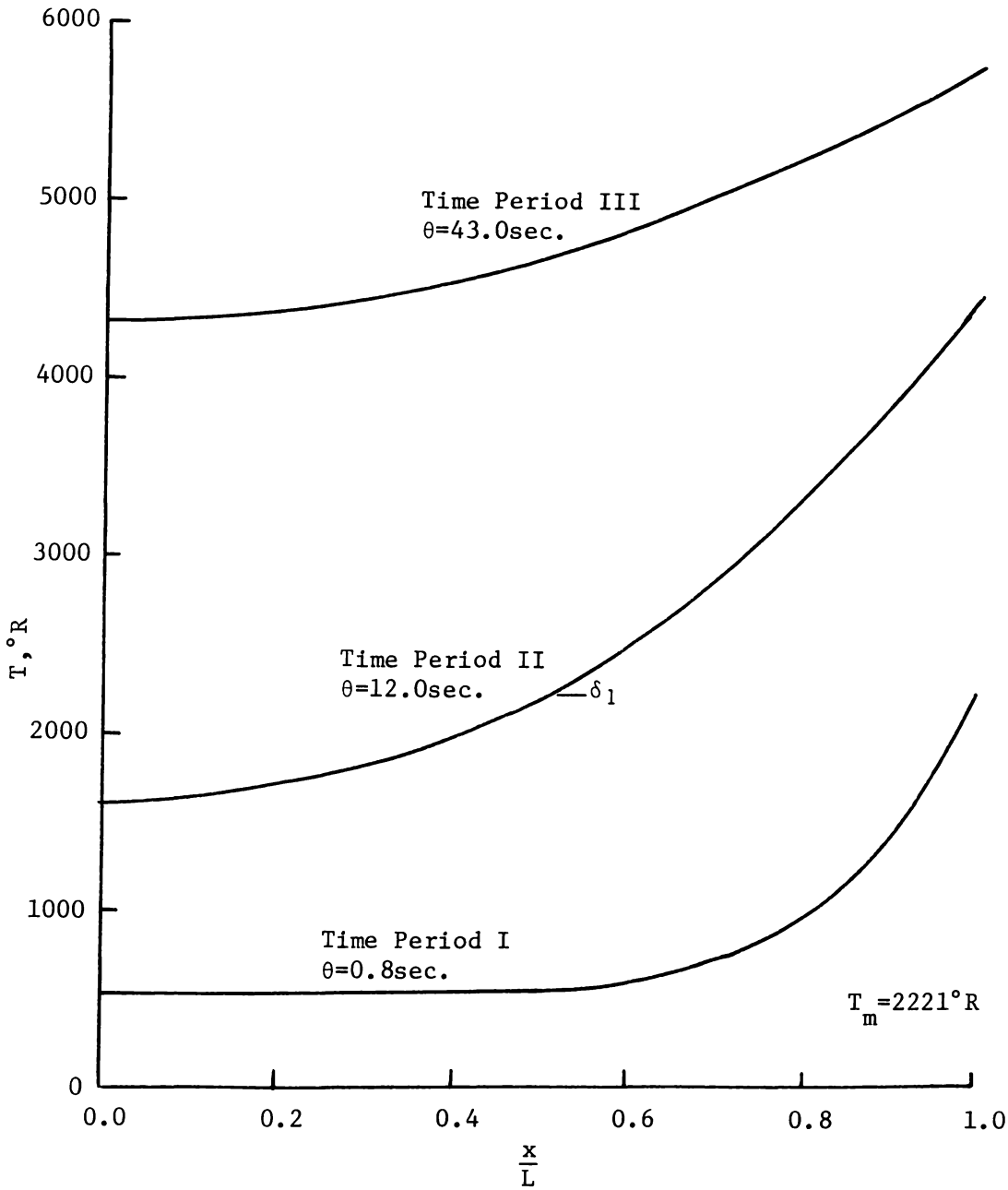

Figure 18: Typical Temperature Distributions, Silver, P=0.2

the curves of Figures 13, 14, and 15 terminate unless otherwise indicated. The temperature response of the original surface for the solid tungsten was obtained as a baseline of comparison by letting the porosity be zero. Data were also obtained for solid tungsten by again letting the porosity be zero and assigning a melting temperature of the coolant in excess of that of the matrix. This kept the analysis in time period I. A comparison of the two methods showed good agreement. A slight divergence of the surface temperature was noted when the equations of time period II were first employed but after a reasonable number of time increments convergence to the solution using time period I only was obtained. The author feels that this was due to assumptions made for the surface temperature relation in the development of the expression to predict the location of the liquid-solid interface, equation (4.42). Also, data were obained for solid tungsten using the thermal properties of (2). A comparison with data reported in (2) showed excellent agreement throughout the entire heating period.

1. Effect of Various Coolants in a Constant Matrix

The data presented in Figures 13 and 18 are for a tungsten matrix of 20 percent porosity. It can be seen in Figure 13 and 14 that the rate of surface temperature rise was retarded to varying degrees by the coolants investigated. Matrices infiltrated with lead, tin, and lithium result in surface temperatures somewhat higher than that of solid tungsten. This does not, however, rule out

the possibility that these may be effective coolants since no comparison is made at times greater than $\theta = \theta_3$. It is possible that the rate of surface temperature rise may be greatly retarded by vaporization of these coolants from within the matrix. The reader is again referred to reference (2) for this effect. The recession rates of the liquid-solid interfaces and the growth and depletion of the liquid layers are compared in Figures 15 through 17 for the various coolants. Typical temperature distributions throughout the composite for the various time periods are shown in Figure 18 for the silver coolant at 20 percent porosity.

Due to the relatively high boiling point of silver, the total time until recession of the vapor-liquid interface to the original surface (θ_3) does not occur until 48.6 seconds. During the early stages of the heating period the temperature of the heated surface is less than that of the solid tungsten slab as a result of the increased conductivity of the composite due to the high conductivity of the infiltrant. This effect diminishes as the boiling point of silver ($5705^{\circ}F$) is approached at the exposed surface of the liquid layer, as evidenced by the approach of the silver curve to that of the solid tungsten curve in Figure 13. The importance of the liquid layer is indicated by the relatively flat portion of the surface temperature response curve, Figure 13, which corresponds to time period III. Even though the maximum possible thickness of the liquid layer is attained (about 1.0 percent of the total composite thickness) the temperature difference across

the liquid layer is small compared to other coolants due to the high conductivity of silver. This factor, as well as the relatively high latent heat of vaporization of silver, accounts for the essentially constant temperature at the original surface during time period III. Since the difference between the melting point ($2221^{o}R$) and boiling point ($5705^{o}R$) of silver is relatively large, there exists a portion of time period II in which the liquid-solid interface has receded to the insulated back face and a constant-thickness liquid layer remains on the surface. This is shown in Figure 16. The relatively flat portion of the surface temperature response curve is an indication of the effect of the melting process. Figure 13 shows that for silver, the rate of rise of the surface temperature is practically eliminated for a considerable period of time.

Since the boiling point of copper at the pressure of the hot-gas stream is higher than the melting temperature of the tungsten matrix, the original surface of the matrix begins to melt while there exists a liquid layer above the surface. Due to the relatively high conductivity of copper, the temperature at the original surface of the composite remains substantially lower than that of the solid slab during the early stages of the heating period. However, the curves converge as the melting temperature of the matrix is approached. Therefore, the advantage of infiltrating with copper is limited.

The behavior of tin, as might be anticipated, is very similar to that of silver since their boiling points are about the same.

Due to the lower melting point of tin (1081°R), liquid-solid interface recession occurs much sooner. Also, due to its smaller volume change on fusion, the maximum thickness of the liquid layer (0.5 percent of total composite thickness) is much less than that of silver. The portion of the surface-temperature response curve that corresponds to time period III is not as flat as that of silver due to the low conductivity of tin. The relatively poor thermal diffusivity of the composite also causes the surface to run hotter than the tungsten slab during early heat-up stages.

Lead possesses the same general characteristics as tin. Due to the lower boiling point of lead (4875°R), however, vaporization of the coolant below the original surface occurs at an earlier time (θ_3 = 13.3 sec.). It is interesting to note that the difference between the melting (1081°R) and the boiling (4875°R) temperatures are such that complete liquid-solid interface recession occurs (10.0 sec.) shortly after vaporization at the exposed surface begins (9.4 sec.). As shown in figure 13, when vaporization begins there is a decrease in the rate of rise of the surface temperature. However, when the flow of liquid onto the surface ceases an increase of the surface temperature is immediately seen.

Lithium, magnesium, and zinc have relatively low boiling points. In all cases, vaporization of the coolant begins well before 5.0 seconds of heating time is completed. Figure 15 and 17 show that complete liquid-solid interface recession is not obtained before vaporization begins (θ_2) and only minimal liquid layer growth is accomplished. However, the effect of the melting process (time

period III) can be seen from Figure 14 to occur during a time when the rate of surface temperature rise is greatest and therefore affords valuable inhibition of the surface temperature rise.

2. Effect of Varying Porosity

All of the cases previously examined have considered variable properties and a constant matrix porosity fixed at 20 percent. Due to its relatively constant surface temperature during time period III, silver was chosen to show the effect of varying porosity. The surface temperature responses for various porosities are shown in Figure 19. Data were obtained for porosities of 10, 20, and 30 percent. A considerable increase in conduction cooling is seen as the porosity is increased for early stages of the heating period due to the high conductivity of silver compared to that of the tungsten matrix. The tendency for conduction cooling effects to diminish as the boiling temperature of the coolant at the exposed surface is approached is apparent. An interesting fact is that recession of the liquid-solid interface for each silver case ceased at essentially the same time (18 sec.). This is again thought to be due to the increased conductivity of the composites as the porosity increases. The major advantage of increasing the porosity is seen to be in the increased length of the flat portion of the temperature response curve (time period III). This does not, however, indicate that longer heating times may be obtained by increasing the porosity. Gessner (2) reports that the surface temperature response curves for

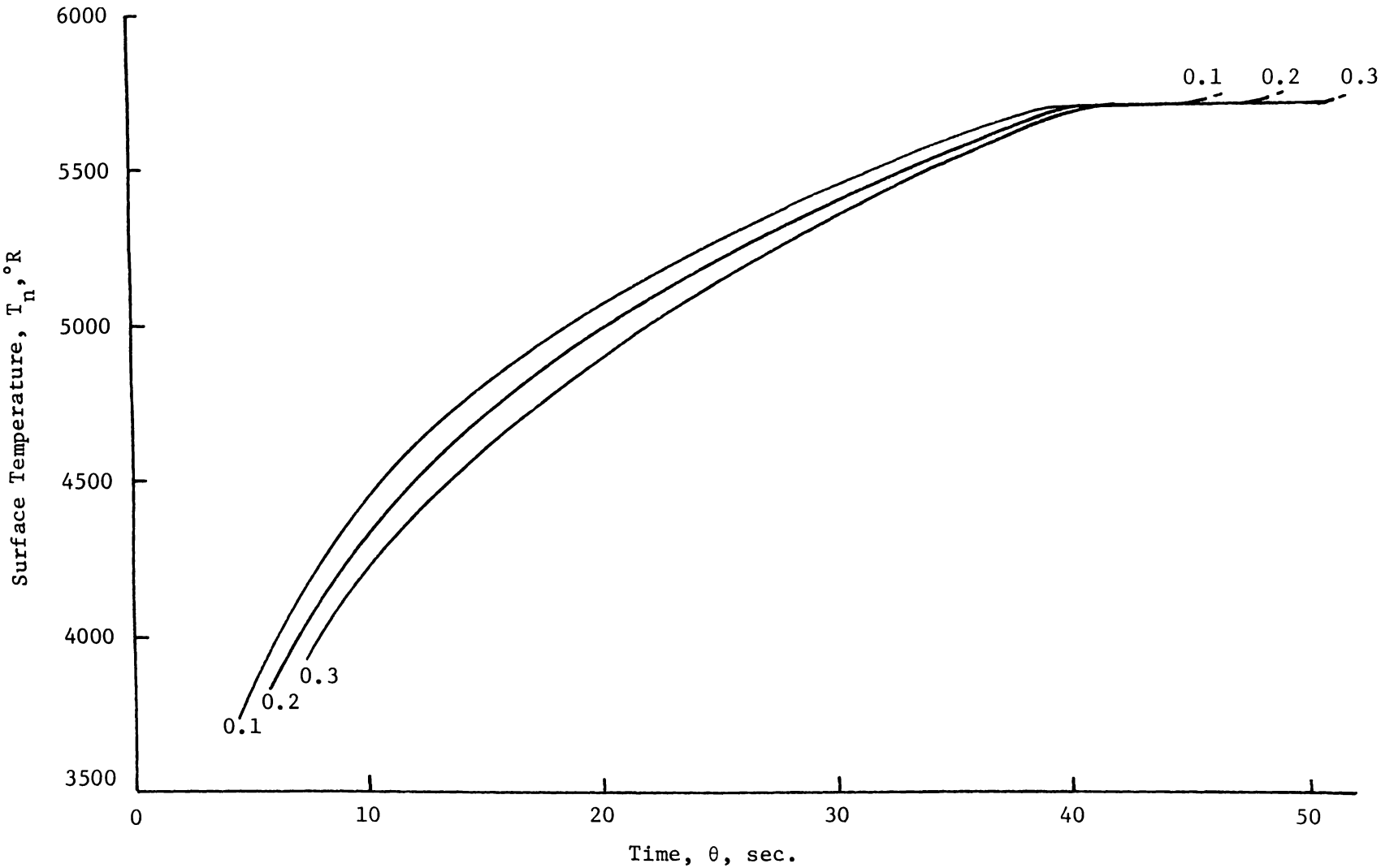

Figure 19: Surface-Temperature Response, Silver, Varying Porosity

silver coolants with porosities of 20 and 80 percents converge as vapor-liquid interface recession below the heated surface preceeds. It is suggested that a graded matrix with highest porosity at the exposed surface would be more efficient in increasing allowable heating time (2). In any case, a compromise between porosity, mechanical strength, and manufacturing limitations must be made.

3. Effect of Variable Properties

All data presented up to this point have been calculated using variable thermal properties as tabulated in Chapter V. To determine the effect of variable property values on the analysis, the data must be compared to data obtained using constant properties. This presents the question as to what constant values to compare with: room temperature, average temperature over the entire temperature range anticipated, or an average over the temperature range for each phase anticipated. The author feels that the most representative constant values that can be used is the average value over the temperature range for each particular phase. This is expected to minimize any effect of using constant properties in the calculation. The values used in (2) appear to be an average over the entire temperature range and are not comparable to this data as previously discussed. A comparison of data obtained using variable and average properties is shown in Figure 20. It is seen that the surface temperatures using average properties are somewhat lower than those when variable properties are assumed. This comparison indicates the necessity of using variable thermal properties.

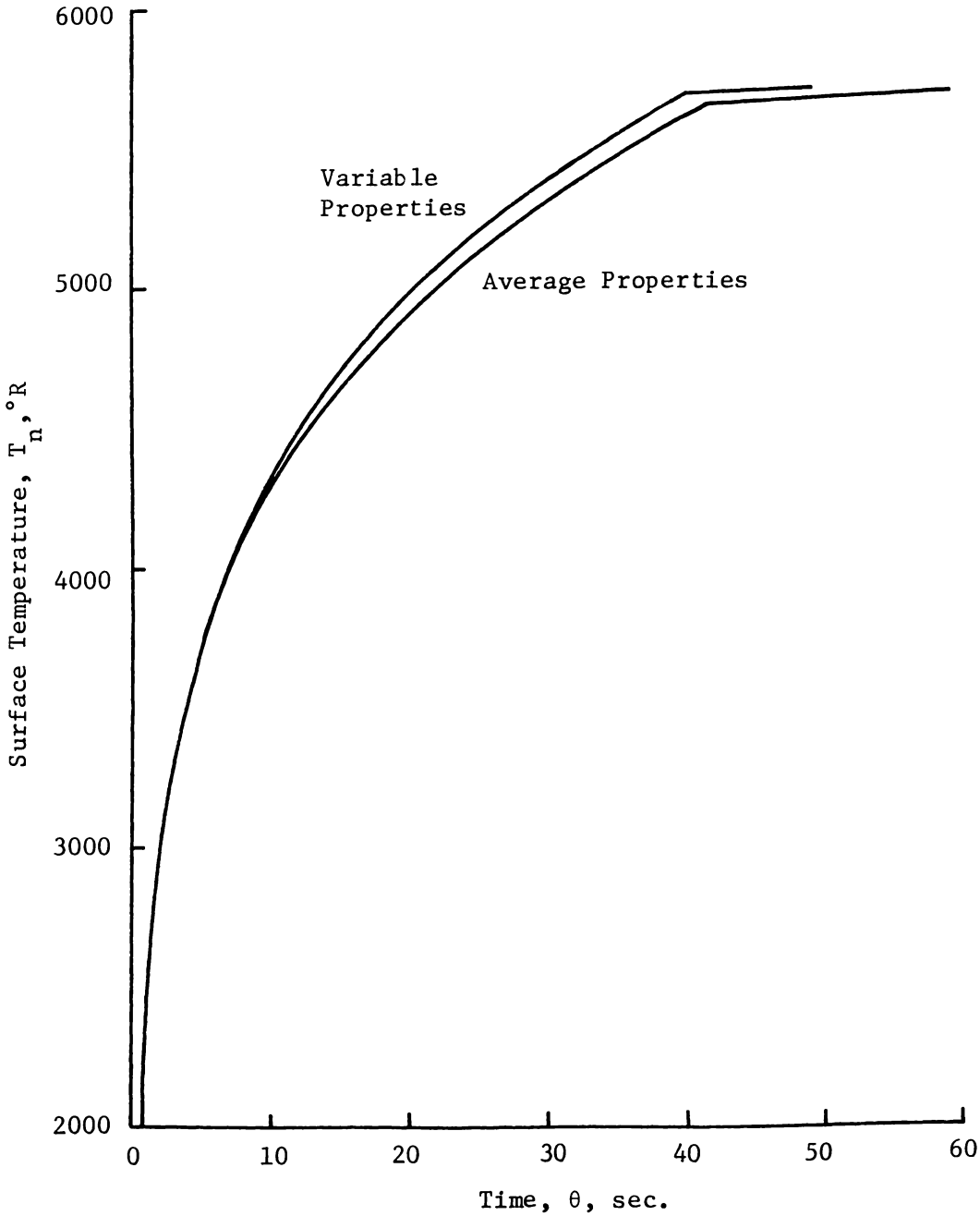

Figure 20: Effect of Variable Properties, Silver, P=0.2

Also, it is noted that in some cases small differences in a particular constant property, especially those of the matrix, lead to large differences in the surface-temperature responses. The increased length of time period III, as indicated by the flat portion of the surface-temperature response curve, for constant property data is misleading in that the amount of liquid that expands onto the surface is directly related to the difference in the densities of the solid and liquid coolant at the melting point. This is normally from 2.0 to 7.0 percent of the solid density. When average values for each phase are used, this becomes nearly 13.0 percent, which increases the maximum liquid-layer thickness by more than twofold.

C. Conclusion

Based upon the results of the case studies using the numerical computer solution of the detailed finite-difference analysis, a fundamental understanding of the early stages of the self-cooling processes was gained. It was shown that the effect of the melting process on the temperature response of the heated composite surface can be of great importance, in that in some cases, the temperature of the surface remains essentially constant while vaporization of the liquid layer occurs. It was emphasized however that any boundary layer shearing or erosion effects have been neglected in this analysis and that the analysis did not consider the latter stages of the heating process when vaporization of the coolant proceeds below the

exposed surface of the composite. The need for accurate thermal properties for both the coolant and matrix materials was demonstrated. Also, the effect of assuming properties that vary with temperature in lieu of constant properties was seen to be significant. The results indicate a coolant with high conductivity or thermal diffusivity increases the contribution of the conduction cooling during the early stages of heating. High volume change on fusion is desired for maximum layer thickness above the surface. Also, a high latent heat of vaporization is desirable in that it decreases the rate of original surface temperature rise during time period III when vaporization of the liquid layer above the surface takes place. The concept of a composite that retards its own heating rate by sacrificing its coolant has been verified as theoretically sound and it is seen that the effect of the melting process can be of considerable significance on the duration of the heating period.

VII. CONCLUSIONS

In this investigation of self-cooling with infiltrated porous tungsten composites, the following significant conclusions are drawn. The conclusions are based on the results obtained from the theoretical analysis up to that time at which the liquid layer vaporizes completely from above the composite surface.

1. The effect of the melting process on the early stages of the self-cooling process is significant for certain combinations of infiltrant thermophysical properties.
2. There exists a period of time during which a stable liquid layer builds up above the original surface due to the expansion of the coolant on melting.
3. The rate of rise of the original surface temperature is suppressed to varying degrees for the different coolants due to the vaporization of the liquid coolant above the surface.
4. Considering thermal properties that vary with temperature has a significant effect on the determination of an accurate value for the temperature at the composite surface.
5. Infiltrants that possess high values of thermal conductivity, volumetric expansion on melting, and latent heats of fusion and vaporization tend to maximize the effect of the melting process.

6. No conclusions are drawn as to the most effective infiltrant since results were not obtained for the time period during which vaporization takes place from within the matrix.

VIII. RECOMMENDATIONS

It is recommended that future studies in the area of self-cooling with infiltrated porous composites be directed toward:

1. Determining the effect of any shearing or erosion at the surface of the liquid layer due to the boundary layer.
2. The expulsion of liquid coolant by mechanisms other than thermal expansion.
3. The effect of evaporation processes other than boiling.
4. Extension of the basic analysis to include capabilities of a graded matrix porosity.
5. Consideration of coolants other than metals.
6. Consideration of matrices other than tungsten.
7. Extension of the analysis for a three-dimensional model.

A complete one-dimensional analysis is of basic importance in a fundamental understanding of the self-cooling concept. However, a three-dimensional geometry which is typical of actual rocket nozzle conditions must be considered before the self-cooling concept can be applied with any reliability to the design of rocket nozzle liners.

IX. APPENDIX A

Presentation and Discussion of the Computer Program

The following discussion applies to the computer program listed at the end of this appendix.

Use of the Program

Equations frequently used in the analysis are listed at the beginning of the program and designated as function statements so that they may be called at any time. In general, symbols used in the program are the same as those given in the nomenclature. It is understood, however, that subscripts must be written as part of the symbol name; for example, KML = $k_{m\ell}$. Greek symbols are partially spelled so they may be recognized as those given in the nomenclature. Throughout the program, all primed quantities are designated by the letters PR following the symbol name. The function statements are, in general, self-explanatory. Possible exceptions are as follows:

TFPR1 - The general explicit finite-difference equation for nodal point 1.

TFPR2 - The general explicit finite-difference equation for an internal nodal point.

TFPR3 - The general implicit finite-difference equation for the nodal point at the original surface.

TFPR4 - The generalized interpolation equation.

The remainder of the function statements are for evaluation of thermal properties.

The read-in procedure is best described with reference to the

sample input data shown at the end of the program. The data are read in as follows:

Card 1 - The coolant name

Card 2 - The total number of nodal points, O1, O2, and O3. The last three numbers refer to the print-out options available within the program and will be discussed later.

The following constants, as given in the nomenclature, are read in on cards 3, 4, and 5:

Card 3 - L, P, T_m, A, B, T_{mm}, T_o

Card 4 - M, T_{nb}, T_c, λ_{nb}, g_c, R, h_o

Card 5 - λ_m, P_o

The next two data cards prescribe the initial temperature distribution for the composite:

Card 6 - The total number of temperatures to be read-in. For the sample data the initial temperature distribution is constant throughout the matrix. Therefore, only one temperature was needed.

Card 7 - The initial temperature at each nodal point. The temperatures are assigned to the nodal points according to the following rule: the last temperature read in is assigned to nodal point n, the next to last temperature to nodal point n-1, etc. The first temperature read in is assigned to the nodal point

next in the above sequence, and also to the remaining nodal points down to the back face, nodal point 1. Additional cards may be needed for the initial temperatures.

The remaining data cards contain the constants needed in the polynominals that calculate the variable properties as discussed in Chapter V. Provisions are made in the program for a fourth-order polynominal whereas one of second order was used in the analysis. The constants are contained on the data cards as follows:

Card 8 - d_{m1}, d_{m2}, d_{cs1}, d_{cs2}

Card 9 - a_{m1}, a_{m2}, a_{m3}, a_{m4}, a_{m5}

Card 10 - b_{m1}, b_{m2}, b_{m3}, b_{m4}, b_{m5}

Card 11 - a_{cs1}, a_{cs2}, a_{cs3}, a_{cs4}, a_{cs5}

Card 12 - $a_{c\ell 1}$, $a_{c\ell 2}$, $a_{c\ell 3}$, $a_{c\ell 4}$, $a_{c\ell 5}$

Card 13 - a_{cv1}, a_{cv2}, a_{cv3}, a_{cv4}, a_{cv5}

Card 14 - b_{cs1}, b_{cs2}, b_{cs3}, b_{cs4}, b_{cs5}

Card 15 - $b_{c\ell 1}$, $b_{c\ell 2}$, $b_{c\ell 3}$, $b_{c\ell 4}$, $b_{c\ell 5}$

Card 16 - $d_{c\ell 1}$, $d_{c\ell 2}$, $d_{c\ell 3}$, $d_{c\ell 4}$, $d_{c\ell 5}$

Card 17 - α_1, α_2, α_3, β

Formats for the input data may be obtained from the program.

As previously mentioned, the program contains several print-out options. The time interval of print-out is controlled by the input value O2. If O2 is an integer greater than zero, print-out is executed every O2 intervals, in addition to the key intervals ($\theta = \theta_1, \theta_2, \theta_3$). For O2 equal zero, print-out is executed at the

nearest time interval to 03. The sample data shows print-out every 0.00027766 hours (1 sec.) as well as at key intervals. The form of the print-out is controlled by the character 01. There are two options. The following data are obtained with either option: θ (sec.), T_m, $\dot{m}_\ell$, δ_1, T_v, $\dot{m}_v$ and δ_2. The options control the following output for each nodal point.

For 01 = 1, Distance from back face, temperature, pressure, conductivity, and thermal diffusivity.

For 01 = 2, Distance from back face, temperature and pressure.

All output, with the exception of time, which is given in seconds, is consistent with the units in the nomenclature.

The program is terminated if one of the following conditions are attained:

a. The end of time period III.

b. The temperature of the original surface exceeds the melting temperature of the matrix.

c. Time exceeds 200 seconds.

Program Limitations

There are certain circumstances that could possibly occur which the program is not designed to handle. They are as follows:

a. Coolants with a difference between melting and boiling points sufficiently small such that vaporization occurs at the surface of the liquid layer before the liquid-solid interface recedes below nodal point n-1.

b. Liquid-solid interface recession of more than two distance increments ($2\Delta x$) in one time increment ($\Delta\theta$).

c. Both liquid-solid and vapor-liquid interfaces lie between two adjacent nodal points.

d. Coolants that contract on melting.

It is suggested that any problems encountered due to circumstances a through c above may be alleviated by sufficiently increasing the number of nodal points.

COMPUTER PROGRAM
SELF-COOLING WITH INFILTRATED POROUS COMPOSITES

```
C DECLARATIONS
      INTEGER O1, O2, V1, V2, V1PR, V2PR
      REAL  L, M, MPR, ML, MLPR, MV, MVPR, MF, MFPR, MLPR1, MVPR1,
     1          MVPR2, K, KPR, KA, KB, KC, KM, KAPR, KBPR, KF, KMS,
     2          KML, KMSPR, KMLPR, KMPR, KCS, KCL, KCV, KFPR, LA,
     3          LB, LC, LAPR, LBPR, LDAM, LDAV, LDA, LDAPR, MUCV,
     4          MUCVPR, MUF, MUFPR, KMF, KCSF, KCLF, MUCVF, LDAVF,
     5          MOLWT, LDAVNB, KMV, KLPR,KL,KFA, KFB, KFAPR, KFBPR
      DIMENSION  T(200), TPR(200), X(200), A(200), APR(200),
     1          K(200), KPR(200), P(200), PPR(200)
C ARITHMETIC-FUNCTION STATEMENTS
      TFPR1(I,J) = TI + 2.0*AF/KF*DLTH/DLX**2*KFA*(TA - TI)
      TFPR2(I,J) = TI + DLTH*AF/KF/DLX**2*(KFB*(TB - TI) + KFA*(TA - TI)
     1          ) + MF*DLTH*AF/KF/DLX*(CCFB*(TI + TB)/2.0 - CCFA*(TI +
     2          TA)/2.0)
      TFPR3(I,J) = (TI*KFPR/AFPR/DLTH*LBPR**2 + 2.0*KFPR*TBPR + (HO*LBPR
     1          /KFPR*(3.0*KFPR - KFBPR - LBPR*MFPR*CCPR))*TO)/(KFPR/AFPR
     2          /DLTH*LBPR**2 + 2.0*KFPR + HO*LBPR/KFPR*(3.0*KFPR - KFBPR
     3          - LBPR*MFPR*CCPR))
      TFPR4(I,J) = (TI/DLTH*(LB*KFA+LA*KFB)/(LB*AFA + LA*AFB)
     1          - MF*CCF/LA/LB*(LB**2*TPRA - LA**2*TPRB)/(LA + LB)
     2          + (KFA*(3.0*LB**2*TPRA + LA*(2.0*LB - LA)*TPRB) +
     3          KFB*(3.0*LA**2*TPRB + LB*(2.0*LA - LB)*TPRA))/LA/LB
     4          /(LA + LB)**2)/ (((3.0*LB - LA)*KFA +(3.0*LA - LB)
     5          *KFB + (LA**2 - LB**2)*MF*CCF)/LA/LB/(LA +LB) + 1.0
     6          /DLTH*(LB*KFA + LA*KFB)/(LB*AFA + LA*AFB))
      TVAP(PV) = B/(A1- ALOG10(PV))
      CMF(TF) = AMF1 + AMF2*TF + AMF3*TF**2 + AMF4*TF**3 + AMF5*TF**4
      KMF(TF) = BMF1 + BMF2*TF + BMF3*TF**2 + BMF4*TF**3 + BMF5*TF**4
      RHOMF(TF) = 1.0/(DMF1 + DMF2*TF)
      CCSF(TF) = ACSF1 + ACSF2*TF + ACSF3*TF**2 + ACSF4*TF**3
```

```
     1          + ACSF5*TF**4
      CCLF(TF) = ACLF1 + ACLF2*TF + ACLF3*TF**2 + ACLF4*TF**3
     1          + ACLF5*TF**4
      CCVF(TF) = ACVF1 + ACVF2*TF + ACVF3*TF**2 + ACVF4*TF**3
     1          + ACVF5*TF**4
      KCSF(TF) = BCSF1 + BCSF2*TF + BCSF3*TF**2 + BCSF4*TF**3
     1          + BCSF5*TF**4
      KCLF(TF) = BCLF1 + BCLF2*TF + BCLF3*TF**2 + BCLF4*TF**3
     1          + BCLF5*TF**4
      RHOCSF(TF) = 1.0/(DCSF1 + DCSF2*TF)
      RHOCLF(TF) = DCLF1 + DCLF2*TF + DCLF3*TF**2
     1          + DCLF4*TF**3 + DCLF5*TF**4
      RHOCVF(TF,PF) =  PF*MOLWT/R/TF
      MUCVF(TF) = SQRT(MOLWT)            *((0.0915*(TF/TNB)**0.645
     1          - 0.0307)/(1.18*TF/TNB)**(0.9*ALOG10(1.18*TF/TNB)))
     2          /TNB**(1./6.)
      LDAVF(TF) = LDAVNB*((TCCR - TF)/(TCCR - TNB))**0.38
      KMV(TF) = KMF(TF)*(1.0 - POR)
      AMV(TF) = KMF(TF)/RHOMF(TF)/CMF(TF)
      KML(TF) = KMF(TF)*(1.0 - POR) + KCLF(TF)*POR
      AML(TF) = KML(TF)/(RHOMF(TF)*CMF(TF)*(1.0 - POR) + RHOCLF(TF)
     1          *CCLF(TF)*POR)
      KMS(TF) = KMF(TF)*(1.0 - POR) + KCSF(TF)*POR
      AMS(TF) = KMS(TF)/(RHOMF(TF)*CMF(TF)*(1.0 - POR)
     1          + RHOCSF(TF)*CCSF(TF)*POR)
      ALPHA(TF) =ALPHA1 + ALPHA2*TF + ALPHA3*TF**2
C READ STATEMENTS
     1 READ(5,9)COOL1,COOL2,COOL3,COOL4
     9 FORMAT(4A6)
       READ(5,10) N, O1, O2, O3
    10 FORMAT(I5,I5,I5,F15.0)
     2 READ(5,20) L, POR, TMELT, A1,B, TMLTMX, TO, MOLWT, TNB,
      1          TCCR, LDAVNB, GC, R, HO,LDAM, PO
    20 FORMAT((7F10.0))
```

```
    3 READ(5,30) N1, (T(I), I=1,N1)
      DO 28 I=1,N
      J = N-I+1
      IF(J-N+N1-2) 27,26,26
   26 J1 = J-N+N1
      T(J) = T(J1)
      GO TO 28
   27 T(J) = T(1)
   28 CONTINUE
   30 FORMAT(I10/(7F10.0))
    4 READ(5,40) DMF1,DMF2,DCSF1, DCSF2, AMF1, AMF2, AMF3, AMF4,
     1          AMF5, BMF1, BMF2, BMF3, BMF4, BMF5,  ACSF1, ACSF2,
     2          ACSF3, ACSF4, ACSF5, ACLF1, ACLF2, ACLF3, ACLF4,
     3          ACLF5, ACVF1, ACVF2, ACVF3, ACVF4, ACVF5, BCSF1,
     4          BCSF2, BCSF3, BCSF4, BCSF5, BCLF1, BCLF2, BCLF3,
     5          BCLF4, BCLF5, DCLF1, DCLF2, DCLF3, DCLF4, DCLF5,
     6          ALPHA1, ALPHA2, ALPHA3, BETA
   40 FORMAT (4E10.0/(5E10.0))
C WRITE OUT ALL QUANTITIES WHICH HAVE BEEN READ IN.
      WRITE(6,110)
  110 FORMAT(1H1,48HSELF-COOLING WITH INFILTRATED POROUS COMPOSITES.//)
      WRITE(6,109)COOL1,COOL2,COOL3,COOL4
  109 FORMAT(1X,12HINFILTRANT =,4A6)
      WRITE(6,111)
  111 FORMAT(1X,14HINPUT VALUES--//)
      WRITE(6,112) N, L, POR, TMELT, A1, B, TMLTMX, TO, MOLWT, TNB,
     1          TCCR, LDAVNB, GC, R, HO, LDAM
  112 FORMAT(1X,2HN=,I5,5X,3HL =,F10.5,5X,10HPOROSITY =,F10.5,5X,
     1           7HTMELT =,F10.5,5X,4HA1 =,F10.5/1X,3HB =,E10.5,5X,
     2           8HTMLTMX =,F10.5,5X,4HTO =,F10.5,5X,7HMOLWT =,F10.5,5X,
     3           5HTNB =,F10.5/1X,6HTCCR =,F10.5,5X,8HLDAVNB =,F10.0,5X,
     4           4HGC =,E10.5,5X,3HR =,F10.5,5X,4HHO =,F10.5/1X,6HLDAM =,
     5           F10.5//)
      WRITE(6,41)DMF1,DMF2,DCSF1,DCSF2,AMF1,AMF2,AMF3,AMF4,
```

```
     1          AMF5,BMF1,BMF2 ,BMF3,BMF4,BMF5,ACSF1,ACSF2,ACSF3
  41 FORMAT(1X,5HDM1 =,E15.7,8X,5HDM2 =,E15.7,9X,6HDCS1 =,E15.7,
     1          //1X,6HDCS2 =,E15.7,7X,5HAM1 =,E15.7,9X,5HAM2 =,
     2          E15.7,//1X,5HAM3 =,E15.7,8X,5HAM4 =,E15.7,9X,5HAM5 =,
     3          E15.7//1X,5HBM1 =,E15.7,8X,5HBM2 =,E15.7,9X,5HBM3 =,
     4          E15.7//1X,5HBM4 =,E15.7,8X,5HBM5 =,E15.7,9X,6HACS1 =,
     5          E15.7//1X,6HACS2 =,E15.7,7X,6HACS3 =,E15.7//)
      WRITE(6,42)ACSF4,ACSF5,ACLF1,ACLF2,ACLF3,ACLF4,ACLF5,
     1          ACVF1,ACVF2,ACVF3,ACVF4,ACVF5,BCSF1,BCSF2,
     2          BCSF3,BCSF4,BCSF5,BCLF1
  42 FORMAT(1X,6HACS4 =,E15.7,7X,6HACS5 =,E15.7,8X,6HACL1 =,
     1          E15.7//1X,6HACL2 =,E15.7,7X,6HACL3 =,E15.7,8X,
     2          6HACL4 =,E15.7//1X,6HACL5 =,E15.7,7X,6HACV1 =,
     3          E15.7,8X,6HACV2 =,E15.7//1X,6HACV3 =,E15.7,7X,
     4          6HACV4 =,E15.7,8X,6HACV5 =,E15.7//1X,6HBCS1 =,
     5          E15.7,7X,6HBCS2 =,E15.7,8X,6HBCS3 =,E15.7//1X,
     6          6HBCS4 =,E15.7,7X,6HBCS5 =,E15.7,8X,6HBCL1 =,E15.7//)
      WRITE(6,43)BCLF2,BCLF3,BCLF4,BCLF5,DCLF1,DCLF2,DCLF3,
     1          DCLF4,DCLF5,ALPHA1,ALPHA2,ALPHA3,BETA
  43 FORMAT(1X,6HBCL2 =,E15.7,7X,6HBCL3 =,E15.7,8X,6HBCL4 =,
     1          E15.7//1X,6HBCL5 =,E15.7,7X,6HDCL1 =,E15.7,8X,
     2          6HDCL2 =,E15.7//1X,6HDCL3 =,E15.7,7X,6HDCL4 =,
     3          E15.7,8X,6HDCL5 =,E15.7//1X,8HALPHA1 =,E15.7,5X,
     4          8HALPHA2 =,E15.7,6X,8HALPHA3 =,E15.7//1X,6HBETA =,
     5          E15.7//////)
      N2=1
      N3=MIN0(10,N)
  120 WRITE(6,130) (I,I=N2,N3)
      WRITE(6,131) (T(I),I=N2,N3)
  130 FORMAT(1X,6H    I =,10I10)
  131 FORMAT(1X,6HT(I) =,10F10.5)
      IF (N3-N) 121,122,122
  121 N2 = N2+10
      N3 = MIN0(N3+10,N)
```

```
      GO TO 120
  122 CONTINUE
C INITIALIZE NECESSARY VARIABLES
      DLX = L/(FLOAT(N) - 1.0)
      DLT1 = L
      DLT2 = L
      DLT1PR= DLT1
      DLT2PR= DLT2
      TH = 0.0
      M1 = N
      M2 = M1 - 1
      M1PR = M1
      M2PR = M2
      TH1 = 1.0E20
      V1 = 3*(N-1) + 1
      V2 = V1 - 2
      V1PR = V1
      V2PR = V2
      TH2 = 1.0E20
      TH3 = 1.0E20
      ML = 0.0
      MV = 0.0
      MLPR = 0.0
      MVPR = 0.0
      TM = TMELT
      TV = TM
      TVPR = TV
      DO 501 I=1,N
      X(I) = DLX*(FLOAT(I) - 1.0)
      P(I) = P0
      K(I) = KMS(T(I))
      A(I) = AMS(T(I))
  501 CONTINUE
C WRITE OUT DESIRED QUANTITIES AT TIME THETA
```

```
      N1 = 0
 1000 CONTINUE
      THSEC = 3600.0*TH
      N1 = N1 + 1
      IF(N1.EQ.1.OR.TH.EQ.TH1.OR.TH.EQ.TH2.OR.TH.EQ.TH3.OR.TH.EQ.
     1          TH4)   GO TO 1060
      IF(O2-1) 1040, 1060, 1020
 1020 IF(MOD(N1-1,O2).EQ.0)  GO TO 1060
      GO TO 1070
 1040 IF(AMOD(TH,O3).LT.0.5*DLTH.OR.(O3  - AMOD(TH,O3)).LT.0.5*
     1          DLTH)   GO TO 1060
      GO TO 1070
 1060 WRITE(6,1061) THSEC, TM, ML, DLT1, TV, MV, DLT2
 1061 FORMAT(//1X,6HTIME =,F10.5//1X,4HTM =,F10.5,5X,4HML =,F10.3,
     1          5X,6HDLT1 =,F10.5/1X,4HTV =,F10.5,5X,4HMV =,F10.3,
     2          5X,6HDLT2 =,F10.5)
      IF(O1.EQ.1) GO TO 1062
      GO TO 1065
 1062 WRITE(6,1063)
 1063 FORMAT(//1X,10X,1HX,19X,1HT,19X,1HP,19X,1HK,19X,1HA//)
      WRITE(6,1064) (X(I),T(I),P(I),K(I),A(I),I=1,N)
 1064 FORMAT (1X,2F20.5,E20.5,2F20.5)
 1065 IF(O1.EQ.2) GO TO 1066
      GO TO 1070
 1066 WRITE(6,1067)
 1067 FORMAT(//1X,10X,1HX,19X,1HT,19X,1HP//)
      WRITE(6,1068) (X(I),T(I),P(I), I=1,N)
 1068 FORMAT(1X,2F20.5,E20.5)
 1070 CONTINUE
C DETAILED CALCULATIONS FOR TIME PERIOD I.
      IF(TH.GE.TH1) GO TO 1499
      AMAX = AMAX1(AMS(T(1)),AMS(T(N)))
      KF = KMS(T(N))
      AF = AMS(T(N))
```

```
      DLTHA = DLX**2/2.0/AMAX
      DLTH4 = (TMELT - T(N))/(2.0*H0*AF/KF/DLX*(T0 - T(N)) -
     1          2.0*AF/DLX**2*(T(N) - T(N-1)))
      IF (DLTHA - DLTH4) 1201, 1202, 1202
 1201 DLTH = DLTHA
      THPR = TH + DLTH
      GO TO 1203
 1202 DLTH = DLTH4
      TPR(N) = TMELT
      DLT2PR = L
      DLT1PR = L
      THPR = TH + DLTH
      TH1 = THPR
      TM = TMELT
      TVPR = TM
 1203 CONTINUE
      TI = T(1)
      TA = T(2)
      AF = AMS(T(1))
      KF = KMS(TI)
      KFA = KMS((TI + TA)/2.0)
      TPR(1) = TFPR1(1,1)
      NM1 = N-1
      DO 1206 I = 2,NM1
      AF = AMS(T(I))
      KF = KMS(T(I))
      CC = CCSF(T(I))
      MF = 0.0
      TI = T(I)
      TA = T(I+1)
      TB = T(I-1)
      KFA = KMS((TI + TA)/2.0)
      KFB = KMS((TI + TB)/2.0)
      CCFA = CCSF((TI + TA)/2.0)
```

```
      CCFB = CCSF((TI + TB)/2.0)
      TPR(I) = TFPR2(I,1)
 1206 CONTINUE
      IF(THPR.EQ.TH1) GO TO 1210
      TPR(N) = T(N)
      TEST = T(N) - 1.0
 1204 MFPR = 0.0
      LBPR = DLX
      TBPR = TPR(N-1)
      KFPR = KMS(TPR(N))
      AFPR = AMS(TPR(N))
      CCPR = CCSF(TPR(N))
      TOPR = TO
      IF(TH.EQ.0.0)  TOPR = (T(N) + TO)/2.0
      HOPR = HO
      TI = T(N)
      KFBPR = KMS(TBPR)
      TPR(N) = TFPR3(N,1)
      IF(ABS(TPR(N) - TEST).LT.1.0E-2) GO TO 1210
      TEST = TPR(N)
      GO TO 1204
 1210 CONTINUE
      DO 1212 I=1,N
      KPR(I) = KMS(TPR(I))
      APR(I) = AMS(TPR(I))
 1212 CONTINUE
      MLPR = 0.0
      MVPR = 0.0
      TEST = 0.0
      NM1 = N-1
 1213 GO TO 1620
 1499 IF (TH.NE.TH1)  GO TO 1500
      M1 = N
      M2 = N-1
```

```
      DLT1 = L
      DLT2 = L
      ML = 0.0
      MV = 0.0
 1500 CONTINUE
C...DETAILED CALCULATIONS FOR TIME PERIODS II AND III.
 1502 IF (TH.GE.TH3) GO TO 2000
      AMAX = AMAX1(AMS(T(1)),AMS(TM),AML(TM),AML(T(N)),AML(T(1)))
      DLTHA = DLX**2/2.0/AMAX
      DLTH = DLTHA
 1504 IF(TH.GT.TH2.AND.TH.LT.TH3) GO TO 1506
      GO TO 1520
 1506 RHOCL = RHOCLF(TV)
      DLTH3 = RHOCL/(MV - ML)*(DLT2 - L)
      IF (DLTHA.LT.DLTH3.OR.DLTH3.LT.0.0) GO TO 1508
      DLTH = DLTH3
      TH3 = TH + DLTH
      DLT2PR = L
      TPR(N) = TVAP(P0)
      TVPR = TPR(N)
      GO TO 1520
 1508 DLTH = DLTHA
 1520 THPR = TH + DLTH
C...REGULAR EXPLICIT CALCULATIONS.
      IF (M2.LE.1) GO TO 1526
      AF = AMS(T(1))
      TI = T(1)
      TA = T(2)
      KF = KMS(TI)
      KFA = KMS((TI+TA)/2.0)
      TPR(1) = TFPR1(1,2)
      KPR(1) = KMS(TPR(1))
      APR(1) = AMS(TPR(1))
 1526 CONTINUE
```

```
C       FOR NODAL POINT 1 WHEN M2 IS LESS THAN 2
        IF(M2.GE.2) GO TO 1540
        IF(DLT1) 1532,1532,1530
 1530   DLT1PR = 0.0
        TPR(1) = TM
        MLPR = 0.0
        KPR(1) = KML(TM)
        APR(1) = AML(TM)
        TI = T(2)
        TPRA = TPR(3)
        LA = DLX
        TPRB = TM
        LB = DLX
        MF = 0.0
        CCF = CCLF(TI)
        KF = KML(TI)
        AMCF = AML(TI)
        TPR(2) = TFPR4(2,2)
        KPR(2) = KML(TPR(2))
        APR(2) = AML(TPR(2))
        GO TO 1540
 1532   AF = AML(T(1))
        TI = T(1)
        TA = T(2)
        KF = KML(T(1))
        KFA = KML((TI + TA)/2.0)
        TPR(1) = TFPR1(1,2)
        KPR(1) = KML(TPR(1))
        APR(1) = AML(TPR(1))
        DLT1PR = 0.0
        MLPR = 0.0
 1540   M2M1 = M2-1
        M1P1 = M1+1
        NM1  = N-1
```

```
      DO 1542 I=2,M2M1
      IF(M2M1.LT.2) GO TO 1542
      AF = AMS(T(I))
      KF = KMS(T(I))
      CC = CCSF(T(I))
      MF = 0.0
      TA = T(I+1)
      TB = T(I-1)
      TI = T(I)
      KFA = KMS((TI + TA)/2.0)
      KFB = KMS((TI + TB)/2.0)
      CCFA = CCSF((TI + TA)/2.0)
      CCFB = CCSF((TI + TB)/2.0)
      TPR(I) = TFPR2(I,2)
      KPR(I) = KMS(TPR(I))
      APR(I) = AMS(TPR(I))
1542  CONTINUE
      DO 1544 I = M1P1,NM1
      IF (M1P1.GT.NM1) GO TO 1544
      AF = AML(T(I))
      KF = KML(T(I))
      CC = CCLF(T(I))
      MF = ML
      TA = T(I+1)
      TB = T(I-1)
      TI = T(I)
      KFA = KML((TI + TA)/2.0)
      KFB = KML((TI + TB)/2.0)
      CCFA = CCLF((TI + TA)/2.0)
      CCFB = CCLF((TI + TB)/2.0)
      TPR(I) = TFPR2(I,2)
      KPR(I) = KML(TPR(I))
      APR(I) = AML(TPR(I))
1544  CONTINUE
```

```
C...CALCULATIONS FOR NODAL POINT N.
      IF(TH.GE.TH1.AND.TH.LT.TH2.AND.M1.LT.N) GO TO 1552
      GO TO 1556
 1552 TPR(N) = T(N) + AML(T(N))*DLTH*(2.0/DLX**2*(T(N-1) - T(N)) +
     1          ((3.0*KML(T(N)) - KML(T(N-1)))/DLX -ML*CCLF(T(N)))*
     2          (TO - T(N)) /  KML(T(N))**2/((DLT2 - L)/KCLF(T(N)) +
     3          1.0/HO))
      KPR(N) = KML(TPR(N))
      APR(N) = AML(TPR(N))
      DLTH1 = 1.0/(2.0*AML(T(N))*(1.0/DLX**2 + 0.5/KML(T(N))**2*HO*
     1         KCLF(T(N))/(DLT2 - L)*((3.0*KML(T(N)) - KML(T(N-1)))/DLX
     2          - ML*CCLF(T(N)))/(HO +KCLF(T(N))/(DLT2 - L))))
      IF (DLTH1.LT.DLTH) GO TO 1554
      GO TO 1556
 1554 DLTH = DLTH1*0.95
      GO TO 1520
 1556 CONTINUE
      IF(TH.GE.TH1.AND.TH.LT.TH2.AND.M1.EQ.N) GO TO 1560
      GO TO 1572
 1560 A5 = (L - DLT1)*(KML(TM)/AML(TM)*(T(N) - TM) + KMS(TM)/AMS(TM)
     1          *(TM - TPR(N-2)))
      A2 = KMS(TM)/AMS(TM)*(TPR(N-2) - T(N-2))*(DLT1 - DLX*(FLOAT(N)
     1          - 3.0))
      Q1 = HO*(TO - T(N))
      Q2 = KMS(T(N-2))**2*((TPR(N-2) - T(N-2))/AMS(T(N-2))/DLTH
     1          - 2.0*(T(N-1) - T(N-2))/DLX**2)/(KMS(T(N-1)) - 3.0*
     2          KMS(T(N-1)))*DLX
      A3 = 2.0*(Q1 - Q2)*DLTH + A5 + 2.0*RHOCSF(TM)*LDAM*POR*(L-DLT1)
      A4 = KMS(TM)/AMS(TM)*(TM - TPR(N-2)) + 2.0*RHOCSF(TM)*LDAM*POR
      DLT1PR = L - (HO*(A3 - A2) - A4*KML(TM) + SQRT((HO*(A3 - A2)
     1          - A4*KML(TM))**2 + 4.0*HO*(A4 + KML(TM)/AML(TM)*(TO - TM)
     2          )*(A3 - A2)*KML(TM)))/2.0/HO/(A4 + KML(TM)/AML(TM)*
     3          (TO - TM))
      IF (TH - TH1)1070,1562,1564
```

```
1562 MLPR = POR*(RHOCSF(TM) - RHOCLF(TM))*(DLT1 - DLT1PR)/DLTH
     ML = MLPR
     GO TO 1566
1564 MLPR = POR*(RHOCSF(TM) - RHOCLF(TM))*(DLT1 - DLT1PR)/DLTH
1566 CONTINUE
     TPR(N) =(HO*TO*(2.0/(L-DLT1PR) - MLPR*CCLF(TM)/KML(TM)) + T(N)*
    1          KML(TM)/AML(TM)/DLTH  +2.0*KML(TM)*TM/(L-DLT1PR)**2)/
    2          (KML(TM)/AML(TM)/DLTH +2.0*KML(TM)/(L-DLT1PR)**2 +HO*(
    3          2.0/(L-DLT1PR) - MLPR*CCLF(TM)/KML(TM)))
     IF (DLT1PR - L + DLX) 1568,1570, 1570
1570 TI = T(N-1)
     TPRA = TM
     LA = DLT1PR - L + DLX
     TPRB = TPR(N-2)
     LB = DLX
     MF = 0.0
     CCF = CCSF(TI)
     AFB = AMS(TPRB)
     AFA = AMS(TPRA)
     KFB = KMS(TPRB)
     KFA = KMS(TPRA)
     TPR(N-1) = TFPR4(N-1,2)
     KPR(N-1) = KMS(TPR(N-1))
     APR(N-1) = AMS(TPR(N-1))
     GO TO 1572
1568 TI = T(N-1)
     TPRA = TPR(N)
     LA = DLX
     TPRB = TM
     LB = L - DLX - DLT1PR
     MF = MLPR
     CCF = CCLF(TI)
     AFB = AML(TPRB)
     AFA = AML(TPRA)
```

```
      KFB = KML(TPRB)
      KFA = KML(TPRA)
      TPR(N-1) = TFPR4(N-1,2)
      KPR(N-1) = KML(TPR(N-1))
      APR(N-1) = AML(TPR(N-1))
1572  CONTINUE
      IF(THPR.LT.TH2) TVPR = (HO*TO*(DLT2 - L) + KCLF(TPR(N))*TPR(N))
     1          /(HO*(DLT2 - L) + KCLF(TPR(N)))
      IF(TVPR.GT.TVAP(PO)) GO TO 1574
      GO TO 1580
1574  DLTH = DLTH*(TVAP(PO) - TV)/(TVPR - TV)
      TVPR = TVAP(PO)
      TH2 = TH + DLTH
      GO TO 1520
1580  CONTINUE
      IF (TH.GE.TH2.AND.THPR.LT.TH3) GO TO 1582
      GO TO 1584
1582  TVPR = TVAP(PO)
      KCL = KCLF((TVPR - T(N))/2.0)
      DLT2PR = DLT2 + 0.5*(ML + MLPR - 2.0*MV)*DLTH/RHOCLF(TVPR)
      TPR(N) = (T(N)*(DLT2PR -L)/AML(T(N))/DLTH + 2.0*TPR(N-1)*(DLT2PR
     1          -L)/DLX**2 + KCL*TV/KML(T(N))**2*((3.0*KML(T(N)) -KML(T(
     2          N-1)))/DLX - MLPR*CCLF(T(N))))/ ((DLT2PR -L)/AML(T(N))/
     3          DLTH  + 2.0*(DLT2PR -L)/DLX**2 +KCL/KML(T(N))**2*((3.0*
     4          KML(T(N)) -KML(T(N-1)))/DLX - MLPR*CCLF(T(N))))
1584  CONTINUE
      IF(M1.LT.N.AND.M2.GT.1) GO TO 1586
      GO TO 1600
1586  Q1 = KML(T(M1+1))**2*((TPR(M1+1)- T(M1+1))/AML(T(M1+1))/DLTH
     1          - 2.0*(T(M1) - T(M1+1))/DLX**2)/((3.0*KML(T(M1+1))
     2          - KML(T(M1)))/DLX - ML*CCLF(T(M1+1)))
      Q2 = KMS(T(M2-1))**2*((TPR(M2-1)  - T(M2-1))/AMS(T(M2-1))/DLTH
     1          - 2.0*(T(M2) - T(M2-1))/DLX**2)/(KMS(T(M2)) - 3.0*
     2          KMS(T(M2-1)))*DLX
```

```
      A3 = (KML(TM)/AML(TM)*(TPR(M1+1) - TM) + KMS(TM)/AMS(TM)*
     1          (TM - TPR(M2-1)) + 2.0*RHOCSF(TM)*LDAM*POR)
      A4 = KML(TM)/AML(TM)*(TPR(M1+1) - T(M1+1))*(FLOAT(M1)*DLX - DLT1)
     1          + KMS(TM)/AMS(TM)*(TPR(M2-1) - T(M2-1))*(DLT1 - (FLOAT
     2          (M2) - 2.0)*DLX) + 2.0*DLTH*(Q2 - Q1)
      DLT1PR = A4/A3 + DLT1
      MLPR = POR*(RHOCSF(TM) - RHOCLF(TM))*(DLT1 - DLT1PR)/DLTH
      TI = T(M1)
      TPRA = TPR(M1+1)
      LA = DLX
      TPRB = TM
      LB = FLOAT(M1)*DLX - DLX -DLT1PR
      MF = MLPR
      CCF = CCLF(TI)
      AFB = AML(TPRB)
      AFA = AML(TPRA)
      KFB = KML(TPRB)
      KFA = KML(TPRA)
      TPR(M1) = TFPR4(M1,2)
      IF(DLT1PR - FLOAT(M2)*DLX + DLX) 1590,1588,1588
 1588 TI = T(M2)
      TPRA = TM
      LA = DLT1PR - FLOAT(M2)*DLX + DLX
      TPRB = TPR(M2-1)
      LB = DLX
      MF = 0.0
      CCF = CCSF(TI)
      AFB = AMS(TPRB)
      AFA = AMS(TPRA)
      KFB = KMS(TPRB)
      KFA = KMS(TPRA)
      TPR(M2) = TFPR4(M2,2)
      KPR(M2) = KMS(TPR(M2))
      APR(M2) = AMS(TPR(M2))
```

```
      GO TO 1592
 1590 TI = T(M2)
      TPRA = TPR(M1+1)
      LA = 2.0*DLX
      TPRB = TM
      LB = FLOAT(M2)*DLX - DLX - DLT1PR
      MF = MLPR
      CCF = CCLF(TI)
      AFB = AML(TPRB)
      AFA = AML(TPRA)
      KFB = KML(TPRB)
      KFA = KML(TPRA)
      TPR(M2) = TFPR4(M2,2)
      KPR(M2) = KML(TPR(M2))
      APR(M2) = AML(TPR(M2))
 1592 CONTINUE
      KPR(M1) = KML(TPR(M1))
      APR(M1) = AML(TPR(M1))
 1600 CONTINUE
      KPR(N) = KML(TPR(N))
      APR(N) = AML(TPR(N))
      IF(THPR.GE.TH2) GO TO 1610
      DLT2PR = L + (L - DLT1PR)*(RHOCSF(TM)/RHOCLF(TM) - 1.0)*POR
      TVPR = (HO*TO*(DLT2PR - L) + KCLF(TPR(N))*TPR(N))/(HO*(DLT2PR - L)
     1          + KCLF(TPR(N)))
      MVPR = 0.0
      GO TO 1620
 1610 MVPR = 1.0/LDAVF(TV)*(HO*(TO -TVPR) - KML(TPR(N))**2*(((TPR(N) -
     1          T(N))/AML(TPR(N))/DLTH  -2.0*(TPR(N-1) - TPR(N))/DLX**2)
     2          / ((3.0*KML(TPR(N)) - KML(TPR(N-1)))/DLX  -MLPR*CCLF(
     3          TPR(N)))))
      IF(THPR.GE.TH3) GO TO 1620
      DLT2PR = DLT2 + 0.5*(ML + MLPR - MV - MVPR)*DLTH/RHOCLF(TVPR)
 1620 CONTINUE
```

```
      M1PR = IFIX(DLT1PR/DLX) + 2
      IF(FLOAT(IFIX(DLT1PR/DLX)).EQ.DLT1PR/DLX) M1PR = M1PR - 1
      M2PR = M1PR - 1
 1630 CONTINUE
      DO 1901  I = 1,N
      K(I) = KPR(I)
      A(I) = APR(I)
      T(I) = TPR(I)
      P(I) = PPR(I)
 1901 CONTINUE
      TV = TVPR
      DLT1 = DLT1PR
      DLT2 = DLT2PR
      ML = MLPR
      MV = MVPR
      M1 = M1PR
      M2 = M2PR
      V1 = V1PR
      V2 = V2PR
      TH = THPR
      IF(THSEC.GT.201.0) GO TO 6001
      IF (T(N) - TMLTMX) 1000, 1000, 6001
 6001 CONTINUE
 2000 CONTINUE
 2250 CONTINUE
      GO TO 1
  170 STOP
      END
```

SAMPLE INPUT DATA CARDS

```
SILVER                                                                          CARD 1
   22     1     0  0.00027766                                                  CARD 2
 0.1666667     0.30      2221.0      8.79       24400.0    6560.0     6660.0   CARD 3
   107.87     4473.0      8940.0    1001.0   416900000.   1545.4     1303.0   CARD 4
    43.4     32600.0                                                           CARD 5
         1                                                                      CARD 6
   530.0                                                                        CARD 7
  8.513E-4  6.154E-9  1.520E-3  5.364E-8                                       CARD 8
  0.030E 0  1.370E-6  0.000E 0  0.000E 0    0.0E0                             CARD 9
  9.390E 1 -1.403E-2  1.155E-6  0.000E 0    0.0E0                             CARD 10
  0.052E 0  7.060E-6  0.000E 0  0.000E 0    0.0E0                             CARD 11
  6.920E-2  0.000E 0  0.000E 0  0.000E 0    0.0E0                             CARD 12
  4.610E-2  0.000E 0  0.000E 0  0.000E 0    0.0E0                             CARD 13
  2.757E 2 -5.180E-2  0.000E 0  0.000E 0    0.0E0                             CARD 14
  1.607E 2  0.000E 0  0.000E 0  0.000E 0    0.0E0                             CARD 15
  6.500E 2 -3.110E-2  0.000E 0  0.000E 0    0.0E0                             CARD 16
  0.371E12  0.000E 0  0.000E 0  1.525E 7                                       CARD 17
```

X. BIBLIOGRAPHY

A. References Used in the Analysis

1. Schwarzkopf, P. and E. D. Weisert, "Self-Cooled Rocket Nozzles," AIAA Preprint 64-129, January 29-31, 1964.

2. Gessner, F. B., R. J. Ingram, and J. D. Seader, "Summary Report, Self-Cooled Rocket Nozzles," Wright-Patterson Air Force Base RTD-TDR-63-4046, Vol. II., March 1964, AD-601574.

3. Ungar, E. W. and K. J. Touryan, "Ablation Mechanisms for Impregnated Tungsten," AIAA JOURNAL, TECHNICAL NOTES, Vol. 3, October 1964, pp 1949-1950.

4. Maloof, S. K., "Development of Ultra-High Temperature Tungsten Base Composites for Rocket Nozzle Applications," ARS Preprint 1573-60, December 1960.

5. Davies, G. F., and W. E. Smith, "Development of Refractory Materials for Rocket Nozzles and Vanes," Clevite Corporation Summary Report NORD 18887, May 19, 1960.

6. Gessner, F. B., J. D. Seader, R. J. Ingram, and T. A. Coultas, "Analysis of Self-Cooling With Infiltrated Porous Tungsten Composites," JOURNAL OF SPACECRAFT AND ROCKETS, Vol. 1, Nov.-Dec. 1964, pp 643-648.

7. Grosh, R. J., "Transient Temperature in a Semi-Infinite, Porous Solid With Phase Change and Transpiration Effects," WADD Technical Report 60-105, January 1960.

8. Resnick, R., C. Wurms, R. Steinitz, and E. Mezza, "Cooling of Porous Tungsten Structures by Evaporation of Infiltrated Material," METALS ENGINEERING QUARTERLY, May 1963, pp 51-59.

9. Schwarzkopf, P. and E. D. Weisert, "Self-Cooled Rocket Nozzles," Wright-Patterson Air Force Base RFD-TDR-63-4046, Vol. III, August 1965, AD-473691.

10. Weinbaum, Sidney and H. L. Wheeler, Jr., "Heat Transfer in Sweat-Cooled Metals," JOURNAL OF APPLIED PHYSICS, Vol. 20, January 1949, pp 113-122.

11. Schnider, P. J., CONDUCTION HEAT TRANSFER, Addison-Wesley Publishing Company, Inc. 1955, pp 258-260.

12. Watson, K. M., "Thermodynamics of the Liquid State, Generalized Prediction of Properties," INDUSTRIAL AND ENGINEERING CHEMISTRY, Vol. 35, 1943, pp 398-406.

13. Greenberg, D. B., and E. Weger, "An Investigation of the Viscous and Inertial Coefficients for the Flow of Gases Through Porous Sintered Metals With High Pressure Gradients," CHEMICAL ENGINEERING SCIENCE, Vol. 12, 1960, pp 9-19.

14. Green, Jr., Leon, and P. Duwez, "Fluid Flow Through Porous Metals,' JOURNAL OF APPLIED MECHANICS, March 1951, pp 39-45.

15. Gambill, Wallace R., "Estimate Low-Pressure Gas Viscosity," CHEMICAL ENGINEERING, September 22, 1958, pp 169-172.

16. Dusinberre, G. M., HEAT-TRANSFER CALCULATIONS BY FINITE-DIFFERENCES International Textbook Company, 1961.

B. References Used in Search of Property Data

17. RARE METALS HANDBOOK, Second Edition, Rienhold Publishing Company, 1961.

18. Thielbahr, W. H., "Transpiration Cooling With Liquid Metals," Part 2, U. S. Naval Ordnance Test Station, NAVWEPS R-8732-2, AD-623020.

19. LIQUID METALS HANDBOOK, Atomic Energy Commission, 1 June 1952.

20. Goldsmith, Waterman, and Hirschhorn, HANDBOOK OF THERMOPHYSICAL PROPERTIES OF SOLID MATERIALS, Armour Research Foundation, MacMillian Co., 1961.

21. INTERNATIONAL CRITICAL TABLES, National Research Council, McGraw-Hill Book Company, 1933.

22. METALS HANDBOOK, 8th Ed., Vol. I, American Society for Metals, 1961.

23. Touloukian, Y. S., Editor, RETRIEVAL GUIDE TO THERMOPHYSICAL PROPERTIES RESEARCH LITERATURE, McGraw-Hill Book Company, 1963.

24. MATERIALS AND METHODS, Vol. 25, No. 1, p. 123, Data Sheet, 1947.

25. Kolsky, H. G. "The Thermodynamic Properties of 54 Elements Considered as Ideal Monotomic Gases," Atomic Energy Commission, LA-2110.

26. Baumeister, Theodore, Editor, MARK'S MECHANICAL ENGINEER'S HANDBOOK, 6th Ed. McGraw-Hill Book Company, 1958.

27. Reid, R. C. and T. K. Sherwood, THE PROPERTIES OF GASES AND LIQUIDS, 2nd Ed., McGraw-Hill Book Company, 1958.

28. Holman, J. P., EXPERIMENTAL METHODS FOR ENGINEERS, McGraw-Hill Book Company, 1966.

29. Hsu, S. T., ENGINEERING HEAT TRANSFER, D. VanNostrand Company, 1963.

XI. ACKNOWLEDGEMENTS

The author wishes to acknowledge Dr. F. B. Gessner, now an Assistant Professor of Mechanical Engineering at the University of Washington, for his suggestion of the basic idea of this investigation and for his advice, assistance and guidance during the preliminary stages of the investigation. Appreciation is also extended to the National Aeronautics and Space Administration for awarding the grant that made the research possible. The author wishes to thank his major professor, Dr. Martin Crawford of the Mechanical Engineering Department, for accepting the responsibility upon the resignation of Dr. Gessner, and who devoted full time during the summer to this investigation. Appreciation is also extended to Dr. H. L. Wood and Dr. F. R. DeJarnette who, as members of the advisory committee, offered their time, comments and criticisms. In addition, the author expresses his gratitude to for typing the complete manuscript.

Thanks and appreciation are extended to the author's parents whose financial assistance and encouragement made a college education possible A most sincere thanks is extended to the author's wife, , whose understanding, encouragement, and assistance made it all possible.

The vita has been removed from the scanned document

AN ANALYSIS OF SELF-COOLING WITH INFILTRATED POROUS COMPOSITES INCLUDING THE EFFECT OF THE MELT LAYER

by

Maurice Robert Berry, Jr.

ABSTRACT

A detailed analytical model was developed to include the effect of the melting process on a porous composite which retards its own heating rate by sacrificing its infiltrant. A transient one-dimensional heat-transfer analysis was conducted considering both the heats absorbed by melting and vaporization of the infiltrant from within the matrix. A finite-thickness liquid layer was seen to exist above the composite surface as a result of the flow of liquid coolant onto the surface induced by the expansion of the coolant on melting. There existed a period of time during which the melt layer was subject to both depletion due to vaporization and renewal by the flow of liquid coolant onto the surface. As the heating process continued the melt layer was depleted and the liquid coolant vaporized from within the tungsten matrix.

The analysis was solved by finite-difference techniques and programmed for the IBM 7040/1401 Digital Computing System. An extensive search was conducted to determine the dependence of temperature on the thermophysical properties of seven different metallic coolants. Data were obtained for the various infiltrants up to that time at which the melt layer vaporizes completely from above the composite surface.

A fundamental understanding of the effects of the melting process and of assuming variable properties on the early stages of the self-cooling process was obtained.